Imperial College of Science, Technology and Medicine
Department of Physics

Entropy Production and the Climate

Goodwin Gibbins

Submitted in part fulfilment of the requirements for the degree of
Doctor of Philosophy in Physics at Imperial College, 2021

Statement of Originality: The work presented in this thesis is my own unless otherwise specified.

Abstract

The entropy production rate of the climate is a topic of active study but ongoing confusion, spurred by the yet-unproven hypothesis that the climate system might be organising itself to maximise its entropy production rate and, more broadly, the potential of probing our climate from unorthodox simplifying perspectives. In this thesis, a re-examination of some fundamentals in this topic is offered.

Two main suggestions for a climate-relevant global entropy production rate have been established in the literature: one which focuses on non-radiative processes only (labelled 'material') and one which includes all radiative and non-radiative processes (labelled 'planetary'). Another physically-motivated entropy production rate is introduced and investigated here – the transfer entropy production rate – which distinguishes radiation according to the role it plays within the system, considering only entropy production due to those transfers of energy which occur within the climate. Various lines of reasoning and evidence point towards the new rate being physically meaningful, which is significant especially as it offers a re-interpretation of the entropy production optimisation hypothesis.

Next, the response of entropy production rates to changing climate conditions is investigated and the results used to verify a simple conceptual model capable of predicting the direction of the changes. The transfer and material entropy production rates are found to be significantly more responsive than the planetary rate to the climate's state and they both are able to resolve changes which surface temperature cannot: a simple solar radiation management scenario is found to be able to restore global average surface temperature but not the entropy production rates.

Finally, the measurement of the entropy production budget via radiation information in observational and GCM datasets is explored. A new method for accounting for entropy storage in the recently published CERES SYN1deg entropy flux dataset is demonstrated, which makes it possible to estimate the material and transfer entropy production rates from that dataset. This reveals that the transfer and material entropy production rates have increased in line with temperature over the past 20 years and that entropy production rates are higher in years with higher solar absorption. Furthermore, there is a hemispheric asymmetry of entropy production, with more occurring in the Northern hemisphere. The global mean material entropy production rate is 55.3 mW/m^{2}K and the transfer entropy production rate, 82.0 mW/m^{2}K in that dataset between March 2000 and February 2018.

As a whole, this investigation deepens our understanding of entropy production in the climate and offers new definitions, frameworks and observed patterns to stimulate further research.

Acknowledgements

The emotional roller-coaster and tangled confusion of embarking on a big research problem is surely best borne with other people. Undertaking this project would have been impossible for me without the warmth, kindness and insights of the people around me, from supervisors to fellow conference attendees, old friends to new office-mates.

Thanks is first and foremost due to my supervisor, Joanna Haigh, whose steadying support lent me such a solid grounding over these tumultuous years. As we explored this project together and the shape of it shifted and reformed, I was privileged to have her scientific experience and astute questioning alongside me. And beyond that, her care, understanding of me as a whole person, and reassuring calm as I navigated other outside problems alongside the research helped me to feel safe and to find the resilience I needed to stay with the work. I have felt very lucky to have had such a mentor.

The wider scientific community in the Atmospheric Physics group at Imperial College supported, inspired and taught me much. Thank you to Helen Brindley and to her group for giving me a second home in this final stretch of the PhD. To Mike, Ed, Peer and Matt for the great conversations and friendly chats, from lunches to journal club. To Ken, who reminds us of other ways of thinking and seeing our climate. To Rich, for his practical support of the whole group and engagement on all sorts of ideas. To Arnaud for his well-placed reassurance and book recommendations. To Apostolos for his enthusiasm. To Erik for leading great outreach. To Heather for her strong example of attention not just to the science but also to how we do it. To Juliet for her warmth and perspective at a critical moment. To Ralf and Marina for their suggestions and re-direction during the course of the PhD. And over in Blackett, to Faye for an outside perspective of encouragement and care at an important time.

For everyone who made the office an oasis of pragmatic, humorous support - thank you. Cups of tea and lunch-time football were wonderful for rainy days and sunny ones, but it was the people who filled it with life. I am so grateful for the fun, warmth, encouragement and commiseration I got in Huxley 709 and the hallways beyond, from Jo, Kieran, Rebecca, Shuai, Sunil, Eric, Pietro, Philipp, Ryo, Rhidian, Ronan, Natasha, Luke, Emma, Peter, Chris, Flo, Jon and everyone else. And from my first home at Imperial, the MPE CDT, and the lovely Oana, Paula, Matt, Thomas, Tasmin, Riccardo, Aythami, Jemima, Lea, Josie, Mike, Zoe and Anna. Thanks especially to Tom, who has always been such a thoughtful, fun and sharp accomplice, from our first maths supervisions through to our PhDs. To Darije for great conversations and support. To Vaiva for understanding and inspiring. And to so many other people who brightened my time at Imperial along the way.

I've also been lucky to have had support and contributions from researchers beyond Imperial. Seiji Kato and Fred G. Rose went above and beyond to respond openly and collaboratively to my questions about their recent work, and I very much appreciate both the calculations they shared and the encouragement their friendliness

Contents

Chapter 1

Introduction

1.1 Motivation

Our climate is an immensely complex system, with richness that emerges from the interaction between the physics of its parts – from temperature and pressure differences, to fluid motions, to phases of water, to radiation. Unlike a biological system, which we know has been arranged by natural selection, the organisation of a climate system is hard to explain with an overarching 'why?'. Yet, there is an urgency to comprehending as much as we can about the workings of Earth's climate. As scientists trying to understand its features, we're driven not only by curiosity about how its beautiful patterns and surprising changes occur, but also by the vulnerability of our reliance as a society and a species on our planet's climate. We are influencing the climate system significantly but without the knowledge to fully anticipate how it will respond.

The climate system is also very challenging to study. We cannot perform experiments on it, nor do we have multiple copies to examine and compare as we do in biology. We have instead invested heavily in simulations which link together the smaller-scale physics that we have been able to ascertain by experiment and observation. Our model-replicas of the climate system allow us to probe and explore the features we observe in our true climate and to run our guesses of what might happen next forward in time.

These simulations are, however, only as good as the pieces of understanding we put into them and even a perfectly accurate simulation would not provide a complete understanding, even if it could supply perfect prediction. The complexity of a global climate model (GCM) mirrors the complexity of the climate system, and this very complexity means it does not itself deliver explanation and comprehension of the climate. For such a vast system as the climate, understanding necessarily comes from a reduction of complexity.

Although the reducing questions in this field typically focus on what mechanistically explains a certain observed feature, in this thesis I am more motivated by the question of what broader things must be true of the climate system as a whole because of the way it is put together. Principles which simplify systems often come from quite

fundamental laws, like the conservation of energy which we know must apply to the whole system because of its universality in the parts. These can be very powerful in building understanding: energy conservation gives the concept of energy balance its meaning, and from that stem the ideas of radiative imbalance and climate sensitivity which are so central to our discussion of anthropogenic climate change.

The entropy production rate of the climate is seen as a potential (still unproven) source of another simplifying principle that may govern, or at least be emergent from, the climate system's intricate behaviour. The idea was 'stumbled upon'[1] by Garth Paltridge during an explicit attempt to get away from the usual simulation-building mode of climate science. It was found by searching widely and speculatively for any variable observed to be extremised by the climate, and which the climate might therefore be self-organising *so as* to extremise, akin to the concept of fitness in natural selection. The variable that was found was the meridional entropy production rate – the horizontal energy flow divided by local temperature.

This is an unusual and exciting scientific approach. If the shot in the dark hit a target, it might turn up a profoundly new aspect of the climate system. However, it also took the field far from firm ground: entropy production was an unfamiliar and undeveloped concept and there was no theoretical basis to make sense of the tantalising hint of a self-organisation principle that Paltridge's results gave, nor a clarity on how to test the principle's applicability or to leverage it. This untetheredness remains the core challenge of conducting and defending research into the climate's entropy production. Studying Earth's rate of entropy production is far from the usual way of doing climate science, which is both a source of strength and confusion.

New simplifying principles can do a lot for our scientific progress, even if they cannot provide as much detail as might a GCM. They are crucial as cognitive aids to make sense of the complexity of the true or simulated system and for communicating about the system to thinkers in other domains. The understanding they supply could let us predict what the system will do without needing to know the details or to use the computational power to simulate it, allowing short-cuts to some of the same answers. They could also help us check our simulations, to confirm that they are working well along meaningful axes. And on the level of curiosity, they are satisfying, revealing emergent elegance in the world around us.

1.1.1   Why entropy?

Apart from Paltridge's observation, why might entropy, and the rate at which it is produced by the climate system, be an interesting and promising place to look for a simplifying principle?

Entropy, although it is far from familiar in our daily experience, is one of the most fundamental thermodynamic variables. On a microscopic level, it measures the number of ways a system can arrange itself to fit each macroscopic constraint and it is an almost mathematical certainty that, if allowed to, systems will find

---

[1]These are the words that the scientist in question used to describe his experience of discovery in *Paltridge* [2005].

themselves transitioning from the less likely to more likely configurations, which is reflected in an entropy increase. In our macroscopic world, the arrangements of these microstates are not apparent but instead we observe that certain energy flows and other changes occur exclusively in one direction because of the requirement that entropy increase. The second law of thermodynamics, which is the one which captures this principle, was actually originally stated by Clauisius as "heat can never pass from a colder to a warmer body without some other change, connected therewith, occurring at the same time" [*Clausius*, 1854]. In fact, the very concept of temperature relies on the directionality of heat flow (and hence the entropy increase requirement) to gain its meaning [*Adkins*, 1983]: an object is described as being at a higher temperature than another exactly when the total entropy would be increased if heat flowed from it to the other. Although we may not note it, entropy is at play wherever temperature differences drive energy flows.

Since the total entropy can never decrease, the only processes that are reversible are those that cause no change in entropy. The rest are irreversible and the rate at which the total entropy of the system increases because of them is called the *entropy production rate*.

The climate is an entropy-producing system. It is not energy alone that drives the motion and activity on the planet, but the movement of energy from the warmer regions, where it is supplied to the climate, to the cooler regions, where it leaves. This transfer is mediated by a myriad of irreversible processes, from wind to rain to life. Each process produces entropy, which must then be exported from the climate system if that system is to be maintained at a near-steady state. This export is by radiation; the supply of low-entropy solar radiation and loss of high-entropy outgoing thermal radiation has the net effect of carrying entropy away from the system and maintaining temperature gradients. Our climate system exists in this balance.

That the climate produces entropy is certain, but what is less clear is exactly how this might be leveraged to advance our scientific understanding of the climate system. Although the rate of entropy production in the climate gains much of its significance from the maximum entropy production principle (MEPP) hypothesis of Paltridge, it is also interesting as a diagnostic variable to test the fidelity of climate models, and as a scalar climate state metric to provide a new lens with which to track the various changes that occur as the climate adopts different states. It is a variable which measures not only the quantity of energy that flows but also its usability and the temperatures involved, highlighting the irreversible activity and the departure from quiescent equilibrium which is so important to our experience as creatures on this planet.

1.1.2 An instructive allegory

What is it to look for new simplifying principles and models from where we stand in climate science? What might the challenges be in terms of the approach we take as a scientific community and barriers to development of the ideas? A somewhat-colourful analogy between climate science and the study of ideal gases tells an

interesting story to which I have found myself often returning while conducting this research (inspired by Garth Paltridge, via *Whitfield* [2005]).

Consider an impossibly tiny scientist living inside a box of an ideal gas and able to see the movement of the molecules. In that world, the first lines of scientific enquiry might likely focus on the kinetics of the molecules: what is conserved during collisions and how can the trajectory of the particles be predicted? If the tiny scientist had access to a super-computer, it is possible to imagine them building a model that could directly simulate the forward-trajectory of particles from a known starting configuration. Even with perfect knowledge of the physics, such a model would, of course, be imprecise - perhaps exhibiting some small energy non-conservation due to numerical integration, or to limited skill due to uncertainty in the starting positions and momenta. That scientist would, however, be satisfied that further work and increases in computational power could improve on these things and that, for the task of predicting the timing of collisions across the domain of the box, their model was evidently the best tool, and thus that they might be quite satisfied with their knowledge and scientific progress.

We macroscopic scientists, however, know there are beautiful features of ideal gases that this microscopic scientist has missed. We have had the luxury of being able to interact with boxes of ideal gases using our body's ability to sense heat transfers and our time-averaged perspective which integrates the impulse of all of the collisions on the side of the vessel to observe pressure and from there allows us to relate it to temperature and volume. Because we have been able to experiment on the box as a whole, the ideal gas law has been a natural discovery for us.

What would it take for the microscopic scientist to discover the ideal gas law? Of course, the law is not inconsistent with the detailed understanding the tiny scientist has from the kinetic model, and it would, in principle, be possible to deduce it by varying parameters within that model and studying the distribution of velocities and collision impulses. But, although it is not precluded, would the microscopic scientist even conceive of doing that? How would they take such a major step away from the normal conception of the system?

Furthermore, what would motivate that microscopic scientist in the single box to study a law which, although providing reliable truths in a wider range of ideal gas scenarios, could give only limited information about aggregated variables in any particular instance, far less completely and precisely than their direct simulation could? It wouldn't be immediately obvious how that different approach could yield any useful new information. Imagine, even, that a technological advance allowed the splitting of the molecules, increasing their number. Although this would be precisely the scenario that the ideal gas law would be well-suited to illuminating, the microscopic scientists would be likely to continue to rely on their imperfect direct simulation model to try to discover the potential impacts of such an intervention.

This is, of course, a thinly veiled analogy for climate science. We exist as small scientists within a complex system, and our GCMs focus on the things we can perceive and are familiar with, via complicated, direct

simulations. If there is a discovery to be found not simply by scaling up laws that exist on the microscopic level to see their global effect (e.g. conservation of energy) but rather by finding new emergent consistent-but-novel laws, it takes very difficult mental gymnastics, especially without the ability to do experiments on the system. But, as we know from this analogy and from statistical physics and thermodynamics more generally, although developing new models or understandings of a system is far-from-trivial, doing so can provide far from trivial new insight, even if the models are somewhat redundant in the sense that they can be derived (in part) from each other.

Entropy production rates are to us like the concepts of temperature and pressure would be to the microscopic scientist. To make a discovery akin to the ideal gas law, we'd need to make two leaps at once: to invent and establish a new concept and, at the same time, to propose a new theory that makes that concept meaningful. Before the law exists, it will not be evident why the variables are worth studying. Furthermore, any law that begins to emerge might also not be an obvious improvement on the GCMs in the realms of study in which the GCMs dominate, and might not seem entirely novel – in some sense they must be written into, or at least consistent with, the other laws we know. At the core of this search, however, is the intuition (or perhaps quixotic hope) that the climate system is rich enough that new simplifying laws could exist, and that they would be scientifically significant enough to warrant the difficult search.

1.2   Thesis overview

This thesis re-examines the foundational aspects of entropy production in the climate in order to develop the fundamentals on which a potential simplifying principle might be built, and to support the use of entropy production rates as diagnostic variables. First, in Chapter 2, a careful study of the existing literature on this topic is offered and the state of the field is summarised to identify the key ideas, approaches, progress and disagreements. In Chapter 3, the two established definitions of global entropy production rates are re-examined and an alternate perspective proposed, introducing a new climate entropy variable – the transfer entropy production rate. It is significant because a new variable gives meaning to new potential theories, and preliminary physical arguments suggest the transfer entropy production rate might be particularly physically relevant. Chapter 4 develops our understanding of these three global entropy production rates by exploring how they respond to changes in climate in a simple radiative-convective model. A new conceptual model for understanding the climate as an entropy-producing system is introduced, which improves our ability to predict and intuit the entropic variables and is supported by the results. Chapter 5 focuses on measurement, exploring how the three entropy production rates can be accurately estimated from observations and more complex models. A recent data product created by the CERES team[2] is adapted to account more correctly for inter-annual entropy storage, and novel patterns that it reveals in the past two decades of global entropy production rates are shared. Finally,

---

[2]Introduced in *Kato and Rose* [2020].

the main conclusions which can be taken from this work are recapped in Chapter 6 and leveraged to supply ideas which might help to further the discussion of the MEPP hypothesis, as well as clarifying our general understanding of entropy production rates as climate variables.

1.2.1 Contributions, publications and statement of originality

The work discussed in this thesis has been conducted by the author with supervision from Joanna D. Haigh. One paper has been published in the *Journal of Atmospheric Science* entitled *Entropy production rates of the climate* [*Gibbins and Haigh*, 2020], which covers some of the content discussed here in Chapters 2, 3 and 4, and a second comment paper [*Gibbins and Haigh*, 2021] has been published in the *Journal of Climate* covering some of the material in Chapter 5. The contributions presented here are my own, except where otherwise stated.

Chapter 2

Background: Entropy Production in the Climate

In the 45 years since its inception, climate entropy production has been an esoteric area of study. An average of four papers have been published per year, going back and forth on the definition of the global entropy production rate, the estimation of its value and components, and the tantalising hypothesis that it might be maximised in the observed climate configuration. These are early questions in the development of a scientific theory and they have not yet been categorically answered. In this chapter, the evolution of this field – the questions it has taken up, the answers which have been found and the confusion and differences which persist – will be summarised.

It was a general search for a simplifying model and understanding of the climate system which led to the initiation of this field:

> In the mid-1970s, the love affair between climatologists and computer models was beginning to blossom. By breaking down the atmosphere and ocean into ever-smaller interacting chunks in simulations, researchers found that they could mimic the behaviour of the global climate with reasonable success. But for Garth Paltridge, a climate scientist at the University of Tasmania in Hobart, Australia, these general circulation models (GCMs) were coming at the problem from the wrong direction. "I felt it was like trying to describe the behaviour of a gas by following the path of every molecule, he says."
>
> *Whitfield* [2005]

Paltridge [1975], which first posits the theory of Earth's entropy production rate optimisation, explains its motivation in its introduction:

> The modern approach [to predicting and understanding the climate] assumes that a solution will be possible when all significant processes affecting weather and climate can be described in sufficient

detail. Vast numerical models have been developed which attempt to simulate global dynamics and climate at the maximum level of detail compatible with available computers (see for instance GARP Report 14 1973). The work is urgent and necessary, but it can be argued that the approach is at variance with a basic philosophy of physics which, when faced with a complex problem, searches for simple laws which may govern the overall situation. Ideally, such laws should be simple in both concept and application.

2.1 Sparking the hypothesis

What was the observation that led Paltridge to put forward the entropy production rate as a climate-simplifying variable and the maximisation of it as a climate-simplifying law?

As he explains, the "work began with the hypothesis that there are sufficient degrees of freedom in the complexity of global dynamics for control by some minimum principle to be possible" [*Paltridge*, 1975]. To search for such a principle, Paltridge designed a zonal energy balance model (with three cells in the initial search phase, extended to ten for further investigations) which had a single unconstrained feature: the meridional energy flow in the ocean and atmosphere. The temperature, cloud cover, incoming and outgoing radiation are all determined within the model for any given meridional energy flow. Testing the state of the model with different meridional flows, he searched for a scalar aggregating variable which was both minimised within the parameter space and the minimisation of which resulted in a recognisable climate state. He hypothesised that if such a quantity existed, it would be of physical importance.

The quantity he landed on was

$$E = \sum_i \frac{(F_i^{in} - F_i^{out})}{T_i}, \tag{2.1}$$

the sum over all cells of the ratio between the difference of incoming and outgoing energy flux and the grid cell temperature. As each grid cell is represented by only a single temperature, this model cannot resolve entropy production due to heat transported in the vertical. However, E can be interpreted as the negative of the entropy production due to meridional energy flows. This led to the hypothesis of the maximisation of entropy production principle, MEPP.

2.2 MEPP in simple models

Paltridge's observation led to a flurry of activity building simple models and testing entropy production rates, including *Nicolis and Nicolis* [1980], *Grassl* [1981] and *Wyant et al.* [1988], which broadly continued in a similar vein, highlighting successes and failures of the entropy production rate maximisation hypothesis in

various simple climate models.

O'Brien and Stephens [1995] re-examines Paltridge's model closely, noting that it makes approximations which amount to assuming that convection is maximally efficient and that these might be partially responsible for the felicity of the entropy production rate maximisation results. There are also less critical follow-ons, such as *Lorenz* [2010] which investigates an even more reduced two-box model of planetary climates in which it appears that a maximisation of the entropy production rate reproduces the equator to pole temperature difference on Earth, Mars and Titan (results which are subsequently questioned in *Goody* [2007]). Recently, *Herbert et al.* [2011] studied the maximisation of entropy production due to meridional and vertical convective heat flux in a two-layer energy balance model, finding reasonable agreement between in the present climate and the Last Glacial Maximum (though without a null hypothesis for comparison).

These, and other papers which take up similar questions [*Noda and Tokioka*, 1983; *Gjermundsen et al.*, 2014], do not provide definitive evidence for or against the MEPP: it seems to have predictive power to some extent in simple models, but there is debate around which model set-up is most meaningful and how to interpret an only-approximate agreement between model and reality, in part due to the ambiguity introduce by the simplicity of the models.

2.3   Disagreement over definitions of global entropy production rate

In Paltridge's zonally-averaged model, the difference in radiative heating was interpreted as the meridional heat transfer rate, as established by *Paltridge* [1978] and *Wyant et al.* [1988], among others.

Essex [1984], however, argued Paltridge's characterisation of the Earth's entropy production rate was fundamentally "incorrect" as it had failed to account for entropy production in the radiation field. In doing so, Essex introduced the quantity labelled in this thesis as the *planetary entropy production rate*, which has been further explored by, e.g. *Lesins* [1990]; *Stephens and O'Brien* [1993]; *Pelkowski* [1994]; *Li et al.* [1994]; *Li and Chylek* [1994]; *Wu and Liu* [2010a].

This insight into the role of radiation in producing entropy instigated the division of the climate into non-radiative (material) and radiative sub-systems and the separate tabulations of the entropy produced in each [*Essex*, 1987; *Goody and Abdou*, 1996; *Goody*, 2000]. Paltridge's meridional entropy production rate was mapped in higher-dimensional models to the *material entropy production rate*, which includes contributions from horizontal and vertical sensible and latent heating (as established by *Pujol and Llebot* [1999]) as well as all other non-radiative processes.

The maximisation principle has been primarily applied to the material perspective, both in experimental and theoretical studies (e.g. *Ozawa and Ohmura* [1997]; *Ozawa et al.* [2003]; *Dewar* [2003]; *Fraedrich and Lunkeit*

[2008]; *Labarre et al.* [2019]). The contributions due to component processes have also been considered separately (e.g. *Pauluis and Held* [2002a,b]; *Volk and Pauluis* [2010]; *Lembo et al.* [2019]).

The debate about which is the "correct" entropy production rate to maximise is ongoing, notably in work by *Bannon* [2015] which lays out six plausible measures, moving away from an analysis that one is 'correct' and the rest 'incorrect'. In this thesis we address this debate further in Chapter 3.

2.4 Investigations of MEPP in more complex models

Research also continues into whether the maximisation of entropy production predicts reasonable states in more complex dynamical climate models. In these studies, as in *Paltridge* [1975], a variable is identified as free to adjust in an otherwise complete model to optimise entropy production rates and the resulting atmospheric state is compared to observations. A striking aspect of this body of research is the wide range of variables which the are identified as free variables, and the mixed success of MEPP in the results.

Ozawa and Ohmura [1997] use a vertical model grey atmosphere with a single exponentially-decaying shortwave heating channel. Their free variable is the convective heat transfer from the surface into the atmosphere, from which is calculated the remaining radiative heating needed for energy balance and thus the implied temperature distribution. The entropy production they focus on is that due to the convective heating in the vertical. Although the match to observation is only approximate, they conclude that "it is suggested from our calculation that the convective heat flux distribution in the atmosphere is determined through a total entropy generation process in the entire atmosphere" (pg 444). This is an overly-confident conclusion.

Pujol and Fort [2002] use a similar vertical model but prescribe the atmospheric lapse rate, fixing convection within the atmosphere. The free variable is instead the surface temperature discontinuity, which is found to be 10K at maximum entropy production, which they note compares unfavourably with the values closer to 2K for more standard radiative-convective models. They maintain a hopeful conclusion on MEPP in some aspects however, as they find that when the optical depth is allowed to vary, a maximum in the entropy production is found with a similar optical depth to the one used to match the real atmosphere in their radiatively-simplified model.

A 10-level column model with detailed radiative transfer calculations and simplified convection is used *Wang et al.* [2008] to study the cloud fraction chosen by MEPP as a function of the lapse rate. The study does not focus on carefully evaluating the fit between MEPP-derived climate and observed but instead proceeds to investigate how the maximally-entropy producing climate changes with climate changes such as an increase in the greenhouse effect.

Pascale et al. [2012] study a gridded energy balance model with horizontal and vertical extent and find that

MEPP is more able to reproduce the meridional character and heat flux than the vertical. In *Pascale et al.* [2011b], the free variables of the convective entrainment rate and the cloud droplet-to-rain conversion rate are studied in a low-resolution atmosphere-ocean circulation model, FAMOUS. It is found that variations in the amount of absorbed solar radiation with the surface temperature mean that no absolute maximum exists in the entropy production rate, which instead increases monotonically with global mean temperature.

More recently, *Labarre et al.* [2019] have attempted to address the issue of unphysical energy transfers being selected for by the MEPP state by adding further physical constraints to the way energy is transferred in the vertical. They use a radiative-convective column model with spectrally-resolved radiative properties which reflect the atmospheric constituents and an energy flux parameterised in terms of a mass mixing between adjacent layers. This means the role gravity plays in convection is taken into account and it results in a temperature profile which is more realistic when MEPP is applied.

2.5   Attempted proofs of MEPP

As these corroborations and challenges to MEPP have been uncovered in studies of model behaviour, some have also attempted more direct theoretical proofs of why the entropy production rate ought to be maximised in an open system driven so far from equilibrium as the Earth.

The primary contributions have been from Roderick Dewar, who takes a statistical mechanics approach, exploring whether the maximum entropy *production* principle might stem from similar considerations to the maximum entropy principle of *Jaynes* [1957a,b]. This has not been an easy task: the arguments in *Dewar* [2003] and *Dewar* [2005] were disputed *Grinstein and Linsker* [2007] . More recently, *Dewar* [2009], *Dewar and Maritan* [2011] and *Dewar* [2014] present further clarification without clinching the problem from the point of view of the climate entropy field at large.

Dyke and Kleidon [2010] builds on Dewar's work, but suggests re-framing the MEPP not as a physical law but as a method of inference useful for deducing additional information about a system about which certain features are already known, information which is then tested and further developed. It argues that the conservation of mass, energy and momentum in the Earth system combine with the informational features of MEPP to result in a law which appears more fundamentally thermodynamic but the principle might be best understood as information-theoretic.

Another relevant work is *Virgo and Ikegami* [2015] which looks for a more mechanistic explanation of how MEPP might arise and be maintained in a system such as the climate. The difficulty of conceiving of a system which is able to deduce and respond to the gradient of the entropy production rate is underlined, but within a simplified framework and assumptions which leaves open questions about the general applicability.

This is still an area of active research and open questions. Each line of argument for proving MEPP posits a different interpretation of what the significance and meaning of the law might be, which means the theorising might change how MEPP is to be applied to and understood in the Earth system, not necessarily following Paltridge's paradigm and the research that has followed.

2.6   Earth entropy budgets

Yet other researchers have put aside the theoretical and predictive questions of the maximisation of entropy production and have instead focused on the entropy production rate as a diagnostic of the climate's state. The work done in this space has prioritised building tools and testing assumptions for deducing the entropy production rate of the complicated Earth system from known variables, as it is not itself a variable which is straightforward to measure.

Some of the early entropy budgets use approximate values for global temperatures and energy fluxes to calculate entropy fluxes and production rates as the difference of those via the simple relationship of entropy as a ratio between an energy and a temperature. *Peixoto et al.* [1991] is a canonical example of this, with entropy production due to certain processes and connected with different fluxes being estimated at the atmosphere and surface. As well as being approximate, however, this budget does not properly account for the entropy carried by radiation (see Section 2.9) and so provides only very preliminary estimates.

More complete analyses of the entropy fluxes carried by radiation are conducted by researchers who try to leverage satellite observations to ascertain entropy budgets. *Lesins* [1990] is an early example of this, exploring the role that temperature variations play in the entropy carried by emitted radiation and employing Planck's relationship between spectral radiation intensity and entropy [*Planck*, 1914]. *Stephens and O'Brien* [1993] calculates these values more precisely from data in the Earth Radiation Budget Experiment. More recently, *Wu and Liu* [2010a] provide a very thorough analysis of entropy in Earth's radiation spectra. On the other hand, even as recently as *Pelkowski* [2012], estimates have continued to rely on the black body or grey body approximations of radiation entropy fluxes rather than using resolved spectra and accurate radiation measurements.

As the focus shifted to the non-radiative portion of the entropy production rate, researchers moved to develop the tools for measuring the entropy produced by material processes only. *Goody and Abdou* [1996] and *Goody* [2000] identified that the entropy production by all non-radiative processes can be deduced indirectly by simply measuring the net heating tendency of non-radiative processes (which in a steady system is the negative of the heating due to net radiative effects), which was applied to deduce an entropy budget in the GISS GCM. The energy fluxes and temperature differences associated with each class of irreversible processes also allows the budget to be separated in terms of the source of the irreversibility. This work was continued by *Pauluis and Held* [2002a], *Pauluis and Held* [2002b] and *Raymond* [2013] to quantify the partitioning of entropy production

between different types of processes, emphasising the dominance of the hydrological cycle in Earth's non-radiative entropy production.

Obtaining more precise direct sums of the entropy production due to each irreversible process within a GCM has been a focus of recent research. *Pascale et al.* [2011a] calculate the entropy budget in the coupled atmosphere-ocean GCM HadCM3, while *Fraedrich and Lunkeit* [2008] do similarly for a different climate model of intermediate complexity. *Lembo et al.* [2019], on the other hand, develops a general diagnostic tool for estimating the entropy budgets across all CMIP6 models. All necessarily provide only approximate estimates, but can still offer insight into the relative entropy production rates between models and the changes of entropy production rate within models over time and due to external changes.

The most recent contribution to the entropy budget project is *Kato and Rose* [2020], which uses detailed radiative-transfer calculations to deduce the entropy fluxes due to non-radiative processes and the exchange of radiation within the atmosphere. This is conducted within the CERES SYN1Deg data product, which is based on ongoing satellite observations, and so this constitutes a major step forwards in terms of the reliability and observational grounding of entropy budgets, which is further explored in Chapter 5.

2.7   Other research questions

As well as allowing the internal features of a climate simulation to vary to see if the observed state is a maximum of the entropy production rate (such as meridional heat transport in Paltridge's original studies), researchers have also studied how changing more external features of the climate system influences the entropy production rate. For example, *Singh and O'Gorman* [2016] investigate the entropy budget in a high-resolution representative radiative-convective model to compare production under different temperature and humidity regimes.

Another issue that is mentioned occasionally in the literature (for example, *Goody* [2007] and *Paillard and Herbert* [2013]) is the distinction between the average of the entropy and the entropy of the average. Because of the diurnal cycle, the actual entropy production cannot be captured by considering the production of some temporally-averaged snapshot. This also applies to seasonal fluctuations and spatial variations.

Researchers have also studied the entropy production by non-physical processes within climate models [*Woollings and Thuburn*, 2006]. *Johnson* [1997] connects this feature to the general coldness of climate models, a systematic under-estimation of certain climatic temperatures by models.

2.8   Connections beyond entropy

Many researchers have sought to map Earth's entropy rate to other simplifying frameworks. Oft-mentioned is the Lorenz Energy Cycle [*Lorenz*, 1960], in which the climate is viewed as a heat engine converting between thermal, potential and kinetic energies such that the maximisation of entropy production is related to an efficiency in the conversion of potential to kinetic energy, as reviewed in *Johnson* [1997]. Other work taking up this topic can be found in *Lucarini* [2009], *Lucarini et al.* [2011] and *Lucarini et al.* [2014]. *Laliberté et al.* [2015] also examine the climate heat engine, but using a high-resolution output from climate models to map convection cycles on thermodynamic diagrams.

More recently, it has been pointed out [*Reis*, 2014] that entropy production maximisations and minimisations might occur as a consequence of a maximally efficient energy flow. This is returned to in Section 6.4.2.

2.9   Mistakes and disagreements

Reading the papers in this field, it is remarkable how many of them point out mistakes or misunderstandings in a paper that came before. Even the first [*Paltridge*, 1975] paper was quickly followed by a comment [*Rodgers*, 1976] that noted that Paltridge had been minimising the negative of the entropy production rate, so had actually found a maximum.

The most common mistake, which has been surprisingly persistent, is in how the entropy flux in radiation is calculated. For a black body radiating towards a vacuum, the radiation carries entropy as $\frac{4}{3}\sigma T^3$, while the material loses entropy at σT^3. This has been explained correctly many times, in the original *Planck* [1914] and recently re-derived in *Wu and Liu* [2010a], and yet continues to be incorrectly applied, as in *Peixoto et al.* [1991], *Ozawa et al.* [2003], *Fraedrich and Lunkeit* [2008] and *Pascale et al.* [2011a]. A very clear derivation of the $4/3$ factor is given in *Feistel* [2011].

More flags are raised in passing: for example, *Peixoto et al.* [1991] refer to entropy 'destruction' in their abstract, which is impossible in the strictest sense, since entropy cannot decrease. Sometimes these are seemingly-minor details: in *Ozawa and Ohmura* [1997], the first term on the right-hand side of equation (4) is labelled as the rate of entropy increase in space, but is actually that in the atmosphere; in *Bannon* [2015], the definition of his MS3 in Equation (2.10) and (2.11) introduces a sign error. Sometimes they are more fundamental misunderstandings, as in *Ozawa and Ohmura* [1997] where it is stated that "when we consider the universe, the isolated system including the earth-atmosphere system, space, and the sun, the entropy in the universe is increasing by a contribution of the thermal convection (the general circulation)", which is untrue because (as will be explored in Section 4.5.2) the radiation incident on and reflected and emitted from the planet captures the impact of the Earth on the universe's entropy production rate and is not directly dependent on the quantity

of entropy produced by the internal processes such as circulation.

There are many more examples of these kinds of lack of clarity in the climate entropy production literature. They evidence a field which which is tentative about its basic understandings and where it is difficult to rely on the conclusions and arguments in other published papers.

2.10   Opinions about entropy research

The story about the climate's entropy production rate that makes it into the published literature is necessarily relatively polished, measured and hopeful. This is in quite striking contrast with the anecdotal evidence I have gathered in discussion with the scientists who are currently working or have worked in the field in the past, and from taking an overview of the literature as a whole. According to my tabulation, there have been 199 papers published[1] on the topic of entropy production in the Earth climate, authored by 193 scientists. The vast majority of these researchers (144) have appeared only on one publication, demonstrating a curiosity with and then dispersal from the field. Of the 49 who have published more than once, I have spoken informally with ten (anonymised here). I have also had countless discussions with other climate scientists who have a more external perspective on the field.

From these conversations, some strong themes in the sentiment towards the climate entropy field have emerged. Among scientists who have worked on entropy, there is often a lot of exasperation, confusion, fatigue and pessimism when talking about the particulars of research design and results, which contrasts with a hopeful glimmer which emerges at the idea of what an organisational principle like entropy could mean for our understanding of the climate. Between those on the inside, there is pervasive scepticism and criticism of the quality of other researchers' work, either as being too imprecise or bombastically over-concluding, or as misunderstanding the essential, most significant features of the problem. Researchers are also often critical of their own work when discussing it informally, expressing that they had had to let go of the aim of really elucidating and had published an increment that, though it might be true, left them confused. Many researchers I spoke to had given up on the field or were pessimistic about whether there was a thesis-worth of useful work to be done, feeling it was intractable and that more mainstream scientific questions were more likely to bear fruit.

This was not dissimilar to the analysis of the situation by scientists from outside the topic area. There, among both the well-established and the novices, there is a sceptical-yet-intrigued curiosity. Entropy, and especially how to see it in the climate, is often only vaguely understood, but comes with a definite appeal for those looking for elegance in the climate system. However, the confusion about the concepts presents a barrier to actual engagement with the ideas, and there is a mistrust in the broader climate science community about the research conducted by those within the entropy production field being over-sold and under-scrutinised.

---

[1]This is likely an under-estimate, but I do not think the true number could be larger than about 220.

This sense of the topic area as being enticing but also a dead-end seems to stymie more concerted research into it, siloing it from the mainstream in climate science and scattering it to individual researchers or groups who return to and question fundamentals rather than building neatly on each other, limiting both the kind of work that is done and the kind of researchers who are willing to undertake it. Many researchers who work on entropy are quite independent thinkers who feel motivated to question the status quo, and at least two in the top 20 are even vocally sceptical of anthropogenic climate change. Entropy production seems to be something of a focal point for researchers willing and curious to leave the more well-trodden lines of research, not necessarily because of evidenced potential for answers but because of the tantalisingness of the questions it raises. This is also reflected in what the introductions of the published papers expound as motivation.

How might this influence how we ought to interpret and contribute to the topic? Firstly, it suggests that the often-frustrating messiness of the topic is a real, unavoidable feature created by the confusion of the researchers who have produced it, and therefore, a pragmatic acceptance of this unsatisfying state of affairs is needed. It secondly underlines that much of the work to be done is in making sense of the fundamentals and defining ways of contributing: these are far from established and are the loci of important ongoing debate. Thirdly, it suggests to me a need for suspending both hope in the promise of MEPP and trust in the published results that have come from such motivated thinking: researchers have clearly wanted something to come out of Paltridge's observation, and those with more scepticism have simply avoided working on the field so that the literature is not necessarily a balanced encapsulation of the scientific views. And finally, it provides reassurance that we also need not place high credence in the wider climate field's dismissal of the potential of entropy production in the study of the climate (e.g. *Caldeira* [2007]), as it is based on a limited connection to and comprehension of the topic.

2.11 Paths forwards

Armed with this picture of how the topic of entropy production and the climate came to be and how it sits as a topic of scientific research, we turn our attention to the question of most relevance to this thesis: how might one contribute to this field?

2.11.1 Facts

To address this, it is useful first to return to and consolidate the reliable facts from the literature. This is non-trivial because of the general confusion and lack of a common narrative, and the prevalence of conceptual and techincal errors.

The following are most reliably known:

- For free-to-vary meridional heat transport given prescribed incoming solar flux and energy emitted in proportion to a representative temperature, entropy production maximisation does a strikingly good job of recovering the observed meridional heat flux and temperatures [*Paltridge*, 1975]. This has not worked as well in the vertical [*Pujol and Fort*, 2002; *Pascale et al.*, 2012].

- There are many ways in which the earth is not at its maximum entropy production rate, for example because it does not have a constant emission temperature [*O'Brien and Stephens*, 1995].

- There have been successful measurements made of the magnitude of different entropy production rates due to different processes. Kinetic energy generation and dissipation accounts for approximately 25% and the hydrological cycle 70% [*Pascale et al.*, 2011a] of the non-radiative component. A smaller fraction $(10-15\%)$ of this non-radiative entropy production is due to processes in the horizontal compared to the vertical [*Pascale et al.*, 2012]. The thermalisation of solar radiation accounts for far more entropy production than the processes which occur on Earth [*Stephens and O'Brien*, 1993].

- Although there have been attempts, there is not yet a theoretical understanding for why MEPP might work.

These can also be found discussed in the published reviews of the field, including *Ozawa et al.* [2003]; *Whitfield* [2005]; *Martyushev and Seleznev* [2006]; *Kleidon* [2009]; *Dyke and Kleidon* [2010]; *Kleidon* [2010]; *Liu et al.* [2011] and *Lucarini et al.* [2014].

2.11.2   Lines of research

In this thesis, I will focus on three lines of inquiry that are familiar from the literature but on which there remains significant work to be done. The first concerns the concept of a climate-relevant global entropy production rate and the breadth of possible interpretations that result in variables that are more and less well-suited to a possible MEPP theory or for use in understanding our climate (Chapter 3). The second considers the features of a climate's state that entropy production rates pick up on, as investigated by varying the climate's features and boundary conditions and studying how the entropy production rate variables respond (Chapter 4). The third (Chapter 5) involves the building of tools for entropy budgets of observations and GCM outputs, particularly by improving on the work in *Kato and Rose* [2020], and offering a preliminary exploration of new patterns in the climate's entropy production rate.

These projects do not directly attempt to respond to or apply the MEPP hypothesis (which is instead returned to in Chapter 6), but are fundamental to developing our understanding of the climate's entropy production rates as concepts, variables and numbers. Even after 45 years of study, we are not yet on a stable foundation with respect to these basics in entropy production. It is precisely because it is an unorthodox field taking an unusual

approach to the study of our climate system that it has been so chaotic and muddled and yet is so potentially pivotal and significant in our study of the climate, and why I feel this return to the heart of the question is a promising scientific avenue.

Chapter 3

A New Definition of a Global Entropy Production Rate

No scientific theory can be crafted without clear definitions of its variables. The global entropy production rate has been a persistently ambiguous concept: there has been much debate and reinterpretation over the history of this subject, often introduced as 'corrections' to previous omissions. Although there have been cases of mistakes which have made some of the proposed definitions inconsistent, *there are also multiple self-consistent perspectives which give rise to fundamentally different global entropy production rates*, which all belong, in some sense, to the climate. Since the entropy production rate is an extensive variable, they differ in how they define the system of interest: the more included within the system, the larger total entropy production rate.

After an introduction to the premise of entropy production in a steady, open system, in Section 3.1, we focus on the specific case of the entropy production in the climate in Section 3.2. A careful framework is presented which makes sense of three possible interpretations of the climate's extent and so three global entropy production rates. Two of them, the *material* and *planetary* entropy production rates, are well-studied in the literature. The third, which we label the *transfer* entropy production rate, is a relatively new framing, building off work by *Bannon* [2015] and *Bannon and Lee* [2017]. This previously unappreciated transfer entropy production rate[1] is significant because there are arguments to suggest that it is more physically meaningful than the existing two global entropy production rates, and so its introduction may open new lines of enquiry into the search for physical laws. The key contribution of this chapter is a careful definition and explanation of the transfer entropy production rate.

---

[1]The work in this chapter was published in *Gibbins and Haigh* [2020]. While that publication was under review, *Kato and Rose* [2020], which is discussed in more detail in Chapter 5, was published which, also building off Bannon's papers, makes measurements of the transfer entropy production rate, but without drawing attention to its significance.

3.1 Entropy production in a general driven non-equilibrium steady system

[A law] is more impressive the greater the simplicity of its premises, the more different are the kinds of things it relates, and the more extended its range of applicability. Therefore, the deep impression which classical thermodynamics made on me. It is the only physical theory of universal content, which I am convinced, that within the framework of applicability of its basic concepts will never be overthrown.

- Albert Einstein, quoted in M.J. Klein, Thermodynamics in Einstein's Universe, in Science, 157 (1967), p. 509.

The reliable thermodynamics to which Einstein refers above is *equilibrium* thermodynamics. Away from equilibrium, it is necessary to define further concepts, appealing, for example, to local thermodynamic equilibrium or statistical mechanics. In what follows, the approach to entropy production which is generally accepted in the climate literature is introduced (Section 3.1.1). The important distinction between entropy *fluxes* and *productions* is emphasised in Section 3.1.2, and in Section 3.1.3 in particular as it relates to radiation. An instructive analogy to the role of entropy production in living creatures in Section 3.1.4 builds intuition before the application of these concepts in the climate is covered in Section 3.2.

3.1.1 The premise

What is an entropy production rate? The Second Law of Thermodynamics states that the entropy of the universe increases due to every irreversible process, stopping only when equilibrium is reached. If these processes occur inside an isolated, closed system, that increase must be reflected in the entropy (S) of the system and they are said to have 'produced entropy' within the system at a rate Σ:

$$\frac{dS_{closed}}{dt} = \Sigma \geq 0 \qquad (3.1)$$

This can also be extended to systems which are open to certain cross-boundary fluxes but are steady, so their properties do not change over time and there is no net storage within the system (a common approximation for the Earth's climate). In terms of ease of thermodynamic analysis, steady systems are second only to equilibrium systems: since their internal attributes are fixed, they can be analysed via the flow across their boundaries without the need for detailed knowledge about the interior. In engineering applications, for example in power plant design, these situations are standard and they are described via fixed control volumes around the region of interest.

For a conserved quantity, such as total internal energy U, in a steady system there must be a balance between

the fluxes, F, into and out of the control volume:

$$\frac{dU_{open,\,steady}}{dt} = 0 = F_{in} - F_{out} \tag{3.2}$$

This feature is already well-mobilized for simplifying, constraining and explaining aspects of the climate system, as in energy balance models and the concept of radiative forcing.

However, as entropy can be created within the system but not destroyed, a different kind of balance emerges: the cross-boundary flow must carry a net outwards flux of entropy ($J_{out} - J_{in}$) which equals the total internal production rate, Σ:

$$\frac{dS_{open,\,steady}}{dt} = 0 = J_{in} - J_{out} + \Sigma. \tag{3.3}$$

which may be presented graphically:
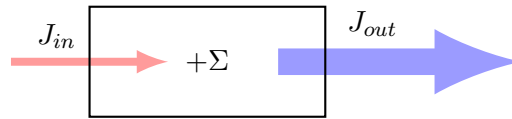
This total entropy production rate can be identified [*Peixoto et al.*, 1991] 'directly' by summing the local entropy productions (σ_i) due to all the irreversible processes which occur within the system:

$$\Sigma = \sum_i \sigma_i. \tag{3.4}$$

or 'indirectly' (but arguably more straight-forwardly) as the difference of the cross-boundary entropy fluxes, relying on the steady state assumption:

$$\Sigma = J_{out} - J_{in} \tag{3.5}$$

This is a potentially-useful identity: although entropy is produced across a wide variety of processes within the system, the total production must be exactly exported by the cross-boundary fluxes in steady-state.

If there is storage within the system, the steady-state assumption breaks down and $\Sigma = \left(J_{out} + \frac{dS_{stored}}{dt}\right) - J_{in}$. This is the case transiently during diurnal and seasonal cycling and systematically for a warming planet, so the results derived here for a steady system would need to be corrected with this in mind (see Section 5.4). However, as a first-order approximation, a steady climate is a very useful model for establishing the concepts and complexities.

3.1.2   Productions and fluxes

There is an important distinction to be made between an entropy *flux*, which moves entropy and energy *across* the boundary, and a *production*, in which transfer of energy *within* a system creates entropy within a system.

Heat delivered at rate F to material at a local temperature T supplies entropy there at a rate $J = F/T$, which is identified as an inward entropy flux, and similarly for energy leaving. By contrast, when heat flows from a T_{hot} to a T_{cold} within a system,
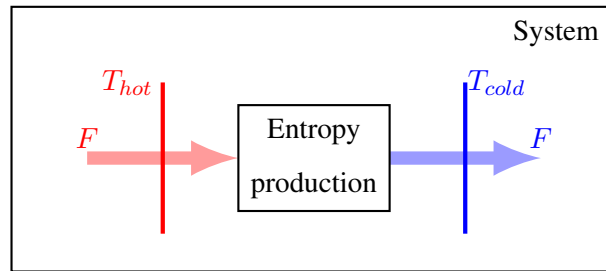
there is an entropy production associated at a rate $\sigma = F(1/T_{cold} - 1/T_{hot})$ (provided that the mechanism which mediates the transfer is returned to its original configuration). As they are the difference of two fluxes, production rates are usually much smaller in magnitude.

Any entropy flux and paired energy flux can be immediately rearranged to recover an entropic average temperature, $T := F/J$, even if the locations of energy delivery or extraction are not isothermal. This is a useful concept as it defines the average quality of the energy at the point of entry or exit from the system. The inflow and outflow temperatures, $T_{in} = F/J_{in}$ and $T_{out} = F/J_{out}$, are sometimes combined into an 'efficiency' $\eta = (T_{in} - T_{out})/T_{in}$, as in the Carnot efficiency for the maximum work per unit heat input which can be extracted by a reversible engine operating between two fixed temperatures. However, the value does not represent work extracted in this case as there is no mechanism for any extraction[2] but instead can be interpreted as a summary metric of the irreversibility of the system or the "lost work" [*Bannon*, 2015]. The total entropy production rate of the system is related to the temperatures, efficiency and energy flow by $\Sigma = F(1/T_{out} - 1/T_{in}) = F(\eta/T_{out})$.

In this way, an entropy production rate can be cast in terms of an energy flux and *two* representative temperatures, but these are not always straightforward to identify: for example in the case of the irreversible evaporation, diffusion or precipitation of water. However, if these irreversible processes are considered together so that their net effect is only a heat transfer (i.e. the mass of water in each phase and location is steady by their combined effect) the amount of energy and the average temperature from and to which the heat is transferred can be calculated. This is generalisable: for a steady system, it is useful to separate those components which do not cross systems boundaries (i.e. water), and so can neither store nor transport entropy from the system, from those which do. The former are catalytic, they move around the system but only as a conduit, with the consequence of moving those quantities which cross the boundary (i.e. heat energy) down-gradient.

This leads to one of the most clear distinctions[3] between productions and fluxes: production within a system is

---

[2]This is an issue which is often missed in applications of the Carnot cycle to the climate system. A thorough discussion of how the recycling of work within the climate system invalidates the Carnot efficiency limit is given in Appendix A.1.

[3]In some places in the literature, both a flux and a production are termed production, because the flux of energy into the system

due to heat moving *from* hot and *to* cold while cross-boundary fluxes deliver heat *to* hotter locations and extract it *from* colder. These opposite roles balance each other in a steady system.

In some cases, the boundary-crossing process will itself be irreversible, causing a production which coincides with the cross-boundary flux. A simple case of this is delivery of heat at a rate F from a surrounding at $T_{surr} > T_{sys}$ to a system:

$$T_{surr} \quad | \quad T_{sys}$$

$$F \longrightarrow$$

$$J_{surr} \longrightarrow \quad J_{sys}$$
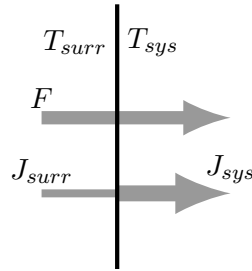
The surroundings experience a loss of entropy at rate $J_{surr} = F/T_{surr}$ while the system experiences an entropy gain due to the same energy flux of $J_{sys} = F/T_{sys} > J_{surr}$. The irreversible transfer of heat from warmer surrounding to system has caused a production of entropy of amount $J_{sys} - J_{surr} = F\left(1/T_{sys} - 1/T_{surr}\right)$. However, this production does not occur within the system - for accurate analysis of the entropy production rate *of the system*, the flux J_{sys} is the appropriate one to use. Why? Suppose that the temperature T_{surr} changed but the thermal conductivity at the boundary also changed to compensate so the rate of energy delivered to the system, F, was preserved. The system would not 'notice' any change, although J_{surr} is different. For analysis of the system, the unchanged J_{sys} is the variable of interest.

3.1.3   Irreversibility in the absorption and emission of radiation

In the climate, the irreversibility in the emission and absorption of radiation often leads to an entropy production which coincides with a cross-boundary flux and so requires particularly careful treatment.

When two sources of the same temperature radiate towards each other the creation of outgoing photons balances the absorption at the surface of each and the process is reversible[4]. When, on the other hand, the characters of the incoming and outgoing photon gases are different because the two sources are of different temperatures, there is an irreversibility. No matter the nature of the incoming radiation, the outgoing emitted radiation is set by the material's characteristics and temperature, and the system cannot be reversed. Heat will flow from the hotter to the cooler, by the Second Law.

---

increases its entropy when it is delivered (see, for example, *Kato and Rose* [2020]). However, the flux of energy out of a system reduces the entropy where it leaves, which would have the unfortunate interpretation as being a negative 'production', which makes this nomenclature less desirable.

[4]This applies even if the spectral absorptivity of the materials differ, thanks to the role of reflection.

As elegantly explored in *Feistel* [2011], this criterion is sufficient to establish that the outgoing radiation must carry a different entropy flux than the loss experienced by the material source. In the case of black body radiation towards a vacuum, the radiation carries entropy $J_{rad} = \frac{4}{3}\frac{F}{T_{mat}}$, compared to the entropy leaving the system of $J_{mat} = \frac{F}{T_{mat}}$. The higher entropy of radiation can be calculated by integrating $dS = \frac{dQ}{T}$ as photons are added one by one to a vacuum, which initially is at 0 K. The derivation of the more general result for the entropy carried in radiation of any wavelength from a statistical physics approach is given in *Planck* [1914] and summarised in *Wu and Liu* [2010a].

3.1.4   Entropy production in biology

The consumption of food by animals is an instructive example of entropy production in a familiar system.

Why do we eat? It isn't just to gain energy: energy is conserved, but there is little doubt that isolating an animal adiabatically from its surroundings is not a substitute for feeding them. In order to stay alive, creatures require a *flow* of energy through our system from high-quality (low-entropy) food to low-quality heat, respired matter and waste (higher entropy). This allows a body to restore itself to an initial configuration, introducing the ability to do work to reverse the irreversible entropy-producing activities which are part of being alive, such as the diffusion in a neuron's firing or the friction as flowing blood slows down against artery walls or the work a creature might do in its surroundings. At death, this restoration ceases and entropy increases towards the well-mixed maximum. A living creature is one which uses a flow of energy through its system to maintain its present configuration against the entropy production happening internally. Food is a low-entropy flux of energy into the system which allows for the internal entropy production to be exported in high-entropy energy returned to the surroundings.

Biological systems are different from the climate in that they have evolved precisely to maintain themselves (and replicate) in their particular out-of-equilibrium state. Entropy production considerations may in fact play a role in explaining the origin of life [*England*, 2013]. Although the selection pressures in biology are necessarily different from those which act on the climate, the climate as we observe it has strong analogues to the way a living being functions, but consuming sunlight instead of food.

3.2   Entropy production rates in the climate

3.2.1   Overview

As energy flows from the sun, into the solar photons, then through the earth system, back into longer wavelength photons and out of the solar system again, its quality decreases and the entropy per unit energy increases. This is shown diagrammatically in Figure 3.1.
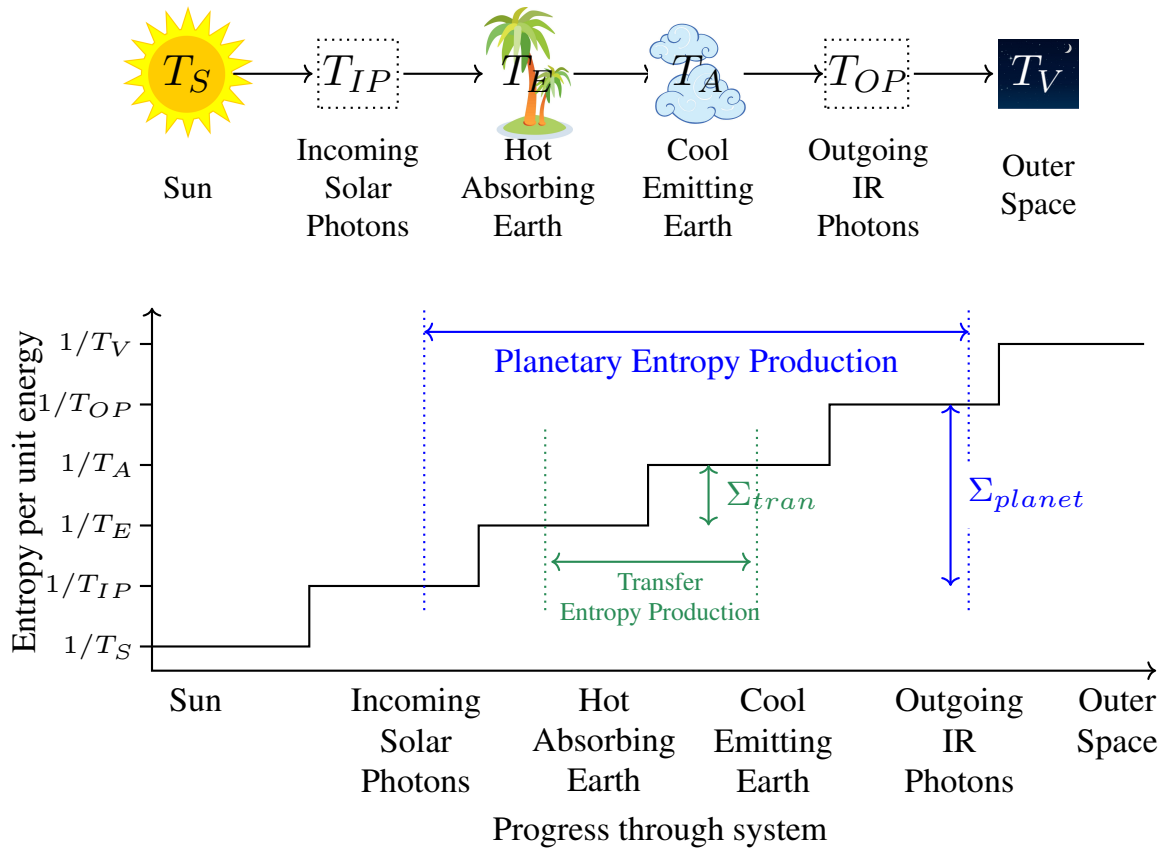
Figure 3.1: A schematic showing the increase in entropy as energy flows from the sun, through earth and ultimately back to outer space. The entropy increase of the universe due to the flow of photons from the sun to outer space (where we assume they are ultimately thermalised) is the same whether or not a planet intercepts the solar photons on their way. We are interested in the entropy production of the climate system, for which there are three proposed interpretations. The larger two, the planetary and transfer entropy production rates, are labelled. *Diagram inspired by Kleidon and Lorenz [2005], Figure 1.1. Note that the y-axis steps are not to scale.*

For the universe, the total entropy production as the energy flows from the sun to outer space (assuming the photons are eventually thermalised) is the same whether or not there is a planet mediating some of that transition. The planet intercepts this flow and harnesses some of the entropy production on Earth, harnessing it to maintain the motion of the atmosphere, oceans and life. Which portion of the entropy production should we take as 'belonging to' the climate system?

I would propose that there are three self-consistent boundaries of the climate system that stem from adopting different approaches to the treatment of radiation. These perspectives give different extents of the system, not in terms of physical space (all extend from the lithosphere to the upper atmosphere) but in terms of how and when radiation or heat crosses into and out of the system:

Planetary: photons carry entropy and energy into and out of the system as they cross a control volume surface beyond the top of the atmosphere.

Transfer: energy enters the system when it is first absorbed by matter on its way from the sun and leaves when it is last emitted on its way to space.

Material: energy is only in the system when it is thermalized in matter, not as photons.

The first two are shown diagrammatically in Figure 3.1. The transfer and material cases are difficult to describe with a control volume boundary in physical space, but they are nested (listed here from large to small), have well-defined and different cross-boundary entropy fluxes and therefore include different sets of irreversible processes. Each measures a different global entropy production rate, although they all, in some sense, describe 'the climate'. This section explains their development, definitions, distinctions, and interpretations; the choice remaining for scientists trying to use entropy production rates as a predictive or diagnostic variable will be which is most physically meaningful and useful. This question is taken up via various lines of reasoning throughout the rest of this thesis.

3.2.2 Energy balance model

Energy balance models (EBMs) are well-suited to summarising the entropics of the climate because they focus on the two key subsidiary variables: energy and temperature.

In order to further explain the definitions of the three entropy production rates and to give preliminary estimates of their magnitude, they are demonstrated in an EBM which has been adapted from *Bannon* [2015] and is shown graphically in Figure 3.2.

The model broadly echoes the familiar global energy budget diagrams of *Wild et al.* [2015], but with a non-standard rearrangement of the radiative energy flux labelling to separate the internal radiation (net flux between surface and atmosphere) from external radiation (fluxes which leave to or enter from the surroundings), reminiscent of the Net Exchange Formulation discussed by *Herbert et al.* [2011]. The two material terms - latent and sensible heating - should be taken as placeholders for the full range of non-radiative heat transfer mechanisms (e.g. creation and dissipation of kinetic energy in the general circulation) which occur in the real system. For simplicity, heat from the planetary interior and the irreversibility of life are not treated here, but the definitions could be adapted to include them.

The model can be solved analytically to give the surface and atmosphere temperatures as a function of albedo, emissivities and latent and sensible heat flux. I have used the same parameter values as *Bannon* [2015] to allow for comparison with those previous results.

The incoming solar flux is $F_{sun} = 340.7$ W/m^2 with a fixed albedo of $\alpha = 0.30$ and a solar temperature of $T_{sun} = 5779$ K. Therefore $F_{SW}^{scat} = \alpha F_{sun} = 102.2$ W/m^2. The atmospheric absorptivity in the shortwave is $\beta = 0.10$, which sets $F_{SW}^{atm} = \beta F_{sun} = 34.1$ W/m^2 and $F_{SW}^{surf} = (1 - \alpha - \beta)F_{sun} = 204.4$ W/m^2, where
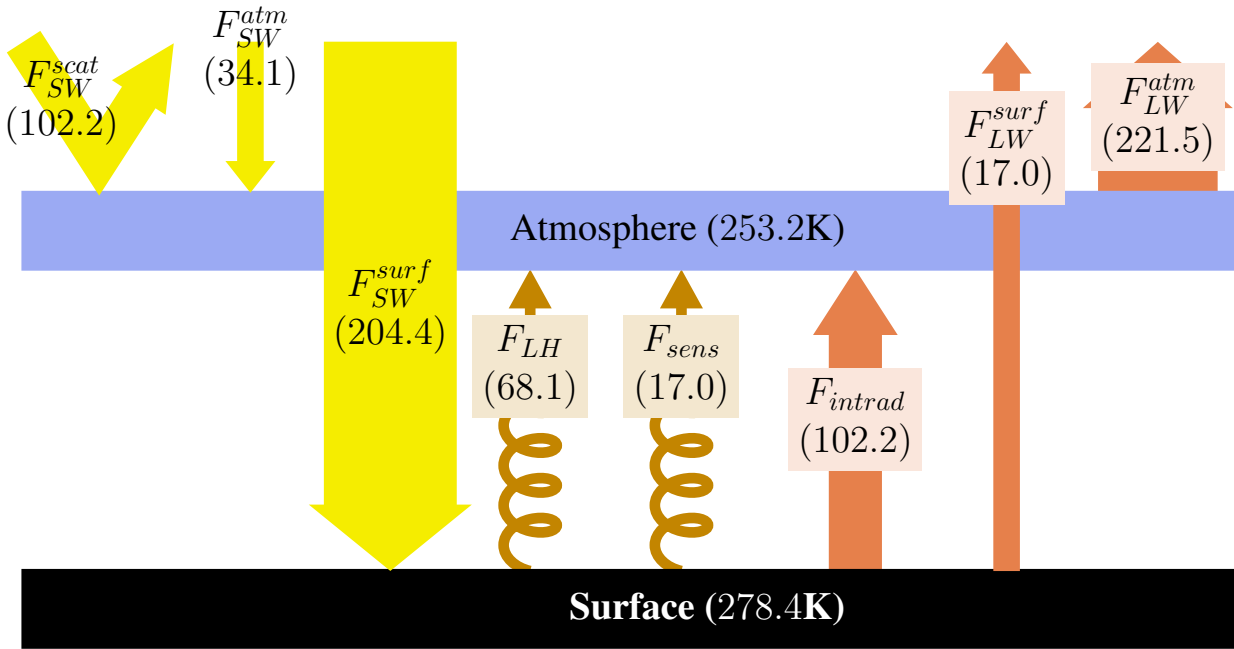
Figure 3.2: The energy balance model which will be used to demonstrate the possible entropy production rates and fluxes. The calculated value of fluxes are shown in units of W/m^2, as is the atmospheric and surface temperature. The model is based on that used in *Bannon* [2015] and the values match.

the issue of surface scattering and subsequent absorption by the atmosphere has been neglected, following *Bannon* [2015]. The surface-atmosphere material heat fluxes are represented by a sensible and a latent heat term which transfer heat as a fraction of the incoming solar flux: $F_{sens} = \gamma_{sens} F_{sun} = 17.0$ W/m^2 and $F_{LH} = \gamma_{LH} F_{sun} = 68.1$ W/m^2 where $\gamma_{sens} = 0.05$ and $\gamma_{LH} = 0.2$, approximately following the energy budget of *Wild et al.* [2015] such that the total $\gamma = 0.25$ matches *Bannon* [2015]. The emissivity of the atmosphere is $\epsilon = 0.95$ and so $F_{LW}^{atm} = \epsilon \sigma T_{atm}^4$, while the surface is a black body such that $F_{surf} = \sigma T_{surf}^4$. Requiring an energy balance for the surface and atmosphere gives the temperatures $T_{surf} = 278.4$ K and $T_{atm} = 253.2$ K. From these, the values of the longwave energy fluxes can be found[5]: $F_{intrad} = \epsilon \sigma T_{surf}^4 - \epsilon \sigma T_{atm}^4 = 102.2$ W/m^2, $F_{LW}^{surf} = (1 - \epsilon)\sigma T_{surf}^4 = 17.8$ W/m^2 and $F_{LW}^{atm} = \epsilon \sigma T_{atm}^4 = 221.5$ W/m^2, as demonstrated in *Bannon* [2015].

3.2.2.1   Entropy production of sub-processes

In the EBM, the entropy production due to each energy transfer process can be calculated based on the energy flow and temperature difference between which it acts.

In general, the entropy production due to an internal heat transfer at a rate F between temperatures T_{hot} and T_{cold} is:

$$\sigma(\text{internal heat transfer}) = F\left(\frac{1}{T_{cold}} - \frac{1}{T_{hot}}\right) \tag{3.6}$$

---

[5]It is coincidental that the internal radiative heat transfer is the same value as the scattered energy

which applies both to the material and to the internal radiation heat transfers. The spectral character of the internal radiation need not be accounted for in the entropy production term because both the creation and destruction of those photons happen within the planetary boundaries; only the resultant heating is relevant.

For the external radiation, we assume a black body spectrum to allow for straightforward estimation of the entropy content of the radiation, as discussed in Section 3.1.3. The absorption of radiation results in an entropy production which is the difference between the entropy of the heat in the material and in the radiation:

$$\sigma(\text{absorb}) = \frac{F}{T_{mat}} - \frac{4}{3}\frac{F}{T_{source}} \tag{3.7}$$

and is the reverse for emission. For black body emission, the temperature of the relevant material T_{mat} will also be the source temperature T_{source}.

These principles can now be applied to the EBM to calculate the entropy production rates for each aspect, as summarised in Figure 3.3.
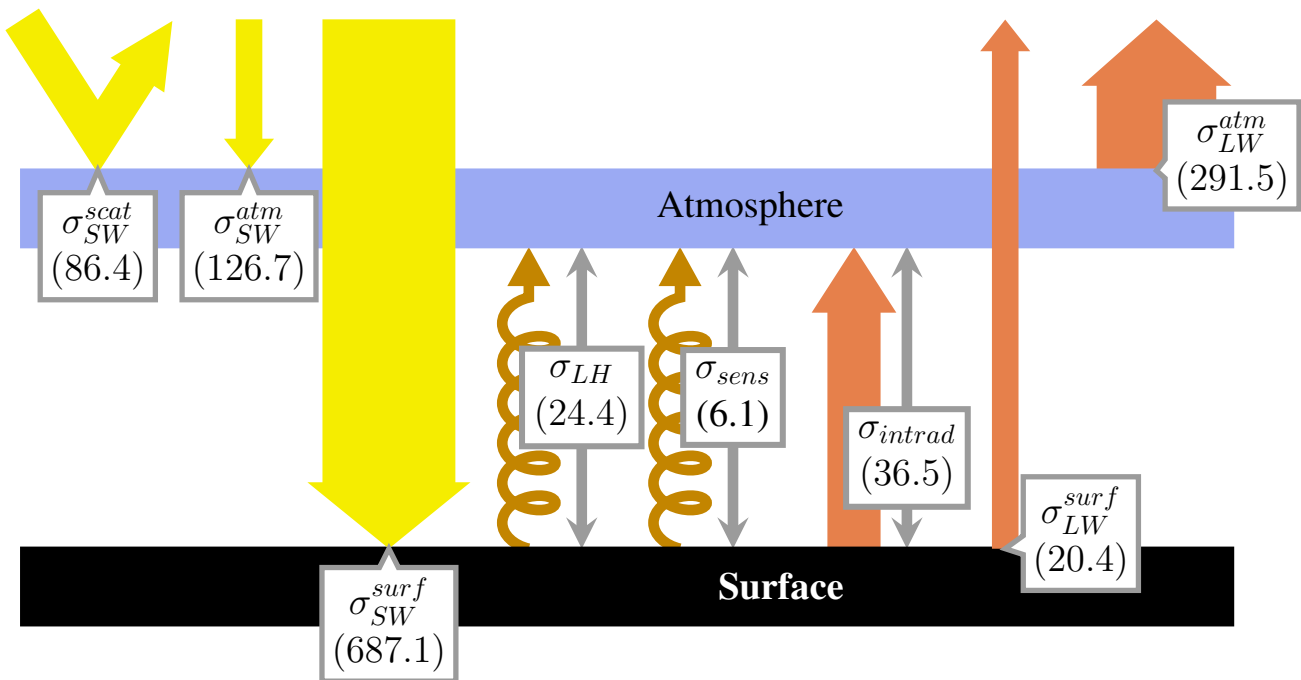
Figure 3.3: Each irreversible energy transfer within the system produces entropy at a rate which can be calculated from knowledge of the temperatures and energy fluxes. The values quoted are in mW/m²K.

The entropy produced upon scattering is generally a function of the change in directional intensity of the radiation. Following *Bannon* [2015][6] and *Wu and Liu* [2010a], $J_{scat} = 110.0$ mW/m²K so that the production

---

[6]There appears to be an inconsistency between the formula for scattered entropy flux given in *Bannon* [2015] on page 3274 and the value found. So that our results are consistent, we used their value for J_{scat} rather than the formula, which is also consistent with *Wu and Liu* [2010a].

rate is:

$$\sigma_{SW}^{scat} = J_{scat} - \frac{4}{3}\frac{F_{scat}}{T_{sun}} = 86.4 \text{ mW/m}^2\text{K}.$$

The thermalization of solar radiation in the atmosphere results in an entropy production of:

$$\sigma_{SW}^{atm} = F_{SW}^{atm}\left(\frac{1}{T_{atm}} - \frac{4}{3T_{sun}}\right) = 126.7 \text{ mW/m}^2\text{K}$$

and similarly, thermalization of solar radiation at the surface is:

$$\sigma_{SW}^{surf} = F_{SW}^{surf}\left(\frac{1}{T_{surf}} - \frac{4}{3T_{sun}}\right) = 687.1 \text{ mW/m}^2\text{K}.$$

The material transport of heat from the surface to the atmosphere results in much smaller entropy productions proportional to the reciprocal temperature difference,

$$\sigma_{sens} = F_{sens}\left(\frac{1}{T_{atm}} - \frac{1}{T_{surf}}\right) = 6.1 \text{ mW/m}^2\text{K}$$

$$\sigma_{LH} = F_{LH}\left(\frac{1}{T_{atm}} - \frac{1}{T_{surf}}\right) = 24.4 \text{ mW/m}^2\text{K}$$

as does the net transport of heat from the surface to the atmosphere via internal radiation,

$$\sigma_{intrad} = F_{intrad}\left(\frac{1}{T_{atm}} - \frac{1}{T_{surf}}\right) = 36.5 \text{ mW/m}^2\text{K}.$$

Emission of longwave radiation from the surface results in an entropy production because the radiation carries more entropy than the cooled matter loses. For the emission from the surface:

$$\sigma_{LW}^{surf} = F_{LW}^{surf}\left(\frac{4}{3}\frac{1}{T_{surf}} - \frac{1}{T_{surf}}\right) = 20.4 \text{ mW/m}^2\text{K}$$

and for the emission from the atmosphere:

$$\sigma_{LW}^{atm} = F_{LW}^{atm}\left(\frac{4}{3}\frac{1}{T_{atm}} - \frac{1}{T_{atm}}\right) = 291.5 \text{ mW/m}^2\text{K}.$$

3.2.3   The planetary entropy production rate

As discussed in Section 2.1, the original entropy production rate put forward by Paltridge [*Paltridge*, 1975] was interpreted as the meridional heat transfer rate by *Paltridge* [1978]; *Nicolis and Nicolis* [1980]; *Grassl* [1981]; *Wyant et al.* [1988], among others. The first suggestion of a more global quantity was made by *Essex* [1984] who contended that Paltridge's entropy production rate was a fundamentally "incorrect" quantity as
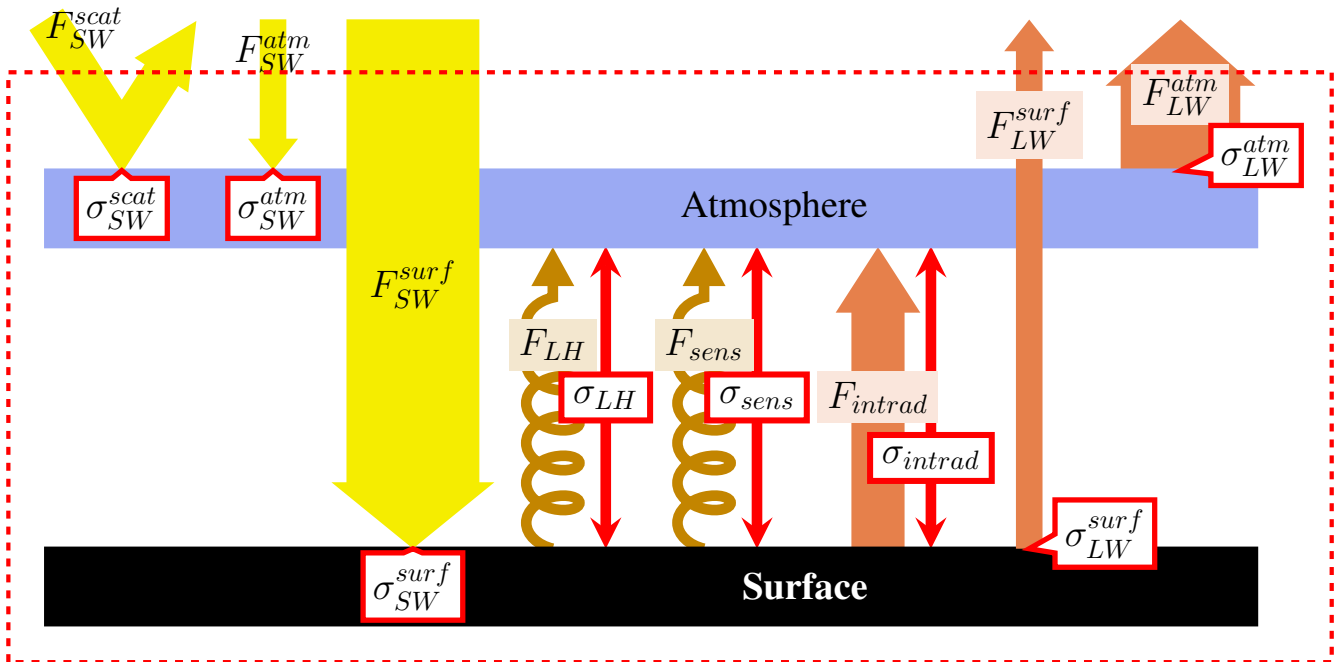
Figure 3.4: The planetary entropy production rate refers to the production due to all processes which occur between the top of the atmosphere and the lithosphere. The cross-boundary fluxes are radiation entering from the sun, scattered and re-emitted to space from the earth.

it had failed to account for entropy production in the radiation field. The Second Law, he argued, makes no distinction between entropy produced in material or radiation and so neither should an entropy production rate of the climate engine. In doing so, Essex introduced the quantity which we label here as the *planetary entropy production rate*: "the entire entropy production of a steady state climate is contained in the difference of the entropy of the outgoing terrestrial radiation from the entropy of the incoming solar radiation", as indicated in Figure 3.1. The planetary entropy production rate accounts for every irreversible process which happens within the planet's sphere of influence.

3.2.3.1 Definition

How is this concept formalised into a definition? The system is contained by a control volume which surrounds the planet somewhere above the top of the atmosphere and includes the entropy production due to all irreversible processes which happen within it, radiative or otherwise. The flux of entropy into and out of the system is carried by the photons flowing across the boundary of this control volume, carrying with them entropy according to the properties of a photon gas. This is shown schematically in Figure 3.4.

To measure the entropy flux in the radiation as it crosses the boundary accurately, the spectral entropy (L_ν) associated with the flow of photons of frequency ν (units of $1/s$) can be calculated as a non-linear function of

their spectral intensity I_ν:

$$L_\nu = (1 + y)\ln(1 + y) - y\ln(y) \tag{3.8}$$

where

$$y = \frac{c^2}{n_0 h\nu^3} I_\nu. \tag{3.9}$$

Here c is the speed of light and the number polarization states $n_0 = 2$. Equation 3.8 can be derived by analysis of photons as a boson gas (*Planck* [1914], further developed by *Rosen* [1954]) or from the relationship $dL_\nu = dI_\nu/T$ where $I_\nu = B_\nu(T)$ is the spectral Planck function intensity which is integrated from zero to the relevant intensity [*Ore*, 1955].

The entropy flux is then calculated by integrating this over all wavelengths, in the inbound or outbound hemispheric directions and over the surface area of the planet:

$$J_{planet}^{in/out} = \int dA \int d\nu \int_{hemi} \cos\theta d\Omega \, L_\nu. \tag{3.10}$$

This entropy flux in radiation simplifies in the case of a black body to a simple dependence on source temperature T_{source}, as explained by *Planck* [1914] and *Essex* [1984] and demonstrated in the appendix of *Wu and Liu* [2010a]:

$$J_{BB} = \frac{4}{3}\frac{F}{T_{source}} = \frac{4}{3}\sigma T_{source}^3 \times SA \tag{3.11}$$

where SA is the surface area.

Defined directly in terms of the quantities labelled in the energy balance model, the planetary rate is the sum of all the entropy budget items, radiative and non-radiative (see Figure 3.4):

$$\Sigma_{planet} = \sigma_{SW}^{scat} + \sigma_{SW}^{atm} + \sigma_{SW}^{surf} + \sigma_{LH} + \sigma_{sens} + \sigma_{intrad} + \sigma_{LW}^{surf} + \sigma_{LW}^{atm} \tag{3.12}$$

Scattered solar photons carry much less entropy than those thermalized and re-emitted by the planet and so the albedo of the Earth is a key determinant of Σ_{planet}. The planetary perspective has been further subsetted in some entropy studies to give related variables, for instance by excluding the production from the fraction of the solar radiation which is scattered (CV2 in *Bannon* [2015]) or by focusing on only the production which occurs within the atmosphere [*Peixoto et al.*, 1991]. These may be interesting quantities, but the definition given here is the one relevant to the global system.

This planetary rate has been explored widely in the literature, for example by *Lesins* [1990]; *Stephens and O'Brien* [1993]; *Pelkowski* [1994]; *Li et al.* [1994]; *Li and Chylek* [1994]; *Wu and Liu* [2010a] and is CV1 in *Bannon* [2015].

3.2.3.2 Estimation

The sun as a black body at temperature T_{sun} emits radiation which carries an entropy flux towards the earth of

$$J_{planet}^{in} = \frac{4}{3} \frac{F_{sun}}{T_{sun}} = 78.6 \text{ mW/m}^2\text{K} \tag{3.13}$$

and the outgoing radiation carries entropy according to its emission temperature,

$$J_{planet}^{out} = J_{scat} + \frac{4}{3} \frac{F_{LW}^{surf}}{T_{surf}} + \frac{4}{3} \frac{F_{LW}^{atm}}{T_{atm}} = 1357.7 \text{ mW/m}^2\text{K}, \tag{3.14}$$

such that the difference is the planetary production rate:

$$\Sigma_{planet} = J_{planet}^{out} - J_{planet}^{in} = 1279.1 \text{ mW/m}^2\text{K}. \tag{3.15}$$

This is exactly the same value as is calculated by adding the terms directly in equation Equation 3.12 and is also in agreement with *Bannon* [2015] for CV1.

The entropy fluxes can also be used to calculate representative temperatures via the relationship $T = F/J$ where $F_{planet} = 341$ W/m^2. Then $T_{planet}^{in} = 4334.2$ K and $T_{planet}^{out} = 250.9$ K, which are lower than the respective source temperatures because of the $4/3$ factor.

3.2.4 The material entropy production rate

The insight into the role of radiation in producing entropy which gave rise to the planetary perspective also laid the foundations for the division of the climate into non-radiative (material) and radiative sub-systems and to a separate tabulation of the entropy produced in each [*Essex*, 1987; *Goody and Abdou*, 1996; *Goody*, 2000].

By virtue of its connection with moving, tangible matter, the material perspective has been preferred for application of a maximisation principle, both in experimental and theoretical studies (e.g. *Ozawa and Ohmura* [1997]; *Ozawa et al.* [2003]; *Dewar* [2003]; *Fraedrich and Lunkeit* [2008]; *Wang et al.* [2008]; *Pascale et al.* [2012]; *Labarre et al.* [2019]). Researchers mapped Paltridge's meridional view to the *material entropy production rate* which includes contributions from horizontal and vertical sensible and latent heating (as established by *Pujol and Llebot* [1999]) as well as all other non-radiative processes. The contributions due to component processes have been considered separately (e.g. *Pauluis and Held* [2002a,b]; *Volk and Pauluis* [2010]; *Lembo et al.* [2019]), and it has been been linked to the conversion between potential and kinetic energy in the Lorenz Energy Cycle (for example *Lucarini et al.* [2011]) but also includes processes which are not related to motion, such as diffusion. In a moist atmosphere, the material rate is dominated by contributions from the hydrological cycle [*Pauluis and Held*, 2002a].

3.2.4.1 Definition

The material entropy production rate avoids dependence on the spectral properties of radiation and the solar temperature by excluding *all* radiative processes from the entropy tally. In this view, the system is exclusively the matter of the climate. The photon gas which permeates the atmosphere is considered part of the surroundings and radiative heating and cooling supply the cross-boundary fluxes of energy [*Bannon*, 2015]. The local temperature distribution of the material is unchanging under a steady state assumption and so the net heating of each parcel by material processes is balanced by radiative cooling to space or within the climate system, and vice versa [*Essex*, 1987; *Goody*, 2000].

In our EBM, the material rate can be directly specified as all non-radiative processes, as shown in Figure 3.5:

$$\Sigma_{mat} = \sigma_{LH} + \sigma_{sens}. \tag{3.16}$$
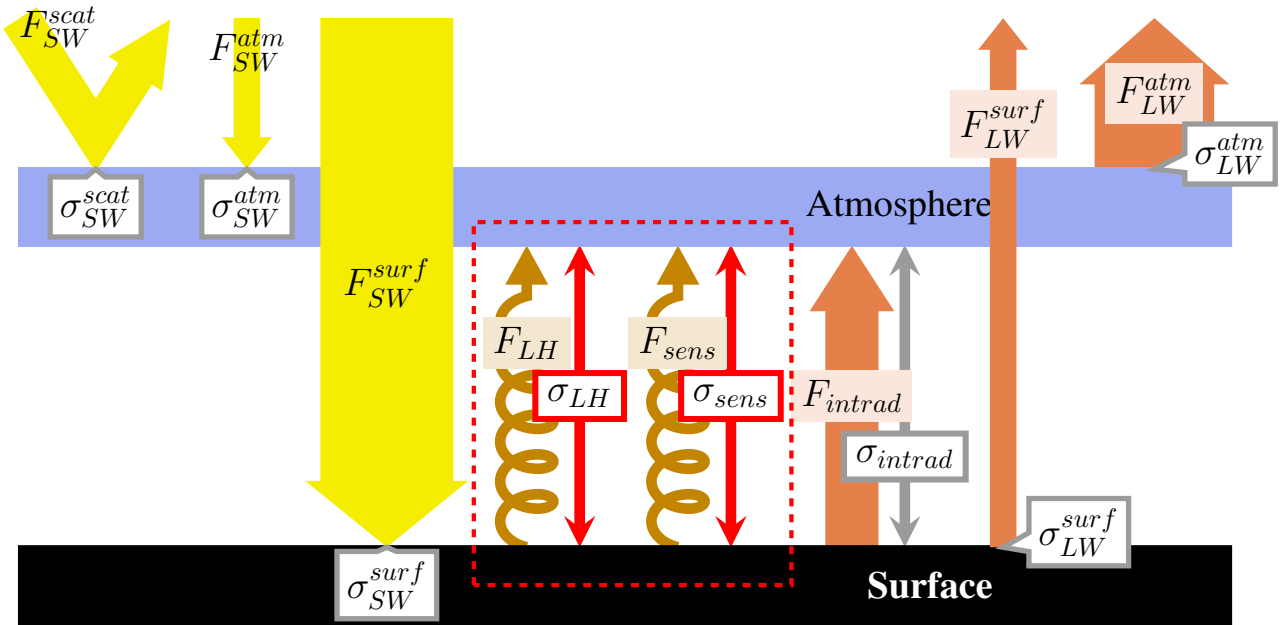
Figure 3.5: The material production rate refers to the production due only to energy transfers within the material of the climate by non-radiative processes. The cross-boundary fluxes are heating of the material supplied by radiation.

The material entropy production rate may be calculated indirectly from the net radiative heating rate, via the entropy flux into and out of the material system:

$$\Sigma_{mat} = J_{mat}^{out} - J_{mat}^{in} = \int dV \, \frac{\dot{Q}_{rad}(\mathbf{x})}{T_{mat}(\mathbf{x})}, \tag{3.17}$$

where $\dot{Q}_{rad}$ is the local radiative heating rate (in W/m^3) which is integrated to give the total heat flux into the system. T_{mat} is the temperature of the material where the heating or cooling occurs. There are multiple options for dividing this net radiative heating into a J_{mat}^{in} and J_{mat}^{out}. One approach is to separate the solar SW

heating from the LW radiative heating and cooling. Another is to separate areas of net positive Q_{rad} from net negative, which is the one we use here. These lead to different analyses of the energy, entropy fluxes, entropic temperatures and efficiency of the material system, but the same production rate, as discussed in detail in Appendix A.2.

Paltridge's original meridional heat transport entropy production rate can be interpreted as the horizontal component of the material entropy production rate, which has been estimated to be approximately $10 - 15\%$ of the total [*Pascale et al.*, 2012].

3.2.4.2 Estimation

To separate flux into and out of the system we take the approach of calculating the net radiative heating rate at each point and distinguish areas of net radiative heating (the surface) from net radiative cooling (the atmosphere):

$$J_{mat}^{in} = \frac{F_{SW}^{surf} - F_{LW}^{surf} - F_{intrad}}{T_{surf}} = 306.0 \text{ mW/m}^2\text{K} \tag{3.18}$$

$$J_{mat}^{out} = \frac{F_{SW}^{atm} + F_{intrad} - F_{LW}^{atm}}{T_{atm}} = 336.4 \text{ mW/m}^2\text{K.} \tag{3.19}$$

The difference is the material entropy production rate:

$$\Sigma_{mat} = J_{mat}^{out} - J_{mat}^{in} = \sigma_{LH} + \sigma_{sens} = 30.4 \text{ mW/m}^2\text{K} \tag{3.20}$$

The flux through this system is $F_{mat} = 85.18$ W/m^2 and the temperatures are accordingly $T_{mat}^{in} = 278.4$ K and $T_{mat}^{out} = 253.2$ K.

3.2.5 The transfer entropy production rate

3.2.5.1 Motivation: internal versus external radiation

The key insight which supports the transfer entropy production rate is that radiative processes can be further categorized according to the role they play within the climate. This is not a new perspective - *Green* [1967] argues for it explicitly - but it has not yet been discussed in detail in the entropy production literature.

Energy is supplied to and exported from the planet by radiation; this *external radiation* on average heats warm places and cools cold places, continually driving the system. By contrast, *internal radiation*, which is emitted and absorbed by the material of the Earth system, gives a net transfer of heat down-gradient, pulling the system towards thermal equilibrium. It is almost accidental that radiation occurs in both of these roles. Internal
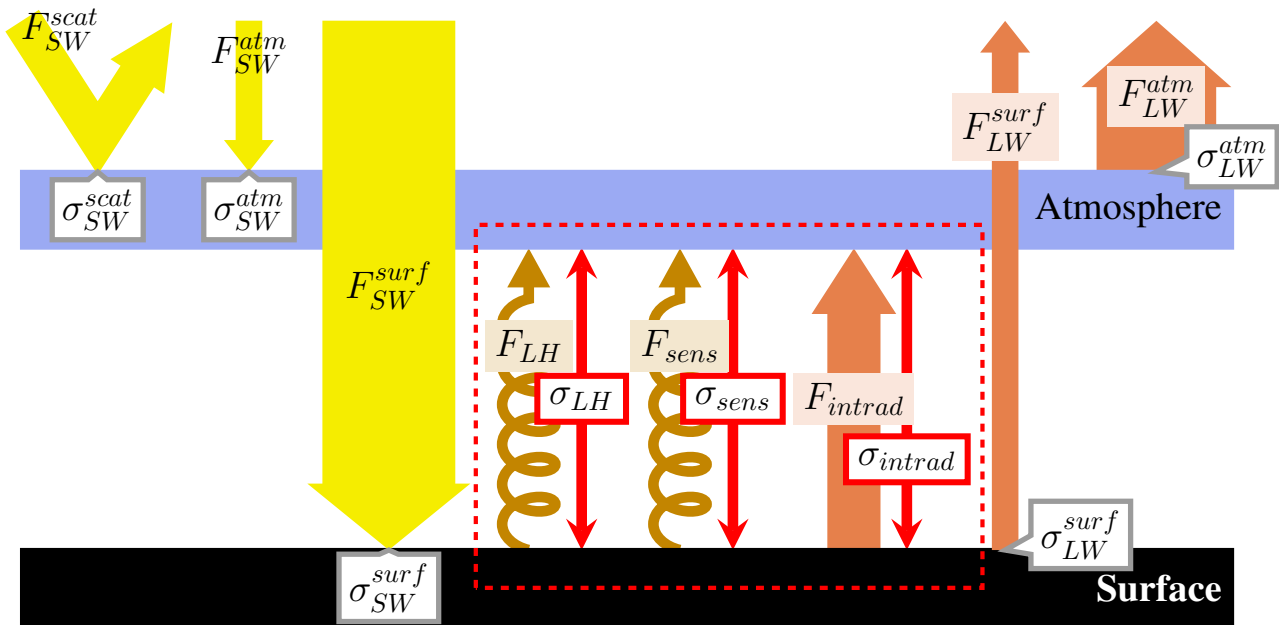
Figure 3.6: The transfer production rate refers to the production due to all processes which transfer energy *within* the climate system - both radiative and non-radiative. The cross-boundary fluxes are heating of the material supplied by external radiation: that which comes from or goes to the sun or outer space.

radiation is an inherent feature of a translucent, warm atmosphere and would occur even if the system were driven by a non-radiative heat source. It is not fundamentally different nor necessarily distinguishable from material heat transfer processes such as conduction. While external radiation determines where and how much heating and cooling drives the system, internal radiation acts in parallel with material processes to also transfer energy between where the external radiation delivers it to and takes it from.

This similarity between internal radiation and material processes suggests that they might be best considered together; this is the transfer entropy production rate. This concept of global entropy production has appeared only occasionally in the literature, and has not yet been thoroughly explored. In *Bannon* [2015], one of the material entropy production rates discussed (his MS3) includes the internal radiative heating processes and so is similar to the transfer rate discussed here. In *Bannon and Lee* [2017], the transfer rate is estimated as an upper bound for the material production rate. Most recently, *Kato and Rose* [2020] presents a study in which the transfer entropy production rate is estimated in Bannon's simple model and from observational data.

3.2.5.2   Definition

The transfer system includes matter and the internal radiation that travels between matter within the climate system but not the external radiation before it has interacted with the matter or after it has been emitted for the last time, which is considered part of the surroundings.

Defined directly for our model (as shown in Figure 3.6):

$$\Sigma_{tran} = \sigma_{LH} + \sigma_{sens} + \sigma_{intrad} \tag{3.21}$$

which makes it intermediate in magnitude,

$$\Sigma_{tran} = \Sigma_{mat} + \sigma_{intrad} \tag{3.22}$$

$$= \Sigma_{planet} - (\sigma_{SW}^{scat} + \sigma_{SW}^{atm} + \sigma_{SW}^{surf} + \sigma_{LW}^{surf} + \sigma_{LW}^{atm}) \tag{3.23}$$

as it includes contributions from the internal radiation which are not in the material entropy production rate and excludes those from external radiation which are included in the planetary rate. It is not coincidental that the entropy production due to internal radiation, σ_{intrad}, takes the same form as the entropy production due to the material processes in our two-layer model: $F(1/T_{atm} - 1/T_{surf})$, where F is the rate of energy transport. By contrast, the five entropy productions relating to external radiation that directly depend on the details of the radiation spectra are excluded.

In the transfer system, the cross-boundary fluxes are the heating or cooling of material upon absorption or emission of external radiation. The incoming entropy flux can be taken to be[7] the heating of the material due to the absorption of solar radiation:

$$J_{tran}^{in} = \int dV \, \frac{\dot{Q}_{sw}(\mathbf{x})}{T_{mat}(\mathbf{x})} \tag{3.24}$$

where $\dot{Q}_{sw}$ is the heating rate due to SW radiation and T_{mat} is the temperature of the absorbing material.

The entropy flux out of the system is then due to the LW emission of radiation which is not reabsorbed within the system. This is the cooling to space, $\dot{Q}_{cts}$, which can be calculated by radiative transfer models if the optical depth and temperature (T) are known [*Rodgers and Walshaw*, 1966; *Wallace and Hobbs*, 2006]:

$$\dot{Q}_{cts}(z) = -\pi \int d\nu \, B_\nu(T) \frac{d\mathcal{T}_\nu(z,\infty)}{dz} \tag{3.25}$$

where $\mathcal{T}_\nu(z,\infty)$ is the transmittance between z and the top of the atmosphere. Then the outwards entropy flux for the transfer system becomes:

$$J_{tran}^{out} = -\int dV \, \frac{\dot{Q}_{cts}(\mathbf{x})}{T_{mat}(\mathbf{x})} \tag{3.26}$$

Note that the cooling to space is everywhere of the same sign and its sum is exactly the outgoing longwave energy flux leaving the planet. It is the temperature from which cooling to space occurs, along with the spectral properties of the radiatively active gases, that determines the shape of the outgoing emission spectra. The average cooling-to-space temperature will generally be close to the emission temperature of the planet.

---

[7]As with the material entropy production case, there is an alternative way to divide the influx and outflux into regions of net external heating and regions of net external cooling. This is explored in Appendix A.2.

In the horizontal, there is negligible net heat transfer by internal radiation and so the horizontal components of the transfer and material entropy production rates converge. Therefore, the meridional heat transfer entropy production rate of Paltridge could just as well be identified as the horizontal component of Σ_{tran} as of Σ_{mat}.

3.2.5.3   Estimation

In the EBM, the flux of entropy into the sub-system is the entropy supplied to the material upon absorption of solar radiation:

$$J_{tran}^{in} = \frac{F_{SW}^{atm}}{T_{atm}} + \frac{F_{SW}^{surf}}{T_{surf}} = 868.8 \text{ mW/m}^2\text{K}. \tag{3.27}$$

The flux of entropy out is the change of entropy of the material which is cooling to space:

$$J_{tran}^{out} = \frac{F_{LW}^{surf}}{T_{surf}} + \frac{F_{LW}^{atm}}{T_{atm}} = 935.8 \text{ mW/m}^2\text{K}. \tag{3.28}$$

The difference, 67.0 mW/m^{2}K, is identical to the result of the direct calculation using Equation 3.21 above for the transfer entropy production rate. The flux of energy in this case is $F_{tran} = F_{SW}^{atm} + F_{SW}^{surf} = 239$ W/m^2 which results in representative temperatures $T_{tran}^{in} = 274.5$ K and $T_{tran}^{out} = 254.9$ K. The out-flux temperature is close to the effective radiating temperature of the planet $T_{eff}^* = ((1 - \alpha)F_{sun}/\sigma)^{1/4} = 254.7$ K, as expected.

3.2.6   Conclusion

The role which radiation plays in transporting energy to, from and within the Earth introduces complications into the description of a global entropy production rate. The absorption and emission of radiation is itself irreversible and, furthermore, radiation plays a role in the irreversible transfer of energy within the climate system. This gives rise to three options for what to include in the climate's entropy production rate. The planetary entropy production rate includes all the radiative irreversible processes, while the material entropy production rate includes none. These are standard approaches in the literature. The transfer entropy production rate takes an intermediate stance, neglecting the irreversibility due to the absorption and emission of external radiation but including that due to internal energy transfers. None of these perspectives can be deemed 'incorrect' global entropy production rates: they are just in reference to different system boundaries. The quantitative values for the resulting entropy-related variables in the EBM are summarised in Table 3.1.

Without a causal physical law relating the climate's state to an entropy production rate, there is not a definitive reason to prefer one entropy production rate variable over another. When such a theory is proposed, it will be unlikely to apply to all three variables, and so part of its development will necessarily be an explanation for why it is relevant to some global entropy production rate variables and not others. Without proposing such a hypothesis, it would be unreasonable to reject any of the three self-consistent options we have summarised here

	Planet	Tran	Mat
$F^{in} = F^{out}$ (W/m^2)	341	239	85
J^{in} (mW/m^{2}K)	79	869	306
J^{out} (mW/m^{2}K)	1358	936	336
T^{in} (K)	4334	275	278
T^{out} (K)	251	255	253
η (%)	94.2	7.2	8.6
Σ (mW/m^{2}K)	1279	67	30

Table 3.1: The energy fluxes (F), associated entropy fluxes (J), temperatures ($T = F/J$), efficiencies ($\eta = (T_{in} - T_{out})/T_{in}$) and production rates ($\Sigma$) for the energy balance model from each of the three system perspectives: planetary, transfer and material.

– all must be considered. However, there are some arguments which build physical intuition pointing towards the merits of the transfer perspective in climatological studies.

Consider, as an analogy to the climate system, a table-top experiment driven into motion by unspecified heating and cooling across its domain. Whatever the mechanism by which the energy is supplied, if the same heat is given to and removed from the system in the same places, the system's behaviour will be identical. A variable which sought to explain that system's behaviour would sensibly focus on the amount of energy and local characteristics of where it was delivered, not the nature of the external supply. This suggests that the planetary perspective might be focused on too broad a system. It is dominated by the production due to the thermalisation of solar radiation, which is highly dependent on the temperature of the sun - a quantity which does not directly impact the climate system (except insofar as it determines where and how much energy is absorbed).

Suppose, next, that this experimental system was made of a translucent medium, so heat could be transmitted by radiation as well as, say, conduction or convection or a hydrological cycle. Should that radiative heat transfer be considered separately from the other processes? As far as the rest of the system is concerned, heat transfer is the same no matter how it is accomplished. If the system cannot distinguish between the mechanisms, why should the non-radiative (material) proportion of the entropy production rate be the predictive quantity[8]?

On our planet, internal radiation plays a limited role in the horizontal and so the transfer and material entropy production rates are approximately the same. Therefore, the promising results about the meridional entropy production studies which emerged from Paltridge's set-up equally suggest the material and the transfer entropy production rate's potential importance. However, in the vertical, where internal radiation is significant, there has been limited success in applying similar principles to the material entropy production rate to find predictive

---

[8]Put another way, excluding internal radiation is as arbitrary as excluding moisture or convection. This does not rule out a subsetted non-radiative entropy production being useful for *diagnostic* purposes, as being, for example, most closely related to convective activity. But if there is a principle explaining the system's behaviour as being for the maximisation of an entropy production rate quantity, that principle is likely to be about the net and not only the fraction of entropy production due to some types of processes.

results [*Ozawa and Ohmura*, 1997; *Pujol and Fort*, 2002; *Wang et al.*, 2008; *Pascale et al.*, 2012]. Could the transfer entropy production rate improve the situation?

Now that the three potential global entropy production rate variables are defined, a natural next question is which aspects of the climate system each can elucidate. This will be the focus of the next chapter.

Chapter 4

How Climate State Influences Global Entropy Production Rates

4.1 Introduction

In this chapter, we turn our attention to how the three different global entropy production rates respond to changes in the climate's state. This is a useful avenue of research for three reasons.

Most straightforwardly, a first step to leveraging entropy-related variables for *diagnostic* purposes is understanding how the entropy productions change with climate properties in simpler models, as it indicates what variations in the values might indicate in more complicated models and observations[1].

Secondly, these experiments will clarify and deepen the intuition we have built from the formal definitions in Chapter 3 about the *significance* of the entropy metrics. The results help us to understand what the transfer entropy production can capture, as compared to the material and planetary perspectives and how internal radiation and material processes share the task of moving energy within the climate system.

And thirdly, as will be further explored in Section 6.4, developing our understanding of the relationship between the entropy production rates and the functioning of the climate system also supports the work to be done challenging and developing *predictive* theories, such as MEPP. The goal of such theories is a tool for explaining or anticipating the state which the climate adopts in response to certain boundary conditions without explicit modelling. Studying the value those variables take in the climate system as a function of the boundary conditions, as we do in this chapter, may provide insight for designing predictive theories. This is a speculative approach – to support hypothesis generation rather than testing – but is an additional motivation for this work.

---

[1]In fact, the results gleaned in this chapter are leveraged for exactly that purpose in Section 5.5.5 and help to uncover a problem with some in recently-published analysis.

The aim of this chapter is to understand how climate changes in the absorbed solar flux, greenhouse effect and efficiency of convection (via the role of latent heating) are manifest in the entropy production rates and related variables. An analytic radiative-convective model (ARCM) of an atmospheric column, detailed in Section 4.2, is used for this purpose because of its balance of fidelity and simplicity. Before the climate-varying experiments were carried out, however, a simple conceptual model of a climate system was developed in order to predict the relative magnitude and direction of the responses. This framework, outlined in Section 4.3, is strikingly successful at anticipating the results from the ARCM (discussed in Section 4.4) and so is likely a useful contribution to deepening our understanding of the entropics of the climate system.

The results we calculate are compared in Section 4.5.1 to those obtained by other researchers for the pairs of climatic changes and entropy production rates where prior studies exist. Studying the climate responses of all three entropy production rates in conjunction also allows us, in Section 4.5.2, to compare their efficacy as climate metrics and offer further arguments for which is most physically relevant. This is especially significant since variables which are responsive diagnostic metrics may be useful predictive variables as they are likely capturing essential information about the complicated underlying system.

Finally, the ability of basic solar radiation management to reverse greenhouse-gas-induced climate changes is investigated using entropy-metrics in Section 4.5.3. The signature of changes in the greenhouse effect and changes to solar radiation are very different when explored from an entropy point of view - differences which cannot be resolved by surface temperature metrics alone but are nevertheless indicative of important differences in the behaviour of the climate. This demonstrates the potential for a societally-useful application of the understanding developed in this chapter and for the Earth's entropy production rate as a tool for studying the climate more broadly.

4.2   Analytic radiative-convective model

Choosing an appropriate model is the first step to to investigating how entropy production rates respond to changing conditions in the true climate. The two-layer energy balance model of Section 3.2.2 is too reduced: with only a single layer atmosphere and convective heat transport which is a fixed fraction of the solar radiation absorbed at the surface, it is not self-evident how to parametrize climatic changes realistically. Conversely, a dynamical model with cloud processes and other feedbacks is over-complicated for this initial investigation, as it is difficult to separate processes, feedbacks and aspects of its behaviour to interpret the results.

An accurate mechanistic model of a simpler climate – one which has the key relevant features of our climate but without some of the complexities present on Earth – is ideal. This is particularly true because it is likely[2]

---

[2]Though not certain: it is also plausible that an entropy production principle could be due to life or a particular process (cloud-moisture feedbacks, say, or convective organisation) which would be missing from the simpler model climate.

that if an entropy production principle exists, it would be universal to any plausible climate – one obeying some reasonably familiar laws of physics – but might be not exist in a more unphysical representation, even if the numerical values appear to more closely match our Earth. For example, a simple model of Mars is arguably more likely to shed light on the how entropy production works in the Earth's climate than would a complex model of the Earth which doesn't conserve energy.

The aspects which are key in an entropy-producing climate are spectrally- and spatially-resolved incoming solar radiation and outgoing thermal radiation, non-radiative heat transport, and internal radiative heat transfer. These are gathered in an elegant form in the analytic radiative-convective model (ARCM) of an atmospheric column by *Robinson and Catling* [2012], further developed in *Robinson and Catling* [2014] and *Tolento and Robinson* [2019]. The model was originally designed to apply to a wide range of planetary climates and so is flexible and able to simulate climate states based on few, physically interpretable variables. It is simple enough to be solved analytically and so is computationally cheap, and the solutions for radiation fluxes and temperature allow entropy production rates to be calculated straightforwardly and precisely. Furthermore, its mode of simplification is to change the basic properties of the climate system (e.g. assuming a grey gas behaviour, fixing humidity for a specified lapse rate) and not via overly-fitted parametrisations. So insofar as it doesn't accurately simulate our climate, it is still a plausible model for *a* climate, in a simpler parallel universe. Although the model has continuous vertical resolution, it has no horizontal extent, so the study is limited to the fraction of entropy production due to heat transfers in the vertical.

There are three main controllable feature of the model: the short wave absorption in two channels (stratospheric and troposphere/surface), longwave emission through the grey atmosphere, and a convective region with a prescribed adiabatic lapse rate. These in turn map to the three climatic changes explored: changes in the albedo, the greenhouse effect and the moisture of the convecting air.

4.2.1 Model definition

As laid out in *Robinson and Catling* [2012, 2014]; *Tolento and Robinson* [2019] the vertical model coordinate of the ARCM is the longwave optical depth, τ, which is related to pressure via a power-law relationship:

$$\tau = \tau_0 \left(\frac{p}{p_0} \right)^n \tag{4.1}$$

where τ_0 is the surface optical depth, p_0 is the surface pressure and n is an observationally-fitted parameter which is typically between 1 and 2 depending on the presence of pressure-broadening and collision-induced absorption in the atmosphere. For the Earth, particularly in the troposphere and lower stratosphere, $n = 2$.

The atmosphere is modelled as a radiatively grey gas in the longwave and as a two-channel approximation in terms of the longwave optical depth in the shortwave, such that the net solar radiative flux at vertical coordinate

τ is given by:

$$F^{\odot}(\tau) = \alpha \left(F_1^{\odot} e^{-k_1 \tau} + F_2^{\odot} e^{-k_2 \tau} \right) \tag{4.2}$$

where α the top-of-atmosphere albedo, F_1 and F_2 are the portion of incident solar radiation destined predominately for the higher (stratosphere) and lower (troposphere and surface) regions of the atmosphere respectively[3], and k_1 and k_2 are their attenuations. The surface is modelled as a black body, absorbing all incident solar radiation and re-emitting in the longwave.

The atmosphere is split into two portions: a upper region which is in radiative balance and a lower region where convection occurs. The location of the interface between the model's convective and stratified regions, labelled the radiative-convective boundary at τ_{rc}, is determined by requiring continuity of upwelling radiative flux and temperature across that boundary. These two conditions allow the model to be solved in terms of two free parameters, for example the surface temperature and location of the radiative-convective boundary.

In the lower portion of the atmosphere, the thermal structure is given by a modified adiabat:

$$T(\tau \geq \tau_{rc}) = T_0 \left(\frac{\tau}{\tau_0} \right)^{\beta/n} \tag{4.3}$$

where T_0 is the surface temperature and the parameter $\beta = a(\gamma - 1)/\gamma$ modifies the dry adiabatic lapse rate (in terms of the ratio of specific heats $\gamma = c_p/c_v$) to account for latent heat release via the rescaling by an empirical factor a, estimated at 0.6 for the Earth climate.

In the upper, non-convecting region the model is solved by requiring that the temperature be such that the net longwave cooling balances the solar absorption. In the convective region the net radiative heating is specified by the prescribed temperature profile and the convective heat flux is calculated as the remainder necessary to achieve local energy balance.

In both regions, the upwelling (F^+) and downwelling (F^-) radiative fluxes are derived from the grey two-stream Schwarzschild equations (assuming a plane-parallel atmosphere):

$$\frac{dF^+}{d\tau} = D \left(F^+ - \sigma T^4 \right) \tag{4.4}$$

$$\frac{dF^-}{d\tau} = -D \left(F^- - \sigma T^4 \right) \tag{4.5}$$

where $D = 1.66$ is the diffusivity factor used. The net upwards longwave flux, $F_{net} = F^+ - F^-$ must satisfy energy balance:

$$F_{net}(\tau) + F_{conv}(\tau) = F^{\odot}(\tau) \tag{4.6}$$

---

[3] In the model definition in the literature, the albedo α is absorbed into F_1 and F_2. It is separated in this version of the model because I intend to run experiments by varying it.

The temperature profile in the non-convective (stratospheric) region can be calculated by noting that $F_{conv}(\tau < \tau_{rc}) = 0$ so $F_{net}(\tau < \tau_{rc}) = F^{\odot}(\tau)$ and:

$$\frac{d^2}{d\tau^2}\left(F^+ - F^-\right) = D\frac{d}{d\tau}\left((F^+ - \sigma T^4) + (F^- - \sigma T^4)\right)$$

$$= D\left[D\left(F^+ - \sigma T^4\right) - D\left(F^- - \sigma T^4\right) - 2\frac{d}{d\tau}\sigma T^4\right]$$

$$\implies \quad \frac{d^2}{d\tau^2}F_{net} - D^2 F_{net} = -2D\frac{d}{d\tau}\sigma T^4. \tag{4.7}$$

Substituting $F^{\odot}(\tau)$ for $F_{net}(\tau)$ (radiative balance) and noting that $F^-(\tau = 0) = 0$ the temperature is recovered:

$$\sigma T^4(\tau \leq \tau_{rc}) = \frac{F_1}{2}\left[1 + \frac{D}{k_1} + \left(\frac{k_1}{D} - \frac{D}{k_1}\right)e^{-k_1\tau}\right] + \frac{F_2}{2}\left[1 + \frac{D}{k_2} + \left(\frac{k_2}{D} - \frac{D}{k_2}\right)e^{-k_2\tau}\right]. \tag{4.8}$$

The upwelling flux is then accessed via $F^+ = \frac{1}{2}F_{net} + \frac{1}{2D}\frac{d}{d\tau}F_{net} + \sigma T^4$, and similarly, $F^- = -\frac{1}{2}F_{net} + \frac{1}{2D}\frac{d}{d\tau}F_{net} + \sigma T^4$.

In the convecting region, the temperature is prescribed and so that

$$\frac{dF^+}{d\tau} = D\left(F^+ - \sigma T_0^4\left(\frac{\tau}{\tau_0}\right)^{4\beta/n}\right) \tag{4.9}$$

which can be integrated by using an integrating factor of $e^{-D\tau}$ and setting $F^+(\tau_0) = \sigma T_0^4$ to give:

$$F^+(\tau \geq \tau_{rc}) = \sigma T_0^4 e^{-D(\tau_0 - \tau)} + \int_{\tau}^{\tau_0} D\sigma T_0^4\left(\frac{\tau}{\tau_0}\right)^{4\beta/n} e^{-D(\tau' - \tau)}d\tau' \tag{4.10}$$

The final integral is recognisable as an incomplete gamma function, which allows F^+ to be calculated via standard integrals. A similar expression can be derived for the downwelling radiation F^- (*Tolento and Robinson* [2019], equation 19).

With these expressions for F^+ and T for both regions $\tau < \tau_{rc}$ and $\tau > \tau_{rc}$, the continuity condition can be applied (numerically) at $\tau = \tau_{rc}$ to solve for τ_{rc} and the other free variable. Figure 4.1 shows the temperature profile and energy fluxes when the parameters given by *Tolento and Robinson* [2019] for Earth are used: $n = 2$, $\tau_0 = 1.96$, $a = 0.6$, $\gamma = 1.4$, $\alpha = 0.3$, $k_1 = 90$, $k_2 = 0.16$. $F_1 = 9.9$ W/m^2 and $F_2 = 330.8$ W/m^2 are rescaled relative to the *Tolento and Robinson* [2019] values so that the total incident solar radiation is $\alpha\sigma T_{sun}^4\Omega_{sun}/4\pi$, to permit more consistent estimations of scattered entropy flux. The resulting surface temperature $T_0 = 287.9$ K and $\tau_{rc} = 0.14$.
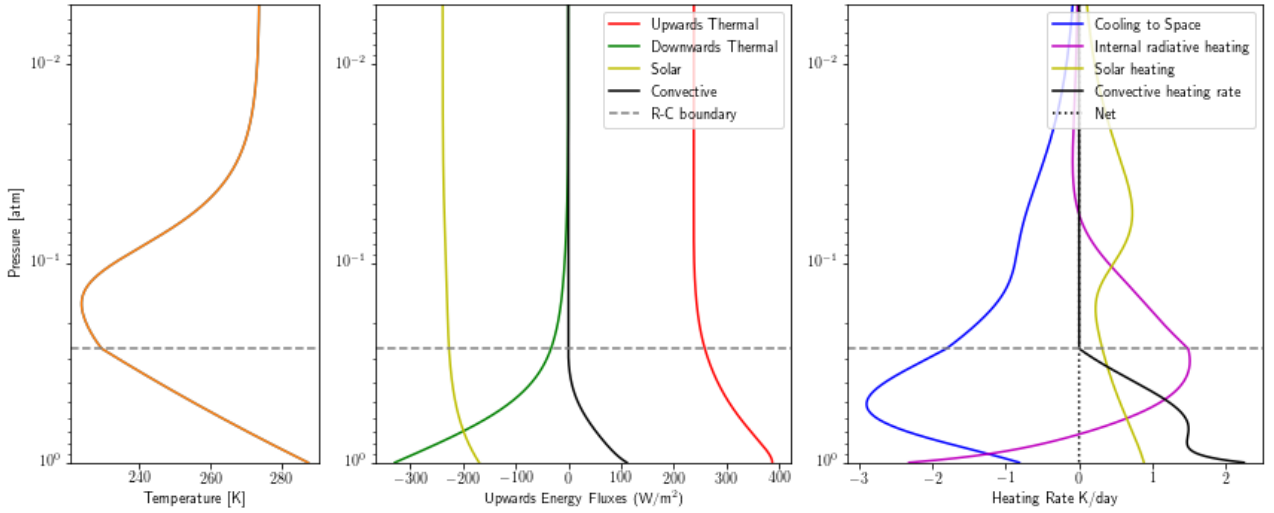
Figure 4.1: The Earth atmospheric profile given by the analytic radiative-convective model of *Tolento and Robinson* [2019] used in this study. The three panels show the temperature, the quantity of convective and radiative energy flux in the vertical and the resulting atmospheric heating rates. There are two portions of the model atmosphere separated by the dashed horizontal line (the radiative-convective boundary): a lower convective region which dominates the troposphere has a prescribed lapse rate which has a power law relationship to the pressure (linear on this semi-log scale), while the upper region is in local radiative balance. The solar heating is supplied in a two-stream semi-grey approximation, such that there is a peak of heating in the model stratosphere and another in the troposphere and surface, as seen in the third panel. The atmosphere is taken to be optically grey in the longwave. In the convective region, the radiation fluxes can be calculated from knowledge of the atmosphere's optical properties and prescribed temperature: convective heating is calculated as the residual needed to maintain steady state in response to the net radiative cooling. In the second panel, the longwave radiative fluxes are separated into an upwelling and downwelling component, but in the third column the radiative heating is separated according to whether it carries energy outside of the system, as cooling to space, or within the system, as internal radiative heating from the surface.

4.2.2   Entropy calculations

As evident from the derivations in Section 4.2, the temperature and radiative fluxes are at the heart of this simple model. This makes it an ideal candidate for the application of the indirect definitions of entropy production rates given in Sections 3.2.3.1, 3.2.4.1 and 3.2.5.2.

For the material entropy production rate, the only region of the model with convective cooling is the surface, so $J_{in}^{mat} = F_{conv}(\text{surface})/T_0$. The convective heating throughout the atmosphere is balanced by net radiative cooling, giving entropy flux out of the material system:

$$J_{out}^{mat} = \int_{\tau_0}^{\tau_{rc}} \frac{1}{T(\tau)} \frac{dF_{conv}(\tau)}{d\tau} \, d\tau \tag{4.11}$$

The material entropy production rate is the difference of these fluxes.

The incoming transfer entropy flux is due to the solar heating:

$$J_{in}^{tran} = \int_{\tau_0}^{0} \frac{1}{T(\tau)} \frac{F_{net}^{\odot}(\tau)}{d\tau} \, d\tau + \frac{F_{net}^{\odot}(\text{surface})}{T_0} \tag{4.12}$$

and the outgoing flux is from the cooling to space:

$$J_{out}^{tran} = \frac{\dot{Q}_{cts}(\tau)}{T(\tau)} \tag{4.13}$$

where

$$\dot{Q}_{cts}(\tau) = (1 - e^{-D\Delta\tau})\sigma T^4 e^{-D\tau} \tag{4.14}$$

which accounts for the emissivity of the layer, the thermal emission of radiation as a function of temperature and the transmittance from that layer to space.

For the planetary entropy production rate, the incoming solar radiation is treated as black body, carrying entropy $\frac{4}{3}F^{\odot}/T_{sun}$ with $T_{sun} = 5779$ K. The entropy of the scattered solar flux is approximated as in *Stephens and O'Brien* [1993]; *Bannon* [2015]; *Wu and Liu* [2010a] by assuming isotropic (Lambertian) scattering, so that the $J_{scat} = \frac{4}{3}\sigma T_{sun}^3 \chi(u_L)$ where $\chi(u) \approx u(-0.2776 \ln u + 0.9651)$ and $u_L = \alpha\Omega_{sun}/4\pi$, where $\Omega_{sun} = 6.77 \times 10^{-5}$ st. We take $\alpha = 0.3$.

For the outgoing planetary entropy flux, the outgoing radiation flux must be calculated spectrally by summing the emission at each wavelength which reaches the top of the atmosphere:

$$I_\nu = B_\nu(T_0)e^{-D\tau_0} + \int d(D\tau)B_\nu(T)e^{-D\tau}, \tag{4.15}$$

to which equation 3.8 can applied to recover the planetary entropy flux. The production is, again, the difference between the incoming and outgoing planetary entropy flux.

4.2.3 Mapping to EBM

It is instructive to attempt a mapping between this ARCM (of Figure 4.1) and the EBM of Section 3.2.2, as it helps explain the structure of the new model, and, insofar as the ARCM is a more realistic representation of the true climate than the EBM, it highlights the important features of the climate that the EBM could not capture.

As in the EBM, the surface in the ARCM receives the majority (71%) of the incoming unscattered sunlight, while the rest is absorbed in the atmosphere at an average pressure of 0.59 atm and an average temperature of 262 K. Similarly, the surface radiates thermally as a black body at $T = 287.5$ K, a small fraction of which (3.9%) is emitted to space. The majority of the radiation emitted to space is from the atmosphere (Figure 4.1, third panel, blue) with an average pressure of 0.52 atm and temperature 255 K. From these we see that in a vertically-resolved atmosphere, the SW and LW external radiation cannot be sensibly represented by a single atmospheric absorption and emission temperature as is the case for the EBM

The limitations of a single-layer approximation for the atmosphere are also evident when we consider convection. Convection is such a comparatively efficient energy transporting mechanism that it effectively determines the temperature profile in the region where it acts: the troposphere remains close to the adiabatic lapse rate, which is the threshold for convective heat transport[4]. However, at that lapse rate, a significant amount of heat is still transferred vertically by radiation internally within the atmosphere, which can be seen in the magenta line in the third panel of Figure 4.1 – a net $43\,\text{W/m}^2$ of internal radiation from the surface and a further $33\,\text{W/m}^2$ from the lower troposphere (at an average of $283\,\text{K}$), which are deposited in the upper troposphere and stratosphere at an average temperature of $241\,\text{K}$. Internal radiation acts in sequence with the convection as well as in parallel: the internal radiative cooling in the lowest portion of the stratosphere is in balance with the convective heating there and is responsible for moving the heat which was convected from the surface further upwards through to where it can be emitted to space.

An updated energy-flow diagram summarises these features in Figure 4.2. It is worth emphasising how many entropy-producing processes cannot be represented in this sketch: at every height in the atmosphere, internal radiation is being emitted and re-absorbed irreversibly. Only by considering the full complexity of the profile in Figure 4.1 can the entropy-producing processes in the vertical be accurately accounted for, even indirectly.

4.3   Building intuition: mapping to a circuit as a conceptual model

> Never make a calculation until you know the answer. Make an estimate before every calculation, try a simple physical argument (symmetry! invariance! conservation!) before every derivation, guess the answer to every paradox and puzzle. Courage: No one else needs to know what the guess is. Therefore make it quickly, by instinct. A right guess reinforces this instinct. A wrong guess brings the refreshment of surprise.   - John Archibald Wheeler, Spacetime Physics

If, as John Wheeler encourages above, we wanted to make estimates of the of the entropy production rates or predictions of how they change when the climate is adjusted before carrying out the calculations, how would we go about it? What conceptual models are available to build instinct around?

This line of questioning is useful both for the project of prediction, as Wheeler makes explicit, but also for understanding. Numerical results are just numbers if they are not mapped to something intuitive. As this is a nascent field, there is not yet a settled set of metaphors or conceptual models to explain entropy production in the climate, like a spring makes sense of a chemical bond or an elastic membrane for gravitational fields. Nor is

---

[4]This is an interesting aspect to note. If convection carried energy simply in proportion to the temperature difference, as in conduction or internal radiation, the temperature difference within the troposphere with convection alone or radiation alone would be larger than if they both acted together. Neither would solely determine the profile. Convection behaves very differently, being so efficient as to dominate but having a threshold for inactivity at which radiative heat transfer is far from inactive. Not many heat transfer processes behave in this way.

Figure 4.2: A sketch of the energy flows in the analytic radiative-convective model, for comparison with Figure 3.2. In an atmosphere with higher resolution in the vertical, it becomes impossible to coherently simplify that atmosphere to a single representative temperature. Different processes deposit and draw energy from different heights within the atmosphere, most notably convection and internal radiation which act in sequence to transfer radiation from the surface to the upper atmosphere. The temperatures shown are entropic averages and the values in parentheses are energy fluxes (W/m^2).

entropy production a familiar, intuitive quantity to the scientist[5] in the way temperature or heat is. This absence of a framework for comprehension limits our ability as researchers venturing into uncertain territory to make sense of the features we might find (and perhaps helps to explain the general confusion in the field discussed in Section 2.9).

In this section, I will describe the conceptual model of the climate which has proved useful and successful during this project, initially for correctly predicting and then for explaining the climate's entropic behaviour. It is not entirely novel but builds from three inspirations: the climate heat engine model, a comment made in *Reis* [2014] about climate processes as resistors, and an approach borrowed from studies on ocean salinity and temperature. The perspective introduced in this chapter will also feature in the discussion of MEPP in Section 6.4; the application of it here provides a partial proof of its plausibility.

4.3.1 Conceptual model inspirations

The heat engine model is often invoked in entropy production, but presents some conceptual problems as a model of the climate system. In engineering usage, a heat engine is specifically a process which transfers energy from a hotter reservoir from a colder *in order to* export work. This mapping makes sense in the case of a

---

[5]It is interesting to consider how our scientific knowledge might be different if we scientists were a different kind of creature who could perceive different variables and aspects naturally (recalling the ideal gas law analogy).

climate component like a hurricane [*Emanuel*, 2006] in which there are external thermal reservoirs (the surface and atmosphere) and the kinetic energy generated can leave the system. However, at the climate scale, the analogy breaks down in two ways. Firstly, there is no way to transport work out of the climate and so motion is created only temporarily and then dissipated again within the system. As explained in Appendix A.1, this means that the Carnot limit for the maximum export of work from a heat engine does not apply, and so there is limited usefulness in a heat engine mapping. Without exporting work, the climate behaves more like a purely heat transfer system such as a heat pipe or a thermosyphon. Secondly, one of the most significant features the climate is that the 'reservoir' temperatures and energy flows *adjust* in order to find a steady state, which is not a feature in the standard heat engine picture with infinite reservoirs. Nevertheless, the basic idea of reducing the climate system to a two-temperature model with energy flowing through it is a useful starting point.

A metaphor-model for climate energy flows which avoids these two pitfalls is suggested in passing in *Reis* [2014], quoting Richard Feynman. Reis points out that the heat transfer processes in the climate system behave somewhat like resistors in parallel, transporting heat (rather than current) from the hot to cold (rather than high to low voltage). Some of these processes involve the temporary creation of kinetic energy or conversion of water to a different phase, but others are more quiescent, like thermal diffusion or internal radiation. All processes, no matter how complicated, must (on net) transfer heat down-gradient because of the Second Law: a resistor, with its linear response to forcing, represents a simplified version of this behaviour. The familiar resistor circuit underlines a key feature: the resistors interact – even when they don't directly feedback into each other – via the mutually-optimised voltage difference and shared current, and this will likely apply to the climate too. This view of the climate underlines that the system is balancing itself in some sense, as automatically as an electrical circuit balances the current through resistors in parallel[6].

Recall that in Section 4.2.3, the aspect which made the mapping between the ARCM and the EBM challenging was the spatial concept of 'the atmosphere'. This is also an issue when attempting to map the climate to the hot and cold reservoirs implied by the heat engine or resistor analogies. The climate is not like a Rayleigh-Bernard cell with physically separated hot and cold plates but is translucent to solar and thermal radiation such that energy is both deposited to and leaves from everywhere within the climate and it is difficult to reduce it to two temperatures. Inspiration is found in the approach taken by Jan Zika and others for studying the ocean[7], where parcels move around in space while its characteristics are preserved. They suggest that by identifying the parcels according to their characteristics and not by location, a different understanding of the system can be gleaned. From this perspective, for example, it is self-evident that the saltiest parcels are those which are being made more salty by evaporation or freezing of freshwater out of the system and conversely for the fresher parcels. These forcings which maintain the most dis-equilibrated parts of the system are balanced by dilutions due to the mixing within the ocean to maintain steady state where the salinity distribution is determined by the

---

[6]*Virgo and Ikegami* [2015] also use a circuit diagram to discuss entropy production in the earth system, but map the whole climate system to a single resistor in series rather than multiple in parallel

[7]These ideas were introduced to me at a talk at Imperial College in 2015, but can also be found in *Zika et al.* [2012, 2015]

relative efficacy of mixing compared the driving evaporation and freshwater sources. This description works absent any spatial location knowledge

The same will be true for the climate: those regions which receive solar energy are necessarily on average the hottest parts of the system, wherever they are. The regions from which energy leaves the systems are cooled and so are necessarily the cooler regions, on average. This is the case even though climate regions often belong to both distributions, to a greater or lesser extent. The existence of the hotter parts which receive energy from outside and cooler parts which emit energy is a certain and simplifying feature of the climate, and allows a schematic representation of temperature without reference to spatial variables. A sketch is shown in Figure 4.3. The external heating (absorbed solar radiation) and cooling (thermal emission to space) stretches the temperature distribution within the climate system and must be exactly balanced by the irreversible processes which mediate down-gradient heat transfer and pull the system toward an isothermal equilibrium. As with salinity in the ocean, the temperatures are set by this competition between the equilibrating influence of internal processes and the dis-equilibration of external radiation.
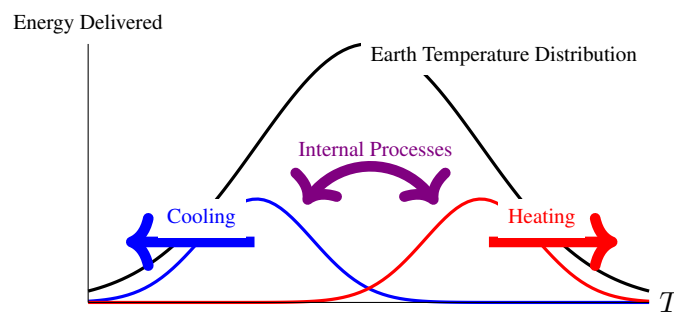
Figure 4.3: A sketch of the temperatures and movement of heat in the climate system. In a non-equilibrium system driven by heating and cooling at different locations, there will be a range of temperatures present. Necessarily, the regions which receive heat from outside of the system are on average warmer than the places where cooling occurs - otherwise the movement of heat within the system would violate the Second Law. The external heating and cooling stretches the temperature distribution of the system, heating the hotter places and cooling the colder which is, at steady state, exactly balanced by the tendency of thermal diffusion, convection, internal radiation and all other irreversible processes to equilibrate the temperature, creating a more peaked temperature distribution. This sketch is not to scale.

4.3.2 Correspondence

Figure 4.3 helps to make concrete the concept of hot and cold reservoirs in the climate. The hot is the aggregate of the places where energy is delivered to the system, and the cold are the places it leaves from. An entropic temperature, $T_H^* = (\frac{1}{F} \int \frac{dF_{in}}{T})^{-1}$ and similarly for T_C, is a natural energy-weighted average temperature with a clear physical interpretation: F/T_H^* is exactly the entropy flux J_{in} for the system, and F/T_C^* is the J_{out}.

This suggests the introduction of the conceptual model of the climate sketched in Figure 4.4 in which the system's hot and cold regions, fed by external radiation, adjust in order to convey sufficient energy through the heat transfer processes available to the system. There are three representative processes labelled to transfer heat from the hotter to the colder regions: internal radiation and two material processes, the hydrological cycle and

kinetic energy generation and dissipation. In each process, heat takes a different form during the transfer but not permanently, so the end-result is just the transfer of heat from the hotter to the colder parts of the system. The hydrological cycle transfers heat by latent heat release – in a steady state system the total mass of water in each phase is constant and so the entropy change of the water as it evaporates or precipitates is cancelled by a reciprocal phase change elsewhere. There is also a generation of motion and subsequent frictional heating which is the result of the dissipation of kinetic energy. Even internal radiation is mediated by the temporary creation of photons, which are destroyed upon absorption such that only the resulting transfer of heat is relevant.
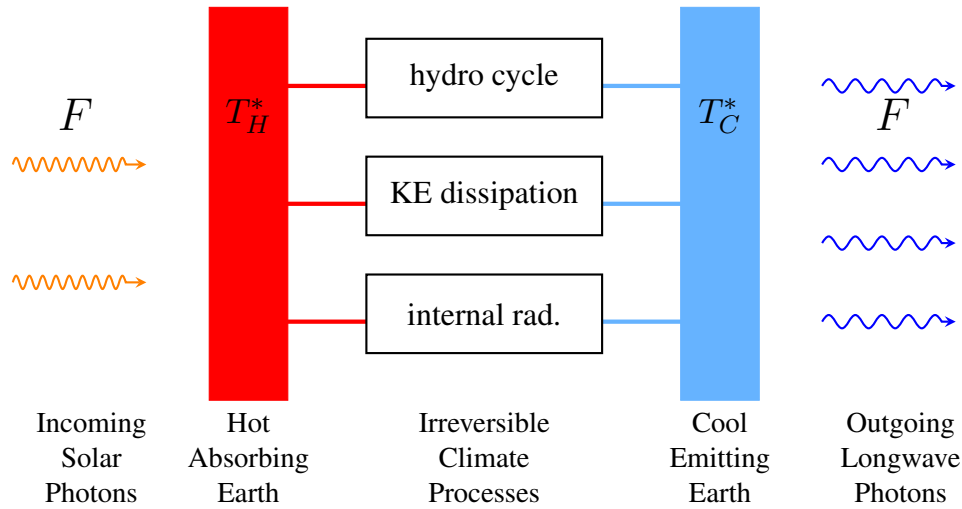
Figure 4.4: A conceptual model of the climate system which emphasises entropy production. Solar radiation approaches the planet, supplying energy to the warmer, absorbing locations. That energy is then transferred within the system by irreversible processes, for example via dissipation of kinetic energy, the latent heat release during the hydrological cycling and by internal radiation. The colder places in the climate are necessarily where energy is emitted to the vacuum of space, and the outgoing photons carry that energy. The entropy production is the amount of energy passing through the system scaled by the appropriate inverse temperature difference. For the planetary perspective, that is the entropic temperature of the incoming and outgoing photons. The transfer perspective considers all energy flowing from the hot absorbing locations to the cool emitting, by material and radiative processes. The material perspective focusses on the subset of processes which are non-radiative, here the hydrological cycle and the creation and dissipation of kinetic energy; only a portion of the energy is transferred in this manner. The diagram suggests a mapping from energy fluxes and temperatures to current and voltage, with the irreversible processes being like resistors in parallel. The temperature of the cool emitting locations are set by the total current through the system (via the Planck constraint on the effective emission temperature), but the hotter locations will find their temperatures increase until there is a sufficient gradient to transfer that energy (current) through the processes (resistors). Within this framework, we expect that changes in the relative conductivity of the irreversible processes will change the fraction of energy transferred by each. Changes in the longwave radiative properties of the climate influence both the location of the emitting areas of the system and the internal radiation, while changes in the albedo influence the system via adjusting the total current. Further discussion of the implications of this model is given in the text.

As emphasised in Chapter 3, there are choices about what to consider the boundaries of the climate system which would change the interpretation (and design) of this model. The perspective which appears most natural to me is based on the transfer point of view, which, interestingly, leaves room for representations of the planetary and material systems. In this approach, Figure 4.4, we map F to the total absorbed solar energy, with $T_H^* = T_{in}^{tran}$ and $T_C^* = T_{out}^{tran}$, which means that T_C^* is approximately the effective radiating temperature of the planet, $T_E^* = (F/\sigma)^{1/4}$. The transfer entropy production rate is then exactly the flow through the system scaled by a difference in inverse temperatures, $\Sigma_{tran} = F(1/T_C^* - 1/T_H^*)$. The material entropy production rate is

approximately the proportion of energy flow through the non-radiative resistors, F_{mat}, scaled by the inverse temperature difference, $\Sigma_{mat} = F_{mat}(1/T_C^* - 1/T_H^*)$, which is only approximate because the temperatures the material processes act between will not be exactly T_C^* and T_H^*. The planetary entropy production rate is approximately the flow through the climate system scaled by the difference of the inverse temperatures *of the radiation* with the 4/3 factor and an extra production due to scattering: $\Sigma_{planet} = \frac{4}{3}F(1/T_C^* - 1/T_{sun}) + \sigma_{scat}$.

Why is the resistor analogy relevant? Fundamentally, activity in the atmosphere and ocean exists to transfer energy from the hotter places where energy is delivered from the sun to the colder places where energy leaves for outer space. In this, the internal radiation and all the material processes act in parallel, experiencing in common the temperature differences and transferring what energy they can according to their natures. Local energy balance is analogous to Kirchhoff's current law - the incoming and outgoing energy flows in each part of the climate system must balance in steady state. The energy transfers are unavoidably dependent on the temperature differential as they must, by the Second Law, be (net) down-gradient, or zero when there is no temperature difference, which suggests a similarity to Ohm's law. The irreversible processes in the climate system all do the job of resistors: they respond to a temperature ('voltage') difference to transfer energy ('current') down-gradient.

This emphasises the key aspect of this model: the same quantity of energy must flow through each stage of the diagram (akin to the current in a circuit). This is a slightly different perspective than the energy balance view of the climate, which emphasises that the temperature of each component changes because of imbalance in deposited energy. Instead, the temperature changes in order to balance the flow. Working backwards from the coldest part of the system, the outflow energy flux is set by the temperature at the places where cooling to space occurs ($F \approx \sigma(T_C^*)^4$). Then T_H^* adjust to drive sufficient energy from where it is deposited in the system to where it can be emitted.

This model emphasises three main ways climate changes can occur. The amount of current through the system, F can change by a change in the global albedo. The resistivity of the resistors can change, for example by a change in the humidity of the climate or the efficacy of the internal radiation. And finally, the physical distance between T_H^* and T_C^* can change by a change in height of emission to space from the atmosphere due to a change in the greenhouse effect (which in practice coincides with a change in the internal radiation 'resistor' as well). As the resistor analogue emphasises, the climate readjusts to each of these changes until it find a configuration in which T_H^* is again hot enough to transfer sufficient energy to T_C^*, which in turn must be hot enough to emit the absorbed F. To anticipate climate changes we need to anticipate this cascade of changes.

4.3.3 Limitations

This resistor-analogue model is instructive, but it also has significant limitations and assumptions.

Firstly, the heat transfer processes in the atmosphere are far from linear with temperature (voltage difference), convection being an acute example of this. The amount of energy transferred will generally increase with increasing temperature difference (because it must be zero at zero temperature difference), but it would be a mistake to try to map convection to a conductivity for numeric predictions because it is not a linear process.

Secondly, in practice the material processes also do not transfer the energy as far through the atmosphere as the internal radiation does and so experiences a smaller temperature difference, as demonstrated in Section 4.2.3. A more accurate representation might show the material resistors a material processes in series with radiation, as much of the convected energy continues its travel in the vertical by internal radiation. This has been omitted here for simplicity, but is a recommended further development.

Thirdly, the model does not feature interactions between resistors and feedbacks on the absorptivity, such as in the humidity influence on the global albedo and the longwave radiative properties, for example. Such a features might be central to the success of a MEP hypothesis – this cannot be ruled out – and so care must be taken to interpret any intuition derived from this simple model as belonging to a simpler system than the climate.

And finally, as the climate system has been projected onto only two temperatures, it is difficult to consider horizontal and vertical heat transfer separately in this simple model.

In spite of these over-simplifications which limit fidelity, the resistor analogue model is useful for anticipating and interpreting the direction of the change of the three global entropy production rates change with climate changes.

4.3.4   Predictions of entropy changes under climate change

One of the key results of this chapter is the usefulness of our simple resistor model of Figure 4.4 in making predictions of entropy responses, which are explored in this section. A retrospective account of predictions should, of course, be treated with caution[8], but the aspect to emphasise here is the utility of the model in making sense of the climate's entropy-behaviour.

The three types of climate changes explored - albedo, greenhouse gas and lapse rate - can all cause an increase in the surface temperature, which we expect to be reflected in an increase in T_H^*. However, an albedo decrease effects this change by increasing F, while the drying of the convection reduces the efficacy of the latent heating transfer process. Changing the greenhouse gas concentration has two impacts: reducing the heat transfer through the atmosphere by internal radiation (more optical depth is more layers to pass radiation through) and elevating the place in the atmosphere from which cooling to space happens[9]. This requires convection (and

---

[8]In writing this section, I have referred to records I kept of my predictions, but chosen to emphasise what the model *can* predict, not just the things I have a record of having thought through.

[9]This is one of the standard explanations of the greenhouse effect which doesn't get much airtime: increased greenhouses gas concentration along with a preservation of the lapse elevates the location of emission to space which tracks back to a warming of the

the internal radiation which is in series with the convection) to act over a longer distance, increasing the total resistance and causing the surface temperature increase. How will these climate changes be reflected in the other entropy production rate variables?

In the albedo decrease case, the increased F through the system should cause the outflow temperature to increase because of the Planck emission criteria. The characters of the resistors do not change, so in order to have an increased F flow from hot to cold, the temperature difference $T_H^* - T_C^*$ must also increase, so the increase in T_C^* will be less than the increase in T_H^*. The increased absolute temperatures would act to reduce the transfer and material entropy production rates, but the increase the flux F and the increase in the temperature difference act to increase the entropy production rates, and it would be plausible to expect these two factors could dominate for a net increase in Σ_{mat} and Σ_{tran}. The planetary entropy production rate is set by inverse difference between the solar temperature (fixed) the emission temperature (increasing), which decreases, and the fraction of radiation thermalised rather than scattered, which increases. The latter effect is expected to dominate for an increase in Σ_{planet} since the entropy difference between scattered and re-emitted radiation is so significant.

When the greenhouse gas concentration is increased, the planetary entropy production rate is expected not to change because the fraction of radiation absorbed, F, is unchanged and so, although the location of T_C^* is different, its temperature is (approximately) fixed at the emission temperature. The decreased efficiency (increased 'resistivity') of internal radiation in transferring energy suggests more energy will be transferred by the parallel material processes which would cause an increase in Σ_{mat} relative to Σ_{tran}. The increasing surface temperature and fixed T_C^* suggests an increased difference in inverse temperatures, which paired with a fixed F suggests an increase Σ_{tran} and a further increase in Σ_{mat}.

If the lapse rate is changed by a drying of the atmosphere, the surface warms but the T_C^* and F are again unchanged, so Σ_{planet} is not expected to change. The transfer entropy production rate ought to again increase because of the increased difference $1/T_C^* - 1/T_H^*$ and the fixed F. The effect on Σ_{mat} is more complicated: it is expected to decrease relative to Σ_{tran} because the less efficient material transfer processes will favour internal radiation. However, the increase in inverse temperature difference points to an increase in both transfer and material entropy production rate and which factor will dominate in Σ_{mat} is not clear.

4.4 Results: entropy production rates under climatic changes on Earth

Armed with a conceptual model of the climate and predictions, we now return to the ARCM specified in Section 4.2 to simulate climate changes and measure how the entropy production rates actually respond. As these three types of climate changes are considered – changes in the global albedo, the greenhouse effect and

surface. Also note that the humidity does not change the optical properties of the atmosphere in this model, though that is a feature of Earth's climate.

the moist adiabatic lapse rate – any feedbacks, for example of surface temperature on water vapour and clouds, are intentionally not featured so that the first-order response can be identified. It is also worth noting that only the re-equilibrated state of the perturbed climate is modelled, not the time-dependent transient response.

The results from the different modes of climate change are compared as a function of the surface temperature change they imply[10] and are explored from three vantage points. Firstly, the vertical profiles of temperature, energy flux and heating rates given by the ARCM under a surface temperature increase of $5.4\,\mathrm{K}$ from $287.5\,\mathrm{K}$ to $292.9\,\mathrm{K}$ by each climate change are compared in Figure 4.5. In the first row, a decrease in the total albedo from 0.30 to 0.25 is shown. The second row focuses on a 25% increase in total the longwave optical depth to simulate an increase in the greenhouse effect, with a total optical depth of 2.45 compared to 1.96 in the pre-industrial case. Finally, in the third row, a change in the lapse rate parameter a is shown, from 0.60 to 0.73, to model changing atmospheric humidity. The atmospheric humidity change is only with respect to convection: the change in the prevalence of water vapour as a greenhouse gas is not reflected in this simple model.

Although the surface temperature is identical in these three perturbed climate states, the heat fluxes and temperature profiles differ significantly because each climate change has a different impact on how energy is transported through the system. In the first column of Figure 4.5 it can be seen that the tropospheric temperature profiles are the same in the albedo and greenhouse gas change cases, while the stratosphere cools in the GHG case but warms in the albedo case. The solar radiative flux (yellow curves, second panel) and heating rates (third panel) are preserved for the reduced moisture and GHG cases but increased in the reduced albedo case. The location of the cooling to space (blue curve, third panel) shifts higher in the atmosphere for a change in GHG but is close to unchanged in the other two scenarios, though there is a marked increase in the amount of cooling to space and upwards longwave radiation in the reduced albedo (increased absorptivity) case because of the increased flow of energy through the system. The trend in internal radiation echoes this, with a shift upwards and increase in the peak heating in the GHG case and an increase in the albedo change case. In the case of the drier convection, more internal radiative heating is delivered lower in the atmosphere as the radiative-convective boundary shifts lower.

Secondly, these differences are also picked up by the entropy production rates and related variables, as tabulated in Table 4.1.

Figure 4.6 gives a third way of visualising the differing impacts of the three classes of climate changes. It shows the change of the entropy-related variables as a function of the degree of climate change (as measured by the surface temperature), emphasising the trends and scaling between variables. Taken together, these paint a rich but complicated picture of entropy variables as global climate change metrics. Drawing out and understanding the results will be the focus of the rest of this section.

Can we use these results to understand why these climate changes influence the global entropy production

---

[10]This is chosen because of the privilege we give in the climate change community to the GMST as a climate change metric.
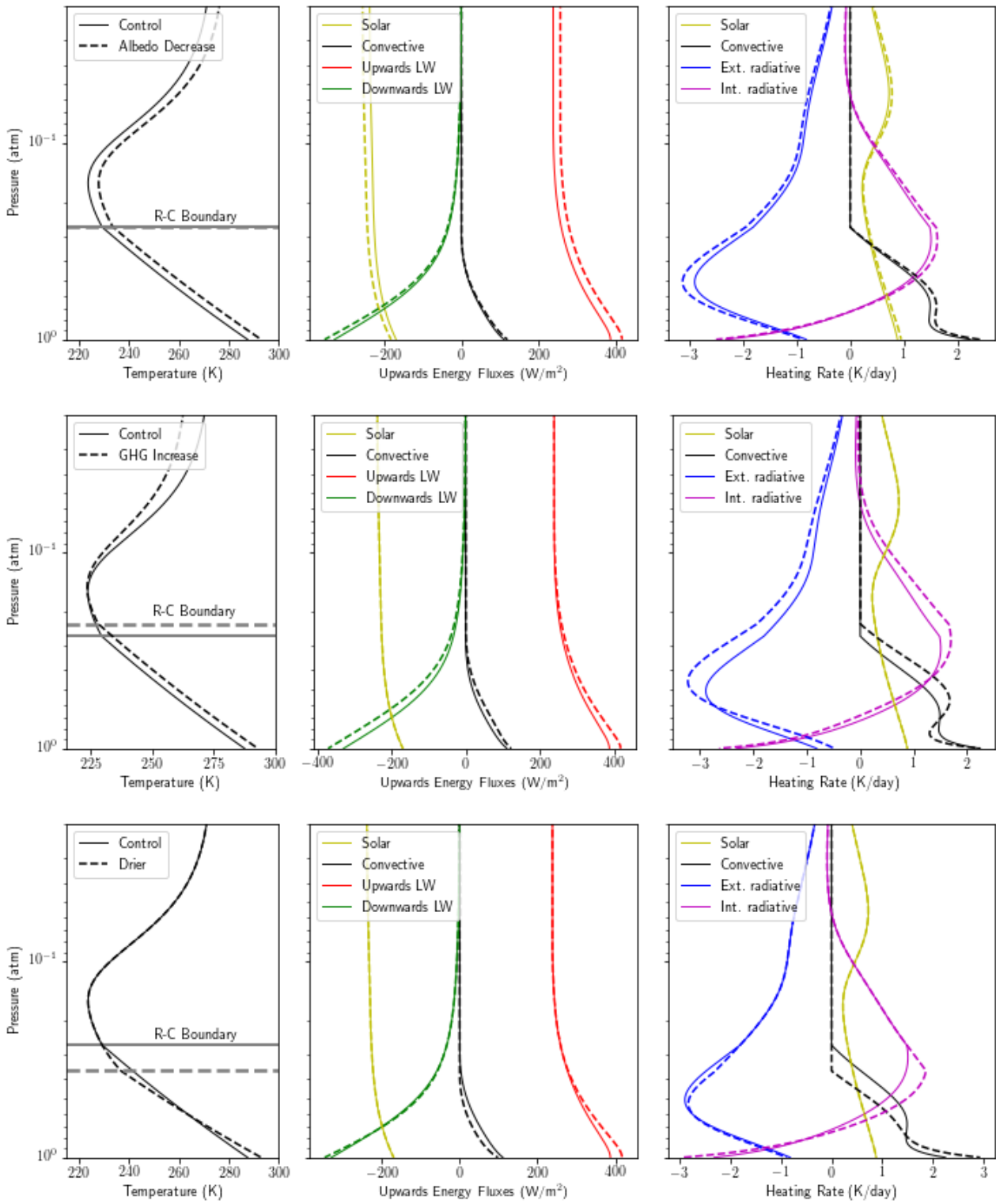
Figure 4.5: The temperature (first column), energy fluxes (second column) and heating rate (third column) atmospheric profiles derived from the analytic radiative-convective model for the control climate and a case in which the global albedo has been decreased from 0.3 to 0.25 (first row), total column optical depth increased from from 1.96 to 2.45 (second row) and adiabatic lapse rate moisture parameter a increased from 0.60 to 0.73 (third row), such that there is an identical surface temperature increase of 5.4K. The entropy production rates and related variables resulting from these climate states are tabulated in Table 4.1.

rates respond in the way they do? The simplest to examine is the planetary entropy production rate, as this is

approximately a function of the fraction of the incident solar radiation which is scattered and the temperature

	Control	Albedo Decrease	GHG Increase	Drier Convect.
T_{surf} (K)	287.5	292.9	292.9	292.9
T_{tp} (K)	223.7	227.9	223.5	223.7
F_{mat} (W/m^2)	111.2	119.9	122.7	98.5
T_{mat}^{in} (W/m^2)	287.5	292.9	292.9	292.9
T_{mat}^{out} (W/m^2)	268.7	273.8	270.3	275.7
η_{mat} (%)	6.54	6.54	7.71	5.87
Σ_{mat} (mW/m^{2}K)	27.1	28.6	35.0	21.0
F_{tran} (W/m^2)	238.5	257.0	238.5	238.5
T_{tran}^{in} (W/m^2)	279.5	284.8	284.3	283.3
T_{tran}^{out} (W/m^2)	256.8	261.6	256.9	257.2
η_{tran} (%)	8.13	8.13	9.64	9.21
Σ_{tran} (mW/m^{2}K)	75.5	79.9	89.5	85.4
F_{planet} (W/m^2)	340.7	340.7	340.7	340.7
T_{planet}^{in} (W/m^2)	4334	4334	4334	4334
T_{planet}^{out} (W/m^2)	250.8	241.3	250.8	250.8
η_{planet} (%)	94.21	94.43	94.21	94.21
Σ_{planet} (mW/m^{2}K)	1280	1333	1280	1280

Table 4.1: The values of the entropy-related variables are tabulated for three types of climate changes which result in the same surface temperature change. The unchanged case (first column) is contrasted with the results in a climate with a decreased global albedo (second column), an increased greenhouse effect (third column), and a decrease in humidity influencing the lapse rate (fourth column). The values are explored in detail in the text.

of the cooling to space, because the total energy flux incident on the planet, F_{planet}, and the temperature of the sun are unchanged by any climatic changes. As shown in Table 4.1 and the third panels of Figure 4.6, the only case where the planetary entropy production rate changes appreciably is the case where the fraction of scattered radiation is altered, where increased absorption causes an increase in the total entropy production rate, as predicted. The planetary entropy production rate is practically unchanged by the greenhouse gas and drier convection climate change because the shape of the outgoing spectrum can only change minutely given the requirement for a fixed total energy flux.

The transfer entropy production rate, on the other hand, increases with surface temperature in all three cases, with the most significant increase in the greenhouse gas increase case. The albedo-mediated increase of $4.4\,\mathrm{mW/m^2K}$ from $75.5\,\mathrm{mW/m^2K}$ to $79.9\,\mathrm{mW/m^2K}$ occurs without any change in the efficiency η_{tran} so must be driven by the increase in flux F_{tran}. The emission to space temperature T_{tran}^{out} ($=T_C^*$) is nearly fixed in the GHG and drier convection cases, but the temperature T_{tran}^{in} increases more steeply in the GHG case than the drier convection case (Table 4.1 and Figure 4.6, second panel). This is explained by the coolness of the upper troposphere in the drier convection case relative to the GHG case, and explains the smaller increase in efficiency in the drier convection case relative to the GHG case and the entropy increase to $\Sigma_{tran} = 85.4\,\mathrm{mW/m^2K}$ rather than the $\Sigma_{tran} = 89.5\,\mathrm{mW/m^2K}$ measured in the increased GHG case.
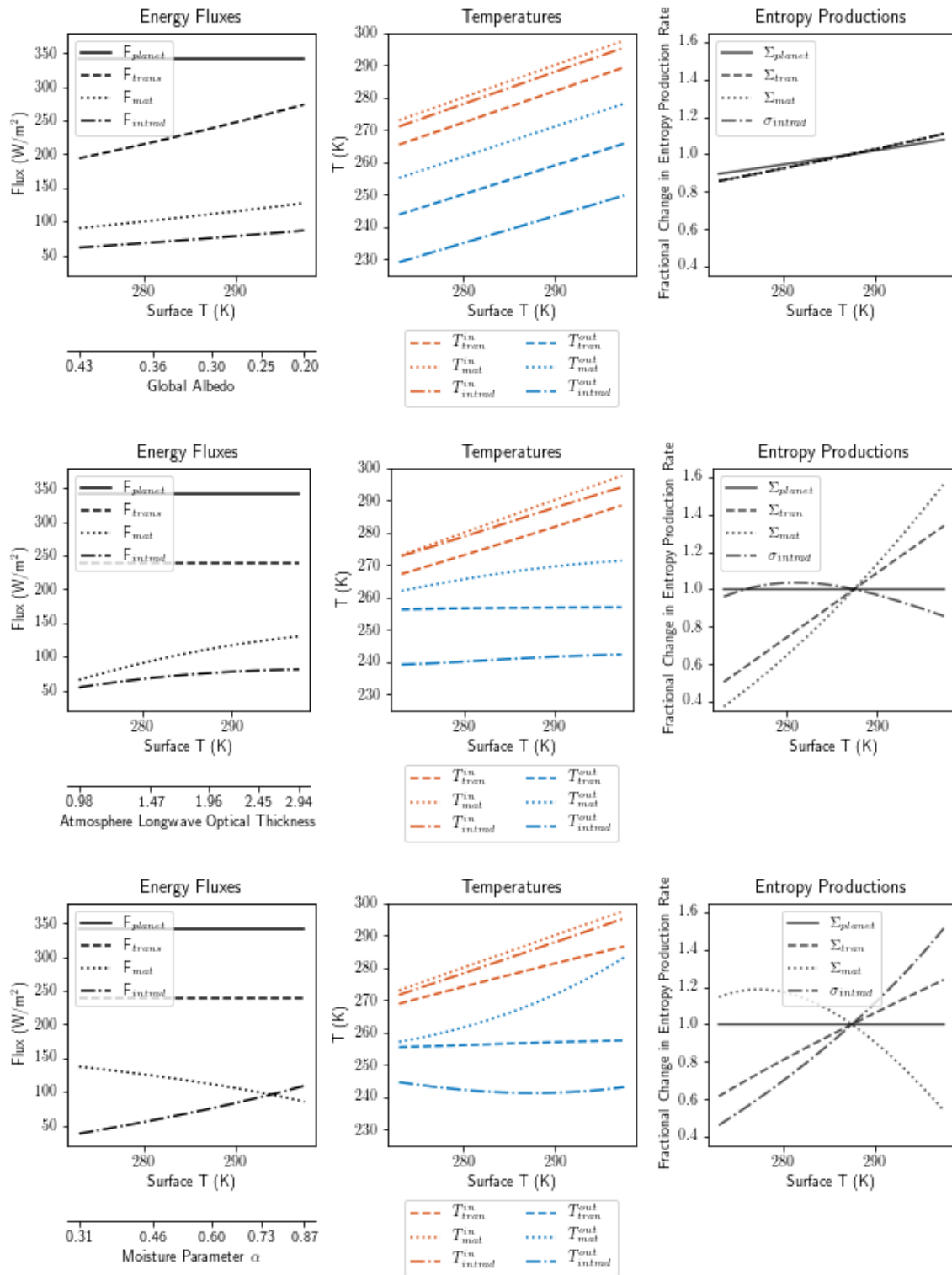
Figure 4.6: The response of the entropy-related variables to climate changes by three mechanism: varied global albedo (first row), varied greenhouse effect (second row) and changes in the moisture of the convecting air (third column). The first column shows the energy flux through the planetary, transfer and material systems, as well as the energy transferred by internal radiation. In the second column, the temperature of input and output of energy into the material, internal radiative and transfer systems are graphed, while in the third column the fractional change in the entropy production rates are shown. In all cases, the same surface temperature range is explored and the horizontal axis in the first column represents the change in the model parameters which achieves this.

The division of entropy production between material and internal radiative heating processes and how they combine to produce the total transfer entropy production in each of the three climate change scenarios is particularly interesting. In the albedo-mediated climate change case, the fraction of the entropy production which is due to internal radiative versus non-radiative process stays the same and so the increase in the material entropy production rate is in proportion to the increase in the transfer entropy production rate. As with η_{tran}, the efficiency $\eta_{mat} = 6.54\%$ is unchanged[11] but as the amount of solar radiation absorbed and thermalised rather than scattered increases by 8%, the effective emission temperature increases by 1.9%, which causes an increase in T_{tp}, T_{mat}^{out} and T_{tran}^{out} and a slightly larger increase in T_{mat}^{int} and T_{tran}^{in}, by $\Delta T_{mat}^{in} = 5.5\text{K}$ and $\Delta T_{tran}^{in} = 5.2\text{K}$ respectively compared to $\Delta T_{mat}^{out} = 5.1\text{K}$ and $\Delta T_{tran}^{out} = 4.8\text{K}$. The higher absolute temperatures would give a decrease in the entropy production rate by 2%, but the increase in energy flux dominates for an overall 6% increase in Σ_{mat} and Σ_{tran}. That these remain in proportion to each other is evident in the third column of the first row of Figure 4.6.

When the greenhouse gas concentration is increased, the amount and location of solar energy absorbed is not changed, but the transport of thermal radiation through the atmosphere is affected. As the peak cooling to space shifts higher in the atmosphere, the amount of heat transported by net internal radiation from the surface decreases from $43.0\,\text{W/m}^2$ in the control case to $39.3\,\text{W/m}^2$. The convective heating necessary to maintain the lapse rate given these altered radiative heating rates is also shifted upwards in the atmosphere and amplified. Although F_{tran}, the total energy transferred, is fixed, the increased optical thickness inhibits net heat transfer by internal radiation, increasing the fraction of energy transferred by material processes (F_{mat}/F_{tran}) by 11% from 0.46 to 0.51. The increase in the surface temperature with a fixed effective emission temperature and total flux through the system explains the sharp increase in Σ_{tran} by 18%. The increased flux through the material system results in an even more dramatic 29% increase in Σ_{mat}.

In the drier convection case, the material entropy production behaves in an opposite way to the GHG increase, which is to be expected given that the GHG case is a reduction of efficiency of the radiative 'resistor' while the drier convection is a reduction of the efficiency of the dominant material heat transfer mechanism. This is reflected in the reduction of the material efficiency η_{mat} from 6.54% to 5.87% in the drier convection case. The energy transferred by material processes decreases while that transferred by internal radiation increases, which causes the decrease in material entropy production rate relative to the control case. There the amount of entropy produced by internal radiative processes increases steeply, in order to sum to the total increase in transfer entropy production rate observed.

These results validate the predictions offered in Section 4.3.4, establishing that the resistor analogue model can be used as a conceptual explanation for why the entropy production variables respond as they do with climate changes. The F, T and Σ variables shed light on each other to explain the results and provide a fuller picture

---

[11]It is striking that the increase in temperatures is exactly the amount necessary to preserve the efficiency η; I cannot explain why this should be the case.

of the entropic behaviour of the climate.

4.5 Significance and implications

The climatic response of the entropy production variables is useful information in its own right and, furthermore, the results strikingly confirm the predictions made using the resistor-inspired model, which lends credence to that perspective. We now return to a discussion of the significance and implications of the results in the broader context of the entropy production field. The first aspect is a comparison with similar results found by researchers in other experimental set-ups, which is provided in Section 4.5.1. The second conclusion concerns the interpretation and physical insightfulness of each entropy production perspective. An argument for the usefulness of the transfer entropy production rate in particular is given in Section 4.5.2.

The results also inform how the global entropy production rate could be used as a *diagnostic* of the climate state. In Section 4.5.3, a particularly important application of this approach is explored with the analysis of solar radiation management. This informs a discussion of the potential role of entropy production variables as climate change metrics, in Section 4.5.4.

4.5.1 Comparison to previously published climate change and entropy results

As the transfer entropy production rate is relatively novel, there is very limited existing research about how it might change with climate changes. In *Bannon and Lee* [2017], the entropy production implied by an energy flow between the solar absorption temperature and the effective emission temperature is studied in an energy balance model similar to that in Chapter 3. This is a close upper bound for the transfer entropy production rate (recall that T_{out}^{tran} is only slightly above T_{eff}), although it is used in the paper as an upper bound for the material entropy production rate (which it is, but much less meaningfully). Unfortunately, the paper focuses on the response to specific features of the climate's state changing independently (albedo, absorption and emission temperature) rather than on the net impact of a climate state change which includes a change in all of these features in tandem. The results are therefore not easily comparable to those found here.

Similarly, the climate-response of the planetary entropy production rate has not been studied in detail before. Many authors have pointed out that a more isothermal output temperature increases the flux of entropy carried by radiation [*Lesins*, 1990; *Stephens and O'Brien*, 1993]. *Li et al.* [1994] estimate entropy fluxes in clear and cloudy skies via a radiative-convective model and find a lower outgoing entropy flux with increased cloudiness, which matches our decrease in planetary entropy production with an albedo increase. A vertical column radiative-equilibrium model similar to the one used in this chapter but without any convection and with only one channel for shortwave absorption was used in *Wu and Liu* [2010b] to obtain analytic calculations of the

planetary entropy production fluxes throughout the vertical atmosphere. Their results suggested a decrease in the net atmospheric outgoing entropy flux by 4% as the longwave optical depth is doubled, which is in contrast to the consistency I find in the greenhouse gas case. However, it is unclear how the authors separate the atmospheric from the surface entropy flux contributions at the top of the atmosphere, and it is possible that this or other approximations being made are contributing to this disagreement. The total top-of-atmosphere entropy flux I calculate is 40% higher than the atmospheric value they report.

There has been more thorough investigation of the response of the material entropy production rate to changes in the climate system.

The role of humidity in the entropy production of a moist atmosphere is explored in *Pauluis and Held* [2002a] and *Pauluis and Held* [2002b]. There it is found that, in a drier atmosphere, more entropy is produced by kinetic energy generation and dissipation than is in an atmosphere where water is present, but that the total material entropy production is dominated by hydrological cycle processes. These results are consistent with our findings that in a drier atmosphere, where moist processes are limited, there is a lower material entropy production rate. It is interesting to note that that our results suggest that the transfer entropy production rate increases in a drier, warmer-surfaced atmosphere even though the material entropy rate decreases. This indicates that more changes are happening to the entropy producing processes upon the introduction of moisture than are explored in these material-processes-focused papers.

In *Lucarini et al.* [2010b] the effect on the material entropy production rate of an increase in the CO_2 concentration and in *Lucarini et al.* [2010a] of changes in the solar isolation are studied. The intermediate-complexity Planet Simulator model is used, and entropy production calculated following *Fraedrich and Lunkeit* [2008]. An increase in the material entropy production rate with increasing surface temperature is found in both cases, of $0.4 \, \text{mW/m}^2\text{K}$ per kelvin for a greenhouse gas change and $1 \, \text{mW/m}^2\text{K}$ per kelvin for the albedo-mediated case. These are in the same direction as my with my results and of a similar order of magnitude but of different relative sizes: I find a $1.4 \, \text{mW/m}^2\text{K}$ per kelvin and $0.3 \, \text{mW/m}^2\text{K}$ per kelvin change for the greenhouse gas and albedo cases respectively. A reduction of the climate efficiency is also found in both cases, which is at odds with our results showing an increase of η_{mat} with a greenhouse gas increase, albedo decrease and wetter convection. However, there is not enough detail about how the temperatures for the efficiency are calculated in these papers to be certain that these results are comparable.

Singh and O'Gorman [2016] study entropy production due to different material sources in a cloud-resolving 3D model. The greenhouse gas concentration is varied and they find an increase in the material entropy production rate with surface temperature, which correlates with an increase in a moister atmosphere. These are consistent with our results.

Labarre et al. [2019] use MEPP to complete a partially-constrained radiative-convective model and study how the MEPP solution changes as the concentration of CO_2 and O_3 are varied. This is a different enquiry to what

is addressed here.

Lembo et al. [2019] study the RCP8.5 scenarios across CMIP6 models and find an increase of material entropy production rate with greenhouse gas increase.

Recently, *Kato and Rose* [2020] have attempted to derive the response of material and transfer entropy production rates to changes in the global albedo by regressing the inter-annual variability of net outgoing entropy fluxes (material and transfer) against shortwave absorption. They have interpreted their results as implying a decrease in entropy production with increasing absorptivity, which would run contrary to the results outlined above. However, their model does not account for storage adequately, which increases during apparent low-production years. Their results are re-examined further in Section 5.5.5.

4.5.2 Advantages of the transfer perspective in capturing climate state

As exemplified in the increased greenhouse gas and drier convection climates, the planetary entropy production rate is not sensitive to changes in the climate for which the albedo remains fixed, as the outgoing entropy flux is approximately determined by the (unchanged) effective emission temperature and the incoming entropy flux is set by the solar temperature. In fact, an atmosphere-less isothermal rock, with identical solar flux and albedo, will have a similar planetary entropy production rate to a planet with a greenhouse effect. This suggests that the planetary perspective is not a good candidate for studying the climate.

The material entropy production rate is, of the three, the most focused on processes relevant to human experience: it is material processes such as the hydrological cycle or convective motion, and not the internal radiation, which directly feature in the weather we experience. However, not all material processes are equally relevant, and it can be more meaningful to consider them separately; for example, the contribution from frictional dissipation around falling precipitation is twice that from atmospheric motions [*Singh and O'Gorman*, 2016], but has a very different significance. The material sub-processes, and even the total material tally, are interdependent portions of a larger system and the energy carried by them can vary because of changes in other parallel processes, such as in internal radiation. This makes interpreting changes in material entropy production rate alone challenging, as they could be due to changes in the proportion of energy transferred rather than in the efficiency or temperature differences.

The material perspective is also limited in its perception of the greenhouse effect, as this is a fundamentally radiative phenomenon. To demonstrate this, consider the extreme case of a climate without material processes but with a variable greenhouse effect. A surface temperature change caused by an increase in that greenhouse effect would be one which Σ_{mat} would be powerless to resolve, material processes being identically null in both cases, even though it would seem to be a climatologically-relevant change. Thus the total material entropy production rate, though meaningful, does not stand out as the natural climate-summarizing global entropy

variable.

We argue that the transfer entropy production rate is of more compelling value from the perspective of the climate system. The F_{tran}, the amount of energy which is absorbed by the planet, is a natural climate-variable, as is the temperature difference between where shortwave radiation is absorbed, T_{tran}^{in}, and where longwave radiation leaves the planet, T_{tran}^{out}. The transfer rate is sensitive to climate changes and captures all processes which move heat in the planet, without distinguishing between mechanism. That the fraction of the transfer entropy production by material processes stays fixed as the albedo is changed but varies as the greenhouse gas concentration or the latent heat release during convection changes suggests that the transfer rate can be leveraged to explain the material entropy production rate and the entropy production due to internal radiation as subsidiary components. Added to that, the consistent increase of Σ_{tran} with surface temperature makes it a promisingly familiar variable.

4.5.3   Application: limitations of solar radiation management

The results outlined in Section 4.4 have an additional significance when they are applied to the question of how the pre-industrial climate state might be restored following the anthropogenic climate emissions of the past century. With surface temperature as the main metric used to evaluate climate state, an increase in the global albedo – solar radiation management (SRM)– appears to counteract the effect of an increased greenhouse effect. However, the entropy variables can distinguish between the climate effects of different modes of warming, underlining that restoring surface temperature is not the same as restoring the climate. Because of the relationship between entropy production and the irreversible activity in the climate, the perspective entropy production rates supply are likely to be far from disconnected from the human experience.

4.5.3.1   Results

To investigate this, the ARCM is studied with an albedo increase to 0.35 as well as an elevated greenhouse effect (an increase in the longwave optical depth by 25%) such that surface temperature is restored. This results in the atmospheric profile shown in Figure 4.7 and entropy variables as tabulated in Table 4.2.

When solar radiation management is used to negate the surface warming of an increase in the greenhouse gas concentration, there is both an decreased flow of energy through the system (from the albedo change) and an increased resistivity in the internal radiative transfer and height of emission to space (from the optical thickness change). These effects on the entropy variables are combinations of the effects seen in Section 4.4, as can be seen by a careful examination of Figures 4.7 and 4.8 alongside Figures 4.5 and 4.6. Although the tropospheric temperature profile is identical in the control and SRM cases, the internal energy transfer by radiation is reduced by the elevated greenhouse gas concentration which leads to a clear change in the convective energy flux
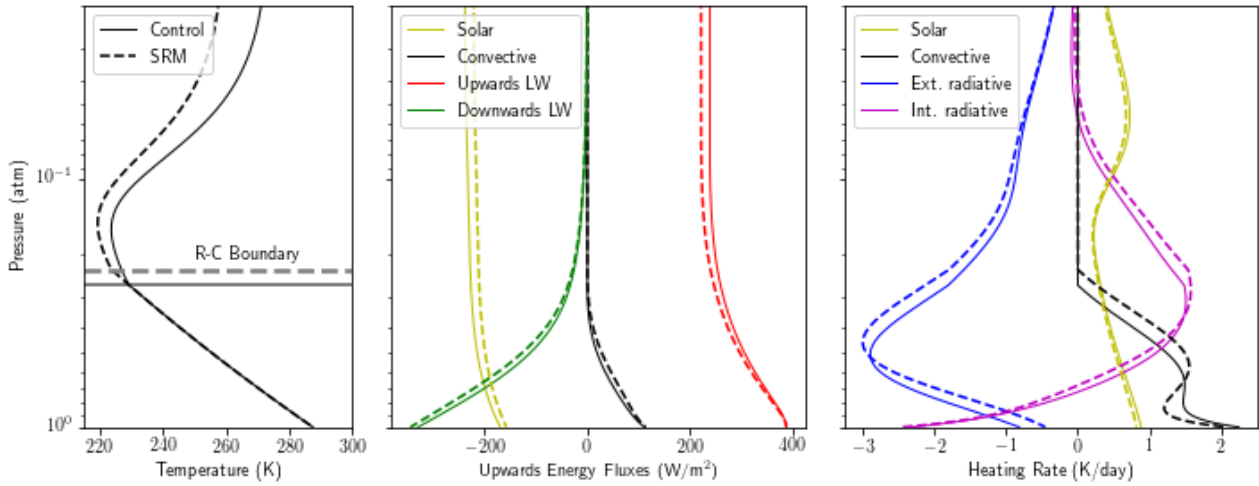
Figure 4.7: The temperature (first column), energy fluxes (second column) and heating rate (third column) profiles derived from the analytic radiative-convective model for the control climate and a case in which the surface temperature is restored by increasing the albedo to 0.35 to balance a 25% increase in greenhouse effect, as in a basic solar radiation management intervention.

	Control	SRM
T_{surf} (K)	287.5	287.5
T_{tp} (K)	223.7	219.4
F_{mat} (W/m^2)	111.2	113.9
T_{mat}^{in} (W/m^2)	287.5	287.5
T_{mat}^{out} (W/m^2)	268.7	265.3
η_{mat} (%)	6.54	7.71
Σ_{mat} (mW/m^{2}K)	27.1	33.1
F_{tran} (W/m^2)	238.5	221.3
T_{tran}^{in} (W/m^2)	279.5	279.0
T_{tran}^{out} (W/m^2)	256.8	252.1
η_{tran} (%)	8.13	9.64
Σ_{tran} (mW/m^{2}K)	75.5	84.6
F_{planet} (W/m^2)	340.7	340.7
T_{planet}^{in} (W/m^2)	4334	4334
T_{planet}^{out} (W/m^2)	250.8	260.5
η_{planet} (%)	94.21	93.99
Σ_{planet} (mW/m^{2}K)	1280	1229

Table 4.2: The values of the entropy-related variables under a solar radiation management scenario, corresponding to the case plotted in Figure 4.7.

and heating rate in the troposphere, as can be seen in the third panel of Figure 4.7. This is identified in the increased material entropy production, which is $\Sigma_{mat} = 33.1\,\text{mW/m}^2\text{K}$, larger than the pre-industrial value of $27.1\,\text{mW/m}^2\text{K}$ but smaller than the GHG-only case of $35.0\,\text{mW/m}^2\text{K}$. The total absorbed radiation (F_{tran}) is

reduced compared to the pre-industrial case, but the fraction transferred by material processes is still elevated at 0.51 due to the greenhouse gases present, which explains intermediate value of F_{mat}. The reduced F_{tran} is counteracted by the increased inverse difference between T^{in}_{tran} and T^{out}_{tran} due to the reduction in the effective emission temperature to result in a net increase in the transfer entropy production rate of 12%. Even the planetary entropy production rate is not restored, but decreases due to the increase in the scattering fraction.
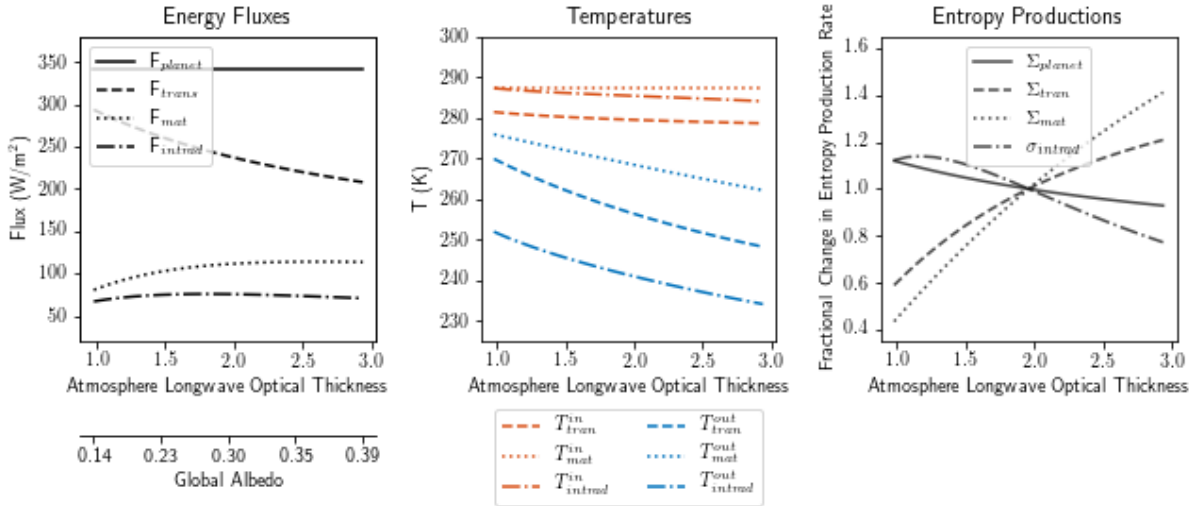

Figure 4.8: Entropy production variables as a function of the degree of greenhouse gas increase and compensating solar radiation management (increase in global albedo). In the first panel, the energy fluxes are shown, in the second the influx and out-flux temperatures and in the third the entropy production rate relative to those in the unperturbed climate state. The control case of Table 4.2 has an optical thickness of 1.96 and the SRM case of 2.45.

4.5.3.2   Discussion

The results offered here are not enough to provide conclusions on the impact of SRM in the true atmosphere because only the first-order responses have been considered. However, they highlight that the entropy production metrics are capable of picking up on aspects of the climate state that temperature alone cannot. The heat transfer aspects of the weather which are of most interest to human concerns (wind, rain) are non-radiative and so the increase in the material entropy production rate underlines that the climate may not be able to be restored by SRM in important ways.

Precipitation is the main non-temperature variable studied in the SRM and climate response literature. As explored in *Samset et al.* [2016] there that there are two ways in which an increase in greenhouse gas concentration affects the precipitation: a fast response due adjustments in the atmosphere with the radiative imbalance, which reduces the precipitation, and a slow response which is an increase in precipitation with the surface temperature increase *Bala et al.* [2010]. In a SRM scenario, in which stratospheric sulphur injections were used to compensate for the surface temperature change [*Laakso et al.*, 2020], the slow response is suppressed and there is an overall decrease in precipitation compared to the unperturbed state.

How does this map to the entropy results? In our simple ARCM SRM scenario, the material and transfer

entropy production rates both increase compared to the unperturbed state, which would seem in conflict to these studies. However, although precipitation plays a major role in the material entropy production rate, the quantity of entropy produced by precipitation is not necessarily a function of the amount of precipitation. This is because, as highlighted in Figure 4.8, the temperature difference within the atmosphere varies as well as the amount of energy carried by non-radiative processes in this SRM scenario, and thus a similar amount of rain depositing might cause more entropy production if it were carrying energy over a larger temperature difference. An aspect that is corroborated in our results is that the material entropy production rate in the SRM scenario decreases relative to the GHG-increase-only scenario, as the precipitation decreases with SRM in more complex model studies [*Bala et al.*, 2008].

4.5.4 Entropy production as a climate change metric

The climate is an unavoidably complicated system, and in considering climate changes, society is interested in many aspects of its behaviour. Nevertheless, there has been a single dominant metric which we use to quantify the climate state: the global mean surface temperature. Temperature increases with the stored energy within the system and so is attractive as an integrated measure of the top of atmosphere energy imbalance.

The results in Sections 4.4 and 4.5.3 underline that very different climates can arise with the same surface temperature change. This is not surprising in a system with as many degrees of freedom as the climate but is significant to how we communicate and think about the climate. The entropy variables offer a metric which, like global mean surface temperature, is a scalar summary the climate, but reveals different aspects. The results suggest that using entropy production rates, particularly the transfer production rate and its internal radiative and material sub-components, in addition to the global mean surface temperature would shed more light on the climate state from a diagnostic point of view.

4.6 Conclusion

The analytic radiative-convective model of *Robinson and Catling* [2012, 2014]; *Tolento and Robinson* [2019] is a versatile tool for investigating how the entropy production rates capture different climate states, in particular via the mechanism of albedo change, greenhouse gas change and moisture changes in convection. In all cases, the transfer entropy production rate increases with surface temperature, but the fraction of transfer entropy production due to material processes decreases when latent heating is suppressed, stays the same with albedo changes and increases with an increased greenhouse effect. The planetary entropy production rate is of limited use in resolving climate changes which do not involve changes the scattered fraction of solar radiation.

The conceptual model introduced which builds on the notion of the climate as resistors in parallel was successful in anticipating and explaining the response of the climate system to the variety of changes, both in terms

of surface temperature changes and entropy-related variables. It is based on a different paradigm from the energy balance models, emphasising the temperature differences necessary to convey energy through the system, leveraging the entropy-based perspective to provide a new lens on the climate system.

In both the conceptual model and the numerical results, the transfer entropy production rate stood out as a useful summary variable for the climate's entropy production state, within which the entropy production due to internal radiative and non-radiative processes are meaningful subsets. This was emphasised by the result the material and transfer efficiencies were a function of greenhouse gas concentration and lapse rate parameter but not albedo, as was the ratio of F_{mat}/F_{tran} and $\Sigma_{mat}/\Sigma_{tran}$

Finally, the fact that manipulating the planet's albedo to balance a greenhouse gas change can restore surface temperature while not restoring these entropy metrics underlines that there is useful additional information in these global scalar variables for climate change discussions and decision-making. Entropy production rates have a more direct relationship to the motion and flows in the climate than does the global mean surface temperature and, although they are less familiar and so less easy to interpret, they warrant further exploration as a supplementary climate diagnostic to allow for thorough summaries of the climate state.

This chapter is immediately applicable to the project of using the entropy production rate as a diagnostic variable. We have proved that entropy production rates are highly sensitive to climatic changes and have offered insight into their behaviour.

Chapter 5

Computing Earth's Entropy Production Rates

So far in this thesis, global entropy production rates have been estimated with simplified models of the climate. This has been useful: when the point to be made is a definition or an explanation, the simpler the model is, the easier it is to understand the implications. However, we cannot be sure that these simpler models behave like the true climate in whatever ways are critical to a MEPP-like theory exactly because we do not know on what such a theory would depend. Also, the potential of entropy production as a tool for characterising the actual climate state relies on first measuring it in the observed climate. The ability to calculate, track and understand entropy production in the Earth's climate is a necessary step towards leveraging the entropy production rate variable, both for predictive and diagnostic purposes.

This chapter is split into two parts. In the first, I explain the approach for making high-precision estimates of entropy variables from atmospheric temperature and composition profiles via radiative transfer calculations on which I worked during the early part of my PhD (Section 5.1.1). This is applied to a standard atmospheric column in Section 5.1.2 and the entropy budget results are compared to those estimated in simplified climate models discussed in the previous chapters.

My initial aim was to apply this tool column-by-column to gridded global datasets, as discussed in Section 5.2. The other approaches which had been explored in the literature are discussed in Section 5.2.1, and the route we planned is explained in 5.2.2. The available data sources from which entropy production rates might be estimated are explored in Section 5.2.3. The significant limitations posed by the computational demands of this approach, which have stymied it for the time being, are addressed in Section 5.2.4 and possible workarounds explored.

During the latter part of my PhD, a dataset was published by the CERES team (*Kato and Rose* [2020], hereafter `KR2020`) which calculates column-wise entropy fluxes from radiative transfer calculations in the

observationally-based CERES SYN1deg dataset. This is a much more developed version of approximately what I had been trying to create (albeit only for a single observational dataset, and without measuring the planetary entropy production rate), and so I pivoted to apply what I had learned from my attempt to see what I could glean from or add to in their project.

This is the focus of the second part of this chapter. In Section 5.3, the CERES entropy data product is introduced in the context of my single column approach. Of particular note is the verification which was conducted in collaboration with Kato and Rose by running our independent, single column entropy budget scripts on an identical simple atmospheric column (Section 5.3.1).

In Section 5.4, the issue of interannual entropy storage, which arises when analysing any system which is not in energy balance (like the changing climate), is explored in the context of the `KR2020` dataset. In the original `KR2020` discussion, entropy storage was not properly accounted for, which leads to some erroneous conclusions. A careful explanation of how to adapt the entropy flux datasets to estimate entropy production rates via estimates of entropy storage rates is offered in this section, building on work published in *Gibbins and Haigh* [2021].

The storage-corrected `KR2020` CERES SYN1deg dataset can then be used to explore entropy flux and production in the climate system. In Section 5.5.1, improved estimates of the annual, globally-averaged entropy production rates and related variables are given. The global entropic temperatures are studied in particular detail in Section 5.5.2, and compared to the global mean surface temperature metric. Hemispheric symmetries and asymmetries of entropy production variables are explored in Section 5.5.3, followed by the seasonal variation in Sections 5.5.4. In Section 5.5.5, the negative correlation between global albedo and entropy production rate found in `KR2020` is re-examined and it is found that accounting for storage reverses the published results, uncovering a positive correlation. Finally, climate change responses which are hinted at during the satellite record are explored in Section 5.5.6. Taken together, these give a new and intriguing picture of the climate as an entropy-producing system.

A discussion of error estimation and the results in the context of the existing literature is given in Section 5.6. Finally, some concluding remarks are offered in Section 5.7, including a discussion of potential further research questions.

5.1   Idealised single-column entropy calculations

Measuring the rate of entropy production in the climate system *directly* by summing the irreversibility due to all constituent processes requires careful analysis of a process-resolving model with high spatial resolution and temporal evolution. Even then, it is hard to avoid omitting entropy-producing sources which impact the

behaviour of the modelled climate but are not explicitly parametrised – for example, numerical diffusion [*Johnson*, 1997; *Woollings and Thuburn*, 2006]. An *indirect* approach is much more versatile and reliable, although it can only provide estimates of the globally-aggregated Σ_{mat}, Σ_{tran} and Σ_{planet} and cannot be used not to separate the contributions of the component σ_i (except $\sigma_{intrad} = \Sigma_{tran} - \Sigma_{mat}$). In the indirect approach, the radiative heating rates and emitted spectra are estimated from an instantaneous vertically-resolved temperature, composition and pressure snapshot of the atmosphere, which allows the rate of entropy flux into and out of the system to be calculated. Provided entropy storage within the system can be accounted for, the difference in flux and storage is the production rate. There is flexibility in this method, as it can be applied to an atmospheric profile derived from any modelled or observationally-based dataset.

In this section, we develop the indirect technique for a single atmospheric column. This work follows a similar approach to that taken by Nikolaos Koukoulekidis during a Imperial College Master's project in 2015 for the planetary entropy production rate, improving on it, re-writing it in `Python`, and extending it to calculate also the material and transfer rates.

5.1.1 Methodology

For this study, I have used `Libradtran` [*Mayer and Kylling*, 2005; *Emde et al.*, 2016], which is a freely available software package which offers a range of tools to perform radiative transfer calculations on atmospheric data. It is designed for high-precision calculations for a single atmospheric column, so is computationally expensive but also highly accurate.

Libradtran is a promising radiative transfer code to use because it is well established, but there are other comparable options. Recently, `Py4CAtS` has been ported to `Python3` and may offer more direct access to the variables of interest, particularly optical depth [*Schreier et al.*, 2019]. The line-by-line radiative transfer model `LBLTRM` is another option [*Clough et al.*, 2005]. Further work might make progress by reassessing which tool is most computationally efficient for calculating the required variables.

Which variables need to be calculated by the radiative transfer model in order to calculate the entropy fluxes? The planetary entropy fluxes are accessed by application of Equations 3.8 and 3.10 to the top-of-atmosphere radiation spectra, which are standard outputs of `Libradtran`. For the material entropy production rate, the net radiative heating and cooling are needed, which are also standard outputs. For the transfer rate, the incoming entropy flux is calculated as in Equation 3.24 from the net solar heating rate, which is a standard output. However, the outgoing transfer entropy flux requires calculation of cooling to space first via Equation 3.25. The cooling to space from each layer is not an output variable of `Libradtran`, so it must be calculated separately from the values which are available[1].

---

[1]Thanks are due to Bernhard Mayer who helped develop `Libradtran` and helped determine the best approach for calculating the cooling to space

Working monochromatically, the molecular absorption of each layer ($\Delta\tau_i$) can be extracted from `Libradtran`'s `verbose` outputs. There are, however, still some careful approximations that need to be made to deal with the vertical discretisation accurately. This is because the atmosphere has an optical thickness of 10^4 at some wavelengths and so it is impractical to divide it into a sufficient number of layers such that a small optical thickness can be assumed.

Suppose that the model layers are numbered from the top of the atmosphere downwards.

$$
\begin{array}{lll}
z_0 \ \rule{2cm}{0.4pt} \ & \tau_0 = 0 \\
\quad \Delta\tau_0 \\
z_1 \ \rule{2cm}{0.4pt} \ & \tau_1 \\
\quad \Delta\tau_1 \\
z_2 \ \rule{2cm}{0.4pt} \ & \tau_2 \\
\quad \Delta\tau_2 \\
z_3 \ \rule{2cm}{0.4pt} \ & \tau_3 \\
\quad \Delta\tau_3 \\
z_4 \ \rule{2cm}{0.4pt} \ & \tau_4
\end{array}
$$

The total optical thickness of the atmosphere(working monochromatically) is then:

$$\text{Optical Thickness} = \sum_i \Delta\tau_i \tag{5.1}$$

And the transmission from the surface to the top of the atmosphere is

$$\text{Transmission} = \exp\left(-\sum_i \Delta\tau_i\right) \tag{5.2}$$

There are discretisation challenges in expressing the transmission between layers because each layer has a finite thickness. It is therefore most sensible to calculate the value we need explicitly:

$$A_{i,j} = \text{energy emitted } \textit{from} \text{ layer i } \textit{to} \text{ layer j} \tag{5.3}$$

The units of $[A_{i,j}] = \text{W/m}^2$ is watts of energy transferred per m^2 of layers i and j.

The exact form for the heating due to emission from slab of height dz' at z' to height z is[2]:

$$h(z, z') = -\pi B(z')\frac{d^2 T(z, z')}{dz\,dz'}dz'$$

---

[2]Rodgers pg 47, third term in penultimate equation.

This must be integrated over all z' in the sources layer i and z in the sink layer j.

$$A_{i,j} = -\int_{z_i}^{z_{i+1}} dz' \int_{z_j}^{z_{j+1}} dz\, \pi B(z') \frac{d^2 T(z,z')}{dz\, dz'} dz'$$

$$= -\int_{z_i}^{z_{i+1}} dz' \pi B(z') \left[\frac{dT(z_{j+1}, z')}{dz'} - \frac{dT(z_j, z')}{dz'} \right]$$

$$= -\pi B(z_i) \left[\Big(T(z_{j+1}, z_{i+1}) - T(z_{j+1}, z_i) \Big) - \Big(T(z_j, z_{i+1}) - T(z_j, z_i) \Big) \right]$$

where have assumed that the temperature varies slowly enough that within a layer that $B(z') \approx B(z_i)$ is constant.

Consider the case $i > j$. Then

$$T(z_j, z_i) = \exp(-(\tau_i - \tau_j)).$$

Now the expanded line above can be re-written:

$$A_{i,j} = -\pi B(z_i) \left[\Big(\exp(-(\tau_{i+1} - \tau_{j+1})) - \exp(-(\tau_i - \tau_{j+1})) \Big) - \Big(\exp(-(\tau_{i+1} - \tau_j)) - \exp(-(\tau_i - \tau_j)) \Big) \right]$$

Now note that $\tau_{i+1} = \tau_i + \Delta\tau_i$ and similarly for j:

$$A_{i,j} = -\pi B(z_i) \Big(\exp(-(\tau_i - \tau_{j+1})) \Big) \left[\Big(\exp(-\Delta\tau_i) - 1 \Big) - \Big(\exp(-(\Delta\tau_i + \Delta\tau_j)) - \exp(-\Delta\tau_j) \Big) \right]$$

which can be rearranged to give:

$$A_{i,j} = -\pi B(z_i) \exp(-(\tau_i - \tau_{j+1})) \Big(\exp(-\Delta\tau_i) - 1 \Big) \Big(1 - \exp(-\Delta\tau_j) \Big)$$

$$= \pi B(z_i) \exp(-(\tau_i - \tau_{j+1})) \Big(1 - \exp(-\Delta\tau_i) \Big) \Big(1 - \exp(-\Delta\tau_j) \Big)$$

And recognising the first term term involving exponentials as the extinction due the layers between (but not including) the two layers i and j:

$$A_{i,j} = \pi B(z_i) \left[\exp \left(-\sum_{k \in (i,j)} \Delta\tau_k \right) \right] \Big(1 - e^{-\Delta\tau_i} \Big) \Big(1 - e^{-\Delta\tau_j} \Big) \tag{5.4}$$

An identical result emerges if $j > i$.

This is not as surprising as it first appears - this formula is just taking into account the finite thickness of the layers. Consider the familiar fact that the fraction of radiation transmitted through a layer of optical thickness $\Delta\tau$ is $e^{-\Delta\tau}$. Therefore, the fraction absorbed must be $1 - e^{-\Delta\tau}$. The absorption must be balanced by emission at thermal equilibrium, so generally the emission from a layer of finite thickness is proportional to $1 - e^{-\Delta\tau}$. Note that at the limit of small τ, $(1 - e^{-\Delta\tau}) \approx \tau$ is returned.

The formula in Equation 5.6 can be interpreted as the emissivity of layer i, $\left(1 - e^{-\Delta \tau_i}\right)$, times the source function of that layer, $\pi B(z_i)$, times the fraction of the radiation which makes it through the intervening layers between i and j, $\left[\exp\left(-\sum_{k \in (i,j)} \Delta \tau_k\right)\right]$, times the fraction absorbed by layer j, $\left(1 - e^{-\Delta \tau_j}\right)$.

For emission from the black surface to height j this becomes:

$$A_{surf,j} = \pi B(z_{surf}) \left[\exp\left(-\sum_{k>j} \Delta \tau_k\right)\right] \left(1 - e^{-\Delta \tau_j}\right) \tag{5.5}$$

And for emission from height i beyond the top of the atmosphere, which is the cooling to space from that layer:

$$A_{i,TOA} = \pi B(z_i) \left[\exp\left(-\sum_{k<i} \Delta \tau_k\right)\right] \left(1 - e^{-\Delta \tau_i}\right) \tag{5.6}$$

and generally $A_{i,i} = 0$.

The heating rate of each layer is now

$$h_i = \sum_{\forall k} -A_{ik} + A_{ki} \tag{5.7}$$

where k covers each atmospheric layer and the surface and top of atmosphere.

The quality of this approximation can be confirmed by comparing the spectral cooling to space with the top-of-atmosphere irradiance as calculated directly by Libradtran. Although this method is successful, it is very computationally expensive: approximations are discussed in Section 5.2.4.

5.1.2　Results: standard atmospheric column entropy budget

We apply this approach to the clear-sky standard atmospheric profile of *Anderson et al.* [1986]. The surface is treated as a black body with temperature 288.15 K and the flux from the overhead sun is scaled such that the incoming and outgoing energy fluxes balance. A standard aerosol profile provided by `Libradtran` is used [*Shettle*, 1989] and the surface albedo is set to 0.3 in the shortwave. The single column is interpreted as representing a zonally- and meridionally-symmetric steady planet (with no storage of energy or entropy). The resulting values are shown in the third columnar section of Table 5.1, contrasted with the values estimated for the EBM in Chapter 3 and ARCM in Chapter 4.

These estimates suggest $\Sigma_{mat} \approx 48\,\text{mW/m}^2\text{K}$, $\Sigma_{tran} \approx 76\,\text{mW/m}^2\text{K}$ and $\Sigma_{planet} \approx 1313\,\text{mW/m}^2\text{K}$, which are broadly in agreement with the values calculated in the literature. The material rate has been estimated by *Bannon* [2015] at $30\,\text{mW/m}^2\text{K}$ in the EBM, by *Pascale et al.* [2011a] at $\approx 50\,\text{mW/m}^2\text{K}$, by *Kato and Rose* [2020] at $49\,\text{mW/m}^2\text{K}$ and by *Lembo et al.* [2019] in the range $38.7 - 43.4\,\text{mW/m}^2\text{K}$ (outlier neglected) by their direct method. The planetary rate is also corroborated in the EBM by *Bannon* [2015] (his CV1), and

	EBM			ARCM			Std. Atmos.		
	Planet	Tran	Mat	Planet	Tran	Mat	Planet	Tran	Mat
$F^{in} = F^{out}$ (W/m^2)	341	239	85	341	239	111	346	260	96
J^{in} (mW/m^{2}K)	79	869	306	79	853	387	79	929	333
J^{out} (mW/m^{2}K)	1358	936	336	1359	929	414	1392	999	382
T^{in} (K)	4334	275	278	4334	280	288	4364	280	288
T^{out} (K)	251	255	253	251	257	269	248	260	252
η (%)	94.2	7.2	8.6	94.2	8.1	6.5	94.3	7.0	12.5
Σ (mW/m^{2}K)	1279	67	30	1280	76	27	1313	71	48

Table 5.1: The energy fluxes (F), associated entropy fluxes (J), temperatures ($T = F/J$), efficiencies ($\eta = (T_{in} - T_{out})/T_{in}$) and production rates ($\Sigma$) for the energy balance model, radiative-convective model and for a clear-sky standard atmospheric column from each of the three system perspectives: planetary, transfer and material.

corroborated by estimates of $1272 - 1284 \,\mathrm{mW/m^2K}$ by *Wu and Liu* [2010a]. The transfer rate calculated by *Kato and Rose* [2020] is $76 \,\mathrm{mW/m^2K}$, and is estimated in *Bannon and Lee* [2017] at $68 \,\mathrm{mW/m^2K}$.

5.1.3 Sources of error

The atmospheric profiles are discretised in the vertical and spectrally to perform radiative transfer calculations. How sensitive are the results to the degree of discretisation? The computation in the previous section takes 13 hours to run on a 3.1 GHz Intel Core i7 processor at medium resolution, which is a challenge if it is to be scaled up.

Libradtran has three spectral resolution options, labelled 'coarse', 'medium' and 'fine', which correspond to spectral band widths of $15\mathrm{cm}^{-1}$, $5\mathrm{cm}^{-1}$ and $1\mathrm{cm}^{-1}$ respectively. The vertical resolution also impacts the results by the approximation that the layer is at a constant temperature. The average temperature of a region with hot and cold patches does not reflect either the energy emitted from that region nor the entropy flux. The results given above were from an atmosphere split into 490 layers at medium resolution, but if 50 layers are used or if coarse is used the results change only marginally.

Radiative transfer calculations are also highly sensitive to the detailed properties of the column. A major challenge is representing realistic cloud parameters, which are often not passed as model outputs as precisely as would be necessary to emulate the atmospheric column in the offline radiative transfer code. The cloud droplet size distribution, the spatial coverage within the grid cell and thickness variation and the vertical location within the atmosphere all significantly affect the radiative behaviour but are often not possible to faithfully represent, which limits the fidelity of single column calculations. These considerations apply to aerosols and other radiatively-active gases as well.

5.2   Scaling up to global observational and GCM datasets: design, limitations and approximations

Entropy production rates are unavoidably global variables: energy enters the system at some locations and leaves at others and the entropy production happens as the energy transits between them. A single-column measure of entropy fluxes and apparent productions is informative for studying how the atmospheric characteristics give rise to entropy fluxes, but is only a first step towards calculating a global value.

In Section 5.2.1 the methodologies in the literature for calculating a global entropy production rate which existed at the outset of this PhD are reviewed. In this context, I worked to develop a tool, `entmap`, for scaling up from the single column estimates to one which could estimate the global entropics for climate model and reanalysis outputs, which is explained in Section 5.2.2.

There were two major challenges which limited the development of this project: the public availability of a data-source which gives sufficient information about the atmosphere and surface to deduce radiative properties (Section 5.2.3) and the computational load of running the radiative transfer calculations on all the columns (Section 5.2.4).

As well as being suspended for these practical reasons (and because it initiated the diverting discoveries of Chapters 3 and 4), this project has also been somewhat superseded by the recently-published global entropy dataset of *Kato and Rose* [2020] which is explored in detail in Sections 5.3 and 5.5. However, `entmap` remains an interesting attempt, and one which might find future relevance because of its versatile applicability.

5.2.1   Existing approaches from the literature

The pre-existing approaches to creating global, spatially-resolved entropy production rate datasets focus either on a particular model, on directly summing the contributions of all non-radiative entropy producing processes, or on both.

Most notable is the recently-released TheDiaTo of *Lembo et al.* [2019]. It is a diagnostic tool designed with versatility in mind, able to estimate a wide range of thermodynamic variables across CMIP6 models, including the material entropy production rate. However, unlike the approach we propose to take here, only the material entropy production rate is tallied, and directly, from approximate estimates of the contributions of each non-radiative irreversible process. This involves estimating the temperatures and energy fluxes involved in each from other variables which are given in the model output, which necessarily limits the accuracy of the results in a way which is difficult to quantify and verify. It remains a powerful tool, however, because of the details it is able to resolve about the sources of entropy production contributions and because it can be applied across models to make comparisons.
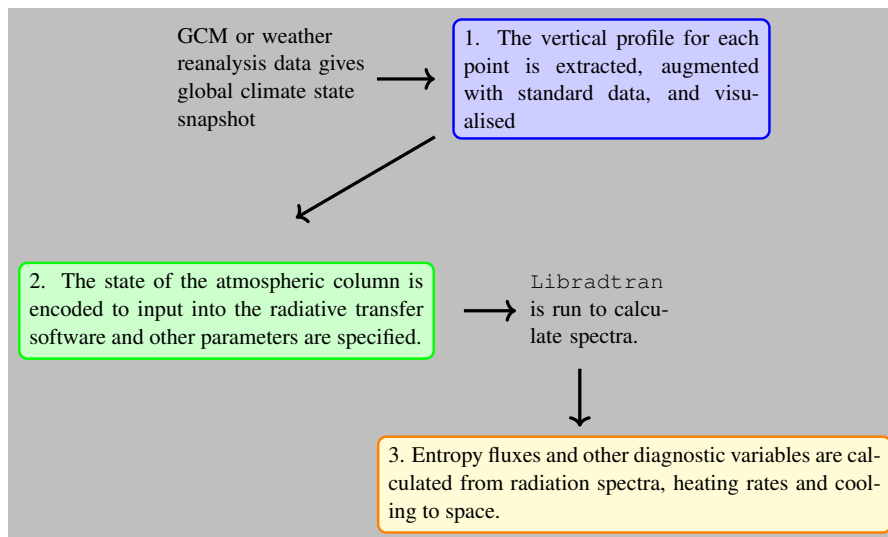
Figure 5.1: The analysis pipeline of the `entmap` tool to calculate entropy production rates from global atmosphere datasets.

Other previous work has taken a similar approach of directly summing material entropy production contributions, but focused on diagnosing a particular model. *Pascale et al.* [2011a] calculates a material entropy production budget in the HadCM3 general circulation model term by term, which results in a very thorough budget. An estimate of the planetary entropy production rate is also offered, but it does not correctly account for the $4/3$ factor in the entropy of radiation (see Section 2.9) and so would need to be adjusted to be applicable. *Fraedrich and Lunkeit* [2008] calculates the material entropy production rate in the intermediate-complexity Planet Simulator using the local temperature tendencies due to each non-radiative process. An earlier paper by *Goody* [2000] improves on the term-by-term estimates in *Peixoto et al.* [1991] using zonally-averaged data from the GISS atmosphere-ocean model.

The planetary entropy production rate has also been calculated from observations of the top-of-atmosphere radiation spectra, as in *Stephens and O'Brien* [1993]. This is, however, limited by the spatial and spectral resolution of the satellite data.

5.2.2 Design of a global entropy estimation tool

The `entmap` tool is a `python` library which calls the `Libradtran` radiative transfer for every column in an arbitrary (standardly-formatted) global atmosphere dataset and uses the spectra and radiative heating rates results to calculate and present the entropy production rates. Figure 5.1 outlines its behaviour. The dataset is specified by the user. Each column is separately read in and any missing temperature or composition data augmented using the US standard profile. `Libradtran` is run on this column and the verbose output is used to re-generate the full layer-to-layer radiative transfer matrix of Section 5.1.1. From these, entropy production rates are calculated and saved into a new netCDF file.

The scripts have been designed to run in parallel, with each column being considered separately. This means it is possible to build up slowly a set of results with global coverage using a higher-performance computer.

5.2.3   Global datasets for entropy production estimates

In climate science, emphasis has been placed on standardised datasets. Thanks to the Climate and Forecast metadata conventions [*Gregory*, 2003], observationally-based reanalyses and global climate model outputs share variable names and units and so the same code can be written to analyse both. An advantage of the indirect approach to estimating entropy production rates from time-slices of the atmosphere's state is that these standardised model outputs – rather than the details of the way processes are handled within the models – can be used to estimate entropy production in a way that is applicable across models.

This approach uses the temperature and composition states of the atmosphere, on which radiative transfer calculations can be performed, but another option would be to use the native radiative heating rates and energy fluxes which are supplied by the GCM. As estimating entropy has not been an aim of these datasets, I have not been able to find the variables needed (especially vertically resolved cooling to space) in any publicly available model output.

In developing `entmap`, I targeted the Geos-5 Nature Run Ganymed dataset. It is a high resolution simulation using prescribed sea-surface temperatures and focusing on the two years from June 2005 and includes simulations of aerosols and, significantly, the radiatively active ozone, CO and CO_2 as well as standard meteorological outputs.

5.2.3.1   Could observational spectra be used directly for entropy estimates?

Using reanalysis datasets to estimate radiative properties seems like a roundabout approach when spectra can be observed directly at the top of the atmosphere. There are, however, several limitations which prevent observational spectra from being used to estimate entropy production rates, such as the restricted temporal coverage and spectral and spatial resolution.

More fundamentally, the radiation spectra can tell us the nature of the energy which crosses the top of the atmosphere, but not the state of the system from where it was sourced or to where it was deposited. This is not a problem for the planetary entropy production rate, which is a function of the top-of-atmosphere spectra[3], but is a major limitation for the transfer entropy production and material entropy production rates. The temperature at which solar radiation is deposited is not available observationally, nor are the temperatures at which internal radiation is transferred within the system. Only the temperature from which external radiation leaves the system, which is useful for J_{tran}^{out}, can be even roughly approximated, by the spectral black-body temperature.

---

[3]Though the limited resolution and spectral coverage of these observed spectra is.

5.2.4 Approximations and shortcuts for GCM and reanalysis datasets

In developing the `entmap` tool, several possible further approximations which might be useful for more efficiently calculating global budgets from this approach were considered.

5.2.4.1 Material and transfer entropy productions from radiative heating and OLR

It is, in principle, more faithful to the model's state to use the radiative heating calculated within the model rather than via the more precise offline radiative transfer code, because the model values, even if they are slightly unphysical, are internally consistent with the climatology of the model.

The material entropy production rate is calculated by the net radiative heating, which is the information most likely to be available.

The shortwave radiative heating is also useful for calculating J_{tran}^{in}. For J_{tran}^{out}, the top-of-atmosphere energy flux provides the amount of cooling-to-space energy, but the source temperature is also needed. This can be roughly approximated by the black body temperature - the temperature a black body would be at in order to radiate that amount of top-of-atmosphere radiation. The difference between the true T_{tran}^{out} and the black body approximation for a longitudinal trace from the CERES SYN1deg dataset (more thoroughly introduced in Section 5.3) is shown in Figure 5.2, highlighting the limitations of this approach. It is interesting to note that the effective emission temperature is an underestimate of the entropic temperature because it comes from a more uniform source: there is further entropy production possible between a varied atmosphere and an isothermal black body source, which is reflected in a higher entropic temperature in the non-isothermal atmosphere (as also discussed in the appendix of *Bannon and Lee* [2017]).
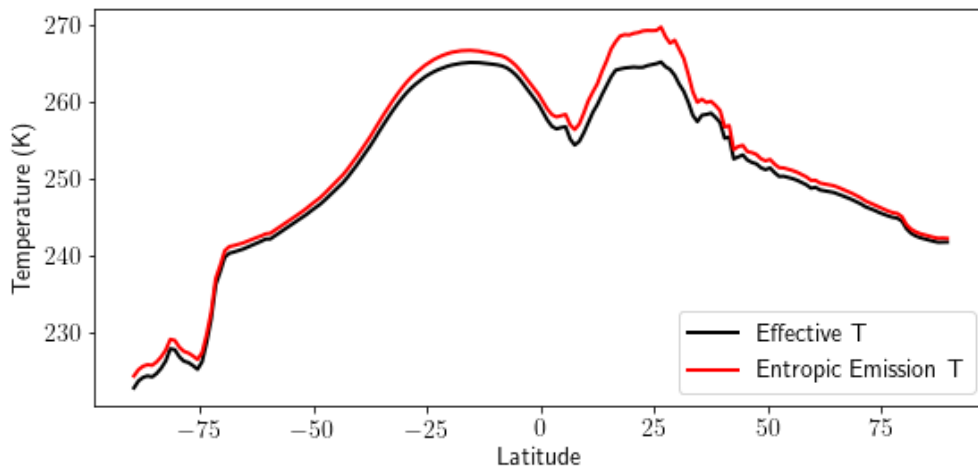

Figure 5.2: A trace along the prime meridian of the 20-year mean entropic cooling to space temperature (red) and effective temperature (black) of black body emission in the CERES SYN1deg dataset.

5.2.4.2   Machine learning - a possible shortcut

A major inefficiency of a column-by-column calculation process is how similar the columns are to each other over time and space and so how repetitive the radiative transfer calculations are likely be. The radiative transfer and entropy calculations perform a complicated mapping from many vertically resolved variables to a handful of scalars. Might it be possible to do these computationally-expensive direct calculations on a smaller training set and use a machine learning technique to circumvent the need to recalculate on similar columns?

A simple proof of concept is explored by comparing the energy fluxes to their related entropy production rates in the CERES SYN dataset, shown in Figure 5.3. Especially for the outgoing thermal radiation, much of the information in the entropy fluxes is contained in the energy fluxes, so there is definite potential in this approach - but including more predictor variables - which might be revisited to if a general `entmap` tool is to be developed further.
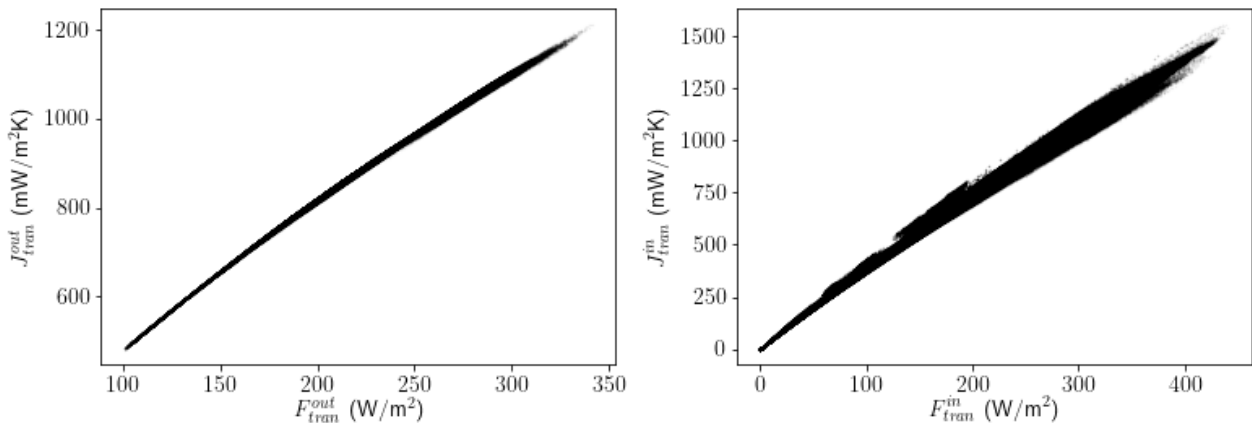

Figure 5.3: Entropy fluxes as a function of the more standard energy flux parameters, strongly hinting at an ability for machine learning to be used to estimate the entropy production from a smaller set of standard parameters. Each point represents a single gridded cell's monthly mean value for the year March 2000- February 2001.

5.3   CERES SYN1deg entropy dataset

Towards the end of this PhD, a new dataset was released by the CERES satellite observation project which estimates the top-of-atmosphere material and transfer entropy fluxes in their dataset [*Kato and Rose*, 2020]. Although it has been produced by a slightly different methodology, it is an example of the kind of data which could be produced by the tool discussed in Section 5.2.

The Cloud and Earth Radiant Energy System (CERES) project captures observations from radiation-measuring satellite instruments and assimilates those with atmospheric reanalyses, cloud observations and other datasets to deduce Earth's radiation budget (ERB). As the website[4] describes, "CERES is the only project worldwide

---

[4]`ceres.larc.nasa.gov/`

whose prime objective is to produce global climate data records of ERB from instruments designed to observe the ERB." *Kato and Rose* [2020] (hereafter, `KR2020`) describes the addition of entropy flux estimates to the dataset, in particular to the CERES Edition 4.1 SYN1deg-Month data product which was introduced in *Rutan et al.* [2015]. The entropy fluxes are estimated by adjusting the source function in the radiation code to include the $1/T$ factor necessary to calculate entropy. The dataset is available to download freely from the CERES website[5].

The CERES SYN1deg dataset implies unphysical energy imbalances: the top-of-atmosphere energy flux suggests a 1.90 W/m^2 average imbalance (July 2005 - June 2015) compared to the 0.71 W/m^2 estimated from observations using the Argo array for the same time period. In `KR2020` the energy-corrected CERES Energy Balance and Filled (CERES EBAF-TOA Ed4.1) product [*Loeb et al.*, 2018], which is adjusted to matched the observed ocean heat storage rate, is used for estimates of the annual shortwave absorption anomaly and for energy flux measurements. Care must be taken, however, not to combine the SYN1deg and EBAF datasets since they correspond to different climates states with different apparent rates of energy storage. The close relationship between energy and entropy flux means that the inaccuracy in the SYN dataset's energy flows implies inaccurate entropy flux estimates, but these require careful interpretation, which is the focus of the next section.

In order to ensure I had a thorough understanding of the `KR2020` dataset, I reproduced their results in detail[6]. In order to match their analysis, I used the range from March 2000 to February 2018 and take March-Feb annual means, accounting for unequal month lengths and adjusting area-averages for the oblate spheroid Earth on which the CERES data is described.

5.3.1 Independent verification CERES entropy estimate approach

Entropy calculation in the CERES SYN1deg dataset works in much the same way as the tool I had been developing: it applies column-by-column radiative transfer calculations to deduce the net shortwave and longwave heating rates and the cooling to space. This means that the two independently-designed calculation tools were able to be used to verify each other, with the help of Seiji Kato and Fred G. Rose. The values are tabulated in Table 5.2 for a simple atmosphere. Agreement between values is generally within a percentage point, which is more likely to be explained by difference in the radiative transfer model than in the entropy calculations. This builds confidence in the SYN entropy dataset.

---

[5]`ceres.larc.nasa.gov/data/`

[6]Reproducing published results isn't a very high-kudos scientific work, but it is important to the quality of the science which is done! It was possible because of care the CERES team takes to make their data publicly available, which is also worthy of acknowledgement. Note that in SYN1deg dataset, the outgoing longwave entropy refers to the entropy of the radiation, so its average is $4/3$ of the value 0.928 mW/m^{2}K quoted in the text. Also `KR2020` Equation (26), $F_{i,LW}^{\uparrow}$ must be the upwards longwave irradiance *from* the ith layer, rather than *at* it.

KR2020 Label	Value	GH2020 Label	Value	Ratio (GH/KR)
Cos_Sol_Zen	0.50	SZA	60°	✓
Skin_Temp	288.20	T_{surf}	288.20	✓
Aer_wavelen	0.55			
Aer_Tau	0.00	libRadtran	`no_scattering aer`	✓
SW_Toa_Down	355.51	F^{in}_{planet}	355.50	✓
SW_Toa_Up	94.61	F^{out}_{scat}	94.17	0.995
SW_Sfc_Down	268.09		269.69	1.006
SW_Sfc_Up	80.43		80.91	1.006
LW_Toa_Up	260.19	F^{out}_{tran}	259.56	0.998
LW_Sfc_Up	390.99		391.41	1.001
LW_Sfc_Dn	286.25		288.17	1.006
net_TOA_SW	260.90	F^{in}_{tran}	261.33	1.002
net_TOA_LW	-260.19	$-F^{out}_{tran}$	-259.56	0.998
net_SFC_SW	187.66	F_surf_SW	188.78	1.006
net_SFC_LW	-104.74	F_surf_LW	-103.24	0.986
		F^{CTS}_{surf}	87.43	
net_ATM_SW	73.23		72.14	0.985
net_ATM_LW	-155.46		-156.32	1.006
Toa_swe_inc	44.52	$(F^{in}_{planet} - F^{out}_{scat})/T_{sun}$	45.23	1.016
		J^{in}_{planet}	96.10	
Atm_swe_inc	12.50			
Sfc_swe_inc	32.02			
Atm_swe_gen	291.34	$J^{in}_{tran}(atm)$	286.45	0.983
Sfc_swe_gen	651.16	$J^{in}_{tran}(surf)$	655.05	1.006
Atm_swe_gen + Sfc_swe_gen	942.50	J^{in}_{tran}	941.49	0.999
Toa_lwe_out	999.80	J^{out}_{tran}	998.36	0.999
Atm_lwe_out	690.45	$\sum F^{CTS}_{atm}/T$	694.98	1.007
Sfc_lwe_out	309.35	F^{CTS}_{surf}/T_{surf}	303.38	0.981
Atm_lwe_gen	615.60	$-\sum F^{LW}_{atm}/T$	619.04	1.006
Sfc_lwe_gen	363.42	-F_surf_LW$/T_{surf}$	358.22	0.986
Trans_Ent_Pro	57.30	$J^{out}_{tran} - J^{in}_{tran}$	56.87	0.992
Mater_Ent_Pro	36.52	$J^{out}_{mat} - J^{in}_{mat}$	35.77	0.979

Table 5.2: A like-for-like comparison between the entropy budgets as calculated by the script used to make the CERES SYN1Deg entropy data product (provided by Seiji Kato and Fred Rose, personal communication) and the budget calculated by my Libradtran-based single column tool (as used in *Gibbins and Haigh* [2020]). Because the focus was any divergence in the entropy calculations and not in radiative transfer calculations, a highly simplified atmosphere was used: US standard profile [*Anderson et al.*, 1986], with no aerosols, no clouds, and a sun with a rescaled solar constant of 711 W/m^2, in order study a column in approximate energy balance.

5.4 Accounting for storage in a global entropy flux dataset

Even once a global entropy flux dataset has been produced, as in the `KR2020` SYN dataset or the one attempted in Section 5.2 with `entmap`, there remains a significant challenge in interpreting a global entropy production rate from it. This is because, unlike in the ARCM and EBM climate models discussed in Chapters 3 and 4, the true climate is not in steady state. There is storage and release of energy – and therefore of entropy as well – during the diurnal cycle, the seasonal cycle and on multi-year trends. This means that the differences in global entropy fluxes cannot be interpreted directly as entropy production rates.

Accounting for entropy storage is one of the fundamental challenges of using the indirect approach to estimate global entropy production rates and has not been sufficiently addressed by the field. In particular, it was not properly undertaken in *Kato and Rose* [2020], which leads to incorrect interpretations of net entropy fluxes as entropy productions (as highlighted in the Comment *Gibbins and Haigh* [2021]). To correct this, new, rigorous conceptual frameworks are needed to distinguish entropy storage production and flux: these are the focus of this section.

Note that the work in this section also appears in a recently-published Comment to the *Journal of Climate*, *Gibbins and Haigh* [2021].

5.4.1 Background: accounting for storage

The framework introduced in Chapter 3 distinguish between possible definitional choices as to the extent of the climate system, which give rise to different entropy production rates. The distinction between the production rates, fluxes and storage rates and how they relate to each other is an orthogonal issue, applying equally to any climate-system-extent perspective.

Entropy production is an extensive process – two Earths would produce twice as much entropy as one Earth – and so whenever a production rate is specified, a system and a boundary between it and the surroundings are necessarily implied. This may be a simple physical dividing line, as in the case of the planetary entropy production perspective, or it may be, for example, the division between matter and radiation, as in the material entropy production perspective. A boundary implies that there can be cross-boundary flows, e.g., of energy in the case of the climate system. If energy crosses a boundary, entropy can be said to *flow* with it into and out of the system, denoted J, and often calculated as the ratio of the energy flow and temperature, F/T.

By contrast, a *production* of entropy, denoted Σ, refers to an occasion where the total entropy of the universe increases. Entropy is special in that it can, and does, increase, being created in a way which conserved quantities cannot be. A conserved quantity can increase locally by flowing, but this is a movement and not a 'production'. Entropy production occurs with an irreversible down-gradient heat transfer, or conversion of energy storage

mechanism (e.g., radiation, phase-changes, kinetic energy conversions), and is always positive. It will generally have the form of a heat transfer rate F multiplied by a difference in *two* inverse temperatures, $1/T_C - 1/T_H$, where T_C is the colder of the temperatures. If there were no cross-boundary flows of entropy to reset the system, internal entropy production would ultimately result in the system achieving equilibrium in a maximum entropy state.

Entropy production can occur within a system, outside of a system, or during the process by which energy crosses into a system. Some flows of energy and entropy into a system involve an entropy production, such as the irreversible thermalisation of solar radiation upon absorption by matter, but some do not, such as the crossing of photons from the sun through the top of the atmosphere control volume (e.g. CV1 in *Bannon* [2015]). The total entropy production rate of a system is the sum of the entropy production which occurs *within* the system. Production occurring outside of the system of interest, for example, the irreversibility within the Sun, is clearly not to be included in a climatological entropy production rate. Likewise, entropy production that occurs at the boundary of a system belongs to the surroundings and not to the system; from the system's point of view, only the entropic impact of energy upon deposit within the system is knowable, and the same energy delivery by a different mechanism involving a different amount of irreversibility would be indistinguishable. Careful description of the system's boundaries is essential for determining the relevant production rate.

Storage of entropy within, or extraction from, the system occurs when the total entropy content of the system changes, either due to production or due to imbalances in the entropy flows. Entropy storage is often associated with a storage of energy or can be due to a change in the distribution of energy and temperatures within the system, and can occur only in a system which is not steady in time. Unlike production, storage can be temporary and reversed: positive storage of entropy in summer months is nearly balanced by extraction in winter months in the climate system. The rate of entropy flow into storage is a time derivative of the entropy of a system S, $J_{stor} = \frac{dS}{dt}$, and can be calculated like a flow of entropy into an internal reservoir at rate F/T_{stor}, where T_{stor} is the appropriately-averaged storage temperature.

Entropy storage, flows and productions must balance and the relationship can be expressed [*Bannon*, 2015; *Bannon and Lee*, 2017]:

$$\frac{dS_{\text{system}}}{dt} = J_{in} - J_{out} + \Sigma \tag{5.8}$$

where J_{in} and J_{out} are the entropy fluxes into and out of the system, as measured from the system's perspective, Σ is the entropy production rate within the system, measuring the total rate of irreversibility, and the storage of entropy within the system is the rate of change of the entropy content of the system, dS_{system}/dt. In a steady system, Equation 5.8 simplifies considerably because $dS_{\text{system}}/dt = 0$ and so $\Sigma = J_{out} - J_{in}$.

In *Kato and Rose* [2020], the net flux of radiation $J_{out} - J_{in}$ is explored and interpreted as the entropy production

rate. This is misleading when there is storage present as:

$$J_{out} - J_{in} = \Sigma - \frac{dS_{\text{system}}}{dt}, \tag{5.9}$$

not the production alone. That storage might impact on their results is acknowledged in passing in `KR2020` but it is not subsequently accounted for, partially because it requires additional calculations to estimate it. In the following section an approach to estimating the rate of entropy storage is offered.

5.4.2   Estimating storage rate from ocean temperature

The entropy content of the climate system is not steady in time but increases as the amount of energy stored in the system increases, or decreases as energy is extracted from the system.

In the climate, the rate of energy storage is the difference in net top-of-atmosphere shortwave incoming irradiance F_{SW} and emitted longwave irradiance F_{LW}: in an equation, $F_{stor} = F_{SW} - F_{LW}$. More than 90% of this energy is stored in the oceans [*Trenberth et al.*, 2014] but to calculate accurately the entropy change of the ocean due to this heat storage, details of its internal temperature structure would be needed. However, since energy enters and exits the ocean at the surface, the average ocean surface temperature is a reasonable proxy for the internally-averaged storage temperature, $T_{stor} \approx \overline{T}_{ocean}$. This is lower than the approximation used in *Bannon and Najjar* [2018], where the energy-influx-weighted ocean temperature is used as the storage temperature; we would argue our approach is appropriate given the role of the cooler deep ocean in heat storage. These two components can be used to estimate the rate of entropy storage in the climate system, $J_{stor} = dS_{\text{system}}/dt \approx F_{stor}/T_{stor}$.

5.4.3   Limitations

There are two approximations taken here which limit the accuracy of the numerical results. Firstly, the global average ocean surface temperature is not a precise measure of the average temperature of entropy storage in the climate system, which ought ideally to take account of storage in the deep ocean, the atmosphere and changes in chemical structure, for example as glacial mass changes. It would be an interesting but non-trivial project to estimate the annual change in the total entropy content of the Earth system, which could then be used to calculate accurately the representative storage temperature $T_{stor} = \Delta S_{system}/\Delta U_{system}$ from the change in internal energy U. However, temperature appears in the storage terms in absolute units, so even a large uncertainty in the storage temperature relative to the temperature range in the climate system of 10K has only a 3% impact on the entropy storage. Since the storage itself is only 10% of the size of the net entropy flux, the storage temperature introduces only less than 0.3% uncertainty per 10K deviation. Far more important is inclusion of a reasonable storage term at all.

Secondly, inaccuracies in the energy budget in the SYN1deg dataset also limit the accuracy with which entropy storage can be estimated from it. However, the estimates of energy and entropy storage from the more-accurate EBAF cannot be directly combined with entropy flow estimates from SYN1deg because doing so would introduce inconsistencies: a system with less storage ought to have a lower top-of-atmosphere energy imbalance, which in turn influences the top-of-atmosphere entropy flux imbalance. Using SYN1deg entropy fluxes but with energy fluxes from EBAF implies non-conservation of energy[7]. Repeating the entropy flux calculations of `KR2020` on a dataset with a more accurate top-of-atmosphere energy imbalance would lead to even more accurate entropy budget estimates for the climate.

5.5   Results: features of the climate's observed entropics

The storage-corrected CERES SYN1Deg data product (hereafter SYN) is a rare treasure trove of potential insights about the climate's entropy production behaviour. We have never before had access to such a complete set of data for the full-complexity observed climate, especially not one which measures the transfer entropy production rate as well as the material.

In this section I will share some initial analysis of interesting patterns and features of the dataset. As with the other studies in this thesis, this serves multiple purposes. One is to deepen our intuitive grasp of entropy production rates as diagnostic climate state variables, demonstrating how they correspond to other more familiar features of the climate system. Another is to probe for unexpected patterns which might shed light on the possibility that the global entropy production rate is a self-regulated potentially-predictive feature of the climate's behaviour. Both of these projects support future hypothesis-generation rather than being hypothesis-testing science; we are building up observations which make more sense of the entropy production story.

5.5.1   Global entropy production rate estimates

Having corrected for entropy storage, the updated estimates of the material and transfer global entropy production rates are shown in comparison with the `KR2020` values in Figure 5.4. The entropy storage in the ocean is identical from the material and transfer perspectives and so the difference between uncorrected and corrected values is the same for both measures. The variance in my corrected entropy production rate estimates is also significantly lower than in the `KR2020` 'productions', i.e. net entropy flux rate. This is because neglecting entropy storage is equivalent to assuming that the temperature of the storage reservoir is infinite ($J_{stor} = F_{stor}/T_{stor} = 0$ if $T_{stor} = \infty$) which means the inter-annual top-of-atmosphere energy imbalance fluctuations have a disproportionate impact on the apparent entropy production rate.

---

[7]*Kato and Rose* [2020] combine entropy fluxes from SYN1deg with energy fluxes from EBAF to calculate representative temperatures in their Table 3, which does not give as accurate an estimate as does using the SYN1deg energy fluxes.
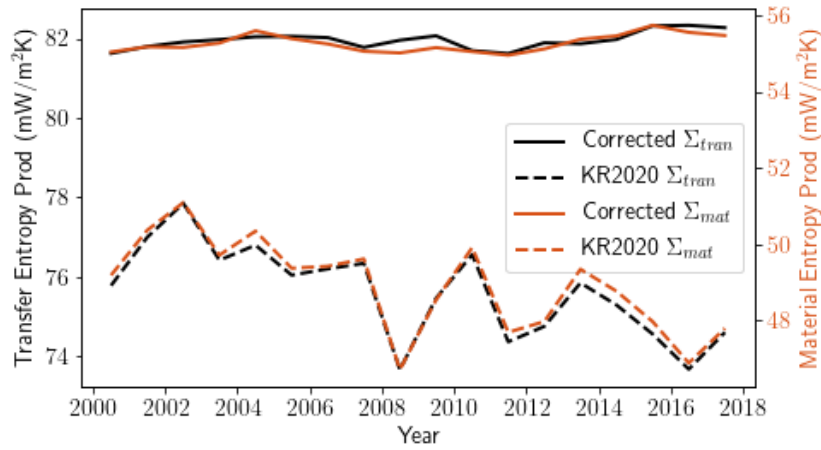
Figure 5.4: The global annual material (red) and transfer (black) entropy production rates from the CERES SYN1deg dataset. The values shown in dashed lines are as calculated in KR2020 without accounting for the storage of entropy in the oceans: they are $J_{tran}^{out} - J_{tran}^{in} = \Sigma_{tran} - J_{stor}$, and similar for the material system. The solid lines are the more accurate, storage-corrected entropy production rates, as calculated in *Gibbins and Haigh* [2021].

Over the 18 year period shown, the material entropy production rate of has an average value of $\Sigma_{mat} = 55.3$ mW/m^{2}K and the transfer entropy production rate an average value of $\Sigma_{tran} = 82.0$ mW/m^{2}K. These are higher than the values in KR2020 because of the consideration of the, on average, 6.3 mW/m^{2}K of entropy storage each year.

It is worth noting that these are the values suggested by the SYN dataset, but are not necessarily the best estimates for the true climate. This is because the mean top-of-atmosphere energy imbalance is significantly over-estimated in the SYN dataset, at 1.8 W/m^2, compared to the more realistic values in the CERES EBAF dataset of 0.7 W/m^2 [*Loeb et al.*, 2018]. However, energy storage rates from one dataset cannot be directly combined with top-of-atmosphere fluxes from another dataset because it suggests a creation or destruction of energy.

Instead, to approximate entropy production rates in the EBAF dataset using the SYN values, the global entropy fluxes values from the SYN dataset can be rescaled by the ratio of energy fluxes between the SYN and EBAF datasets:

$$J_{EBAF} \approx J_{SYN} \frac{F_{EBAF}}{F_{SYN}}. \tag{5.10}$$

This approximation makes the implicit assumption that just the quantity of the energy and not the temperatures nor absorption and emission locations vary between the EBAF and SYN datasets, which is necessarily not true. Nevertheless, it brings us closer to an observationally-consistent entropy budget for the climate.

Table 5.3 shows the values of the entropy budget and related variables from the KR2020 paper (i.e. neglecting storage), the storage-adjusted SYN dataset and two rescaled-to-EBAF approximations, one using point-wise rescaling by local monthly-mean EBAF energy flows in each grid cell[8] and the other using hemispherically averaged values. It is particularly noteworthy that the large discrepancy in the entropy storage estimate between the EBAF and SYN datasets does not imply an equally large difference between the entropy production rates:

---

[8]The EBAF dataset has negative solar absorption in some polar gridpoints while the SYN dataset does not. A cut-off is used for the rescaling: any grid cell with less than 0.1 W/m^2 of solar absorption is not rescaled.

this is because, physically, energy passing through the climate system and then being sequestered in the ocean is not so different from it being passed out of the climate system in terms of the entropy production rate it implies (and certainly much less different than neglecting the storage process).

Variable	KR2020	SYN	EBAF (cell)	EBAF (hemi)
T_{surf} (K)	288.4	288.4	288.4	288.4
F_{in} (W/m^2)	240.9	240.2	240.9	240.9
F_{out} (W/m^2)	240.2	238.3	240.2	240.2
F_{stor} (W/m^2)	–	1.8	0.7	0.7
J^{in} (mW/m^{2}K)	853.1	853.1	855.2	855.5
T^{in} (K)	281.6	281.6	281.6	281.6
J^{out}_{mat} (mW/m^{2}K)	902.0	902.0	909.0	909.0
T^{out}_{mat} (K)	266.3	264.2	264.2	264.2
J^{out}_{tran} (mW/m^{2}K)	928.7	928.7	935.9	935.9
T^{out}_{tran} (K)	258.6	256.7	256.7	256.7
J^{stor} (mW/m^{2}K)	–	6.34	2.34	2.33
T^{stor} (K)	–	292.1	292.1	292.1
η_{mat} (%)	5.42	6.08	6.16	6.13
η_{tran} (%)	8.14	8.76	8.84	8.82
Σ_{mat} (mW/m^{2}K)	48.9	55.3	56.1	55.8
Σ_{tran} (mW/m^{2}K)	75.6	82.0	83.0	82.7

Table 5.3: The global entropy production rates and related variables (first column), as estimated in the KR2020 with storage neglected (second column), in the SYN dataset accounting for inter annual entropy storage (third column) and as approximated for the EBAF dataset using the rescaling of Equation 5.10 grid cell-by-grid cell (fourth column) and hemispherically (fifth column). For the KR2020 values I follow the publication in using EBAF values for energy fluxes and to calculate the entropy temperatures.

5.5.2   Globally-averaged temperature metrics

Temperature is a well-established global climate metric. The standardised aggregated measure, the global mean surface temperature (GMST), is at the core of our international climate action commitments, our simplifications of the climate system in the concept of climate sensitivity, and our model verification projects.

Entropy flux is a combined measure of temperatures and energy flows and is a naturally globally-aggregated variable; that is to say, for the climate system as a whole, the global entropy flux is a more physically fundamental variable than the global mean surface temperature. The global average entropic input and output temperatures, which can be calculated from the ratio of entropy fluxes to energy fluxes, are the focus of this subsection.

Because the SYN entropy dataset is aggregated by column, the entropy temperatures implied by calculating F/J in each grid cell are column averages and do not resolve the full range of temperatures within the column. For example, for the single atmospheric column studied in Section 5.1, an energy-weighted histogram of absorption and emission temperatures *within the column* (Figure 5.5) shows a wide range of temperatures at which energy is supplied to and removed from the system. The SYN column values average out these

vertically-resolved values, so do not demonstrate the full range of temperatures in the true climate.
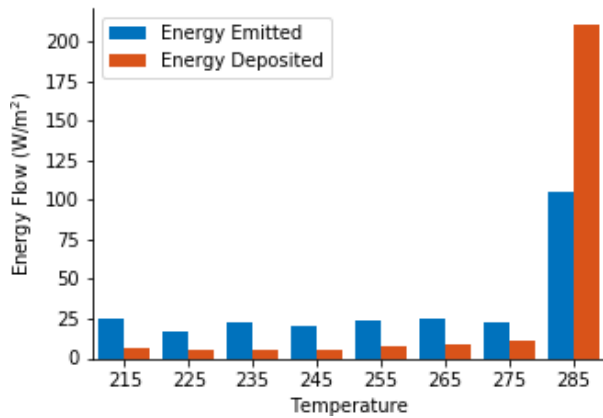

Figure 5.5: A histogram of the amount of energy flowing into (red) and emitted from (blue) each 10K temperature bin in the standard atmospheric column of Section 5.1. The majority of energy is both delivered and emitted from the surface, but there is net energy absorbed at the warmer temperatures and net energy emitted at the cooler temperatures. This demonstrates the energy flow from warmer to cooler within the atmospheric column which is responsible for entropy production, as well as the broader spread of entropic temperature in a vertically-resolved column, which is averaged away in the two-dimensional SYN dataset.

The global coverage of the SYN dataset does, however, permit a spatial analysis of how the entropic input and output variables are composed, and how this contrasts with the GMST. In Figure 5.6, the GMST (first row) is compared with the entropic input temperature (second row) and the output temperature (third row) in terms of the temperatures they summarise (first column) and the variables which serve as a weighting (second column). While the GMST averages the surface temperature uniformly across the globe, the entropic temperatures are inversely weighted by the local energy flux. This is best expressed in equations:

$$T_{GMST} := \frac{\int T_{surf} dA}{\int dA} \qquad (5.11)$$

$$T_{ent} := \left(\frac{J}{F}\right)^{-1} = \left(\frac{\int \frac{F}{T} dV}{\int F dV}\right)^{-1}. \qquad (5.12)$$

where T is the temperature field, A is surface area and F is energy flow, either into the system as solar heating (for T_{in}) or cooling to space (for T_{out}). This means that, relative to the GMST, both entropic average temperatures give less weighting to the poles. The input temperature particularly picks out the tropics, where there is absorption of solar energy supplied to the climate system. The output temperature captures the cooling-to-space sink of energy within the climate system, and is dominated by regions which have warmer cloud-top temperatures or are clear and so emit more energy to space.

At all longitudes, the heat delivered is to warmer temperatures than the heat ejected from. Figure 5.7 shows a heat-map histogram of the temperatures of T_{tran}^{in} (red) and T_{tran}^{out} (blue) at each latitude, weighted by the amount of energy flow and normalized within each latitude band. The difference between temperature spreads over land and ocean hints at different production rates in these different environments.

Another perspective on these temperatures can be gleaned from examining their distributions without their spatial position, as shown in Figure 5.8, which is reminiscent of Figure 5.5 but using a 2D dataset and of the sketch in Figure 4.3. This plot makes clear the temperature difference between those locations where energy is supplied to the system (red) and those where it leaves the system (blue); the climate's activity mediates the
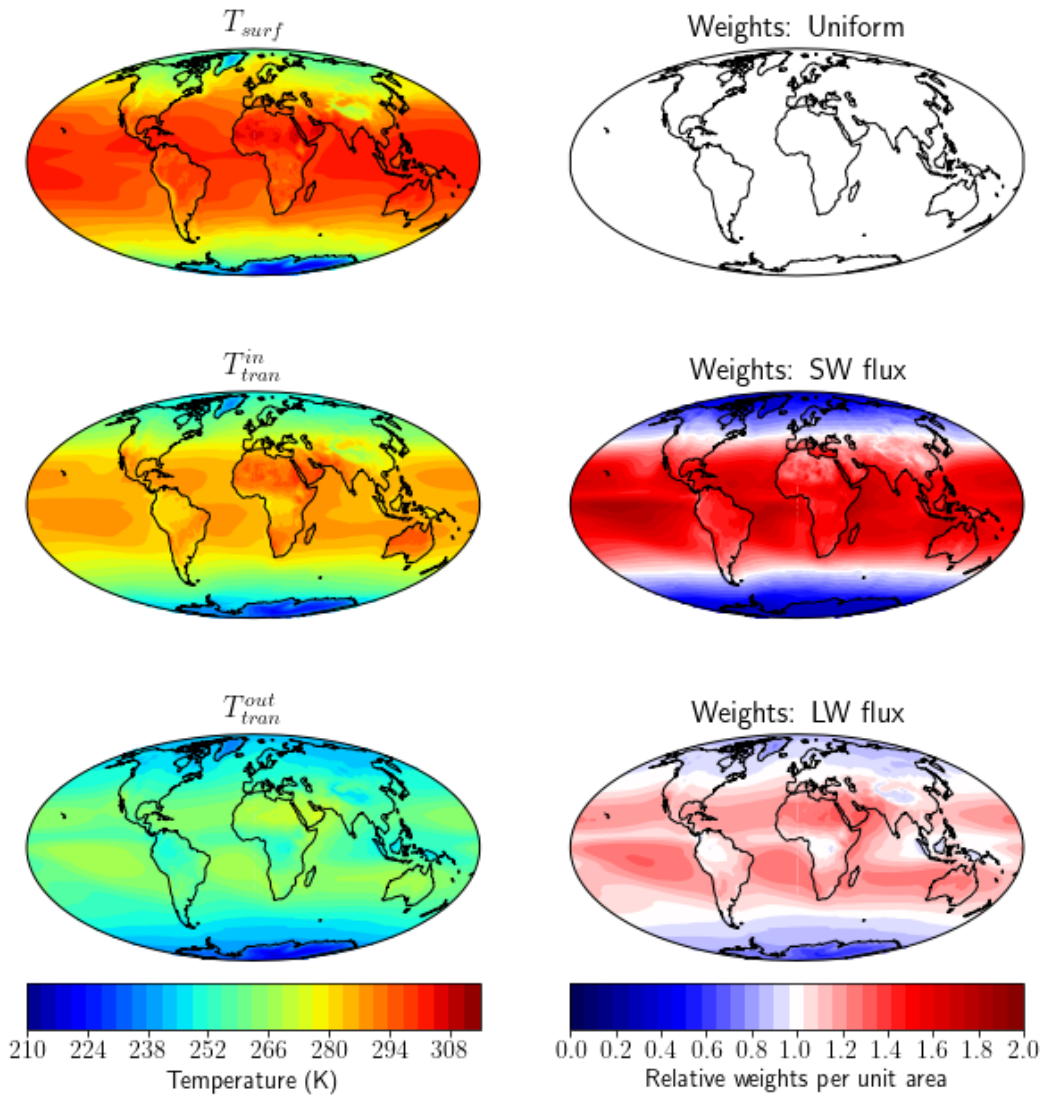
Figure 5.6: (first column) The temperature field and (second column) the normalised variable which multiplies it as in equations 5.11 and 5.12 to calculate the standard global mean surface temperature (first row), entropic input temperature, T_{tran}^{in} (second row) and entropic output temperature, T_{tran}^{out} (third row). The energy-flow weighting of the entropic temperatures gives significantly less relative weighting to the polar regions than the uniform area weighting used for the GMST does.

down-gradient transfer of energy from input to output. This is a numerical validation of the conceptual sketch which was provided in Figure 4.3. As well as being clearly distinguishable from each other, the different shapes of the input and output temperature distributions are notable: the cooling to space output temperatures are symmetric, while the input temperature distribution is significantly peaked in a way which echos the peaked surface temperature distribution and exhibits very broad tails. Note that, were the vertically-resolved temperatures used, the spreads would be wider: for example, T_{tran}^{in} ought to include a significant amount of heating at the surface temperatures.
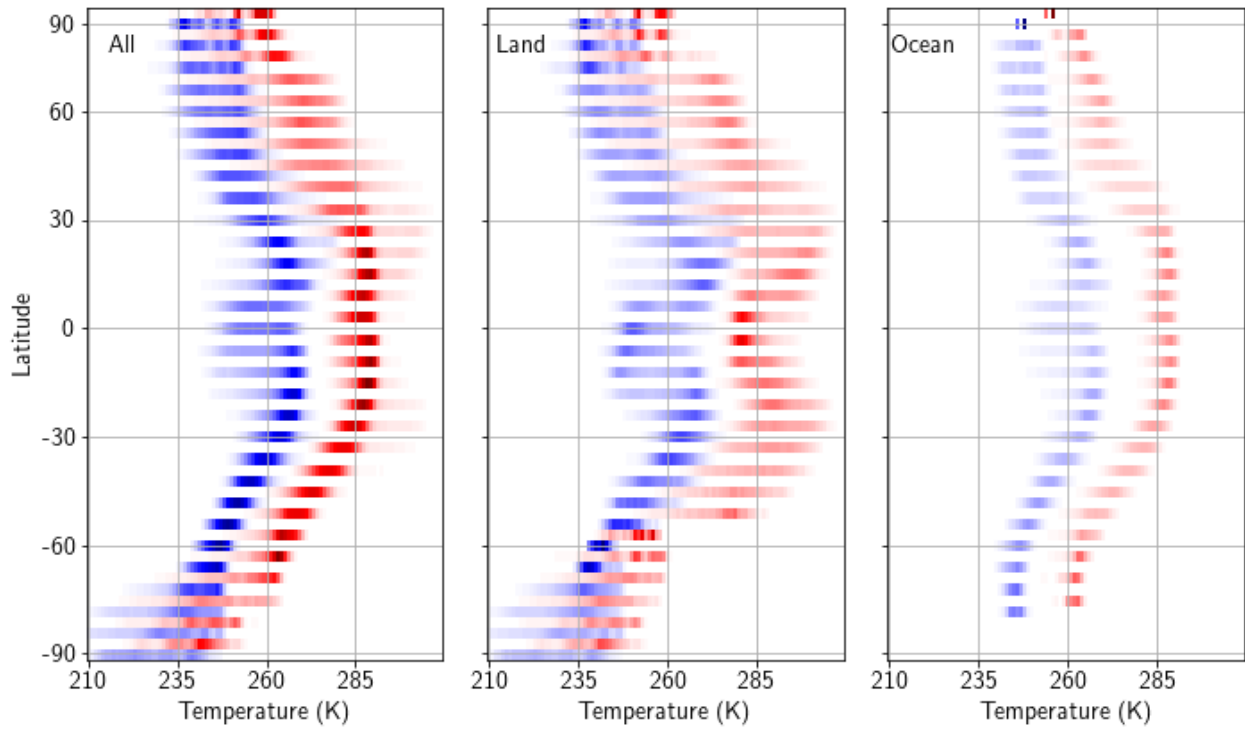
Figure 5.7: Each band shows the distribution of temperatures at that latitude as a heat map, with the entropic input temperatures T^{in}_{tran} in red and output temperatures T^{out}_{tran} as blue. All surface cover is shown in the first panel, which is divided into the land and ocean components in the second and third panels respectively. Within each band, the temperatures appearing are weighted according to the energy flow, but the bands are normalised relative to each other.
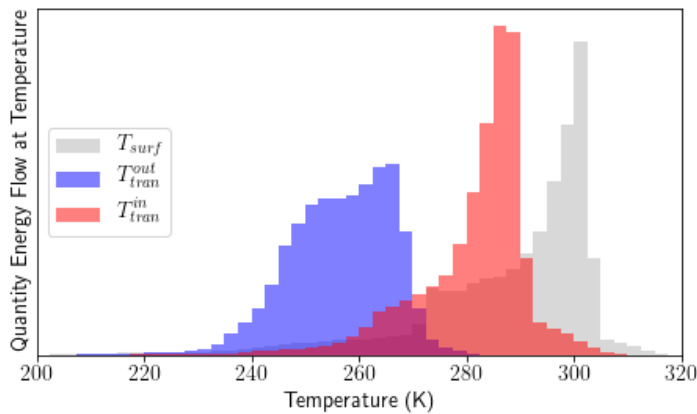

Figure 5.8: Histograms of the column-averaged entropic temperature of solar absorption, T^{in}_{tran} (red), and of thermal radiation emission to space, T^{out}_{tran} (blue), compared with the global mean surface temperature (grey) for the 18-year monthly-average SYN dataset. Values are weighted by the related energy flow as shown in Figure 5.6.

These three global temperature measures are related to each other. Figure 5.9 shows the correlation between the two entropic temperatures and the GMST. In both cases, the slope of the correlation is less than 1, in line with the observation that the inter annual spread of GMST in the 18-year record studied (0.55K) is more than that of the input temperature T^{in}_{tran} (0.46K) or the output temperature T^{in}_{tran} (0.24K). The correlation between GMST and the input temperature is stronger than with the output temperature, which is to be expected as the surface is the location of more solar absorption than it is of thermal emission to space. The third panel shows the very strong correlation between the output temperature and the quantity of longwave emission: theory shows that T^{out}_{tran} is quite similar to T_{eff}, so this is to be expected.
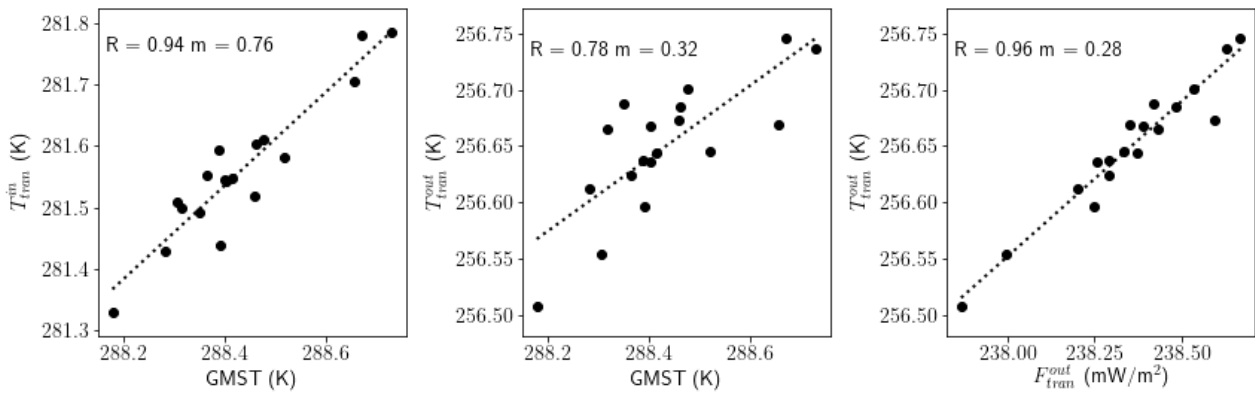
Figure 5.9: (left) The correlation between the entropy-averaged input temperature (T_{tran}^{in}) in the SYN dataset and the global mean surface temperature over the 18 year record. (middle) The less pronounced correlation between the output temperature (T_{tran}^{out}) and GMST. (right) The strong correlation between the outgoing longwave radiation (F_{tran}^{out}) and the output temperature.

5.5.3   Hemispheric symmetry

Although the clear sky albedo differs between the hemispheres because of the difference in surface albedo, it has been observed that compensating cloud cover results in a striking symmetry in the all-sky annual mean hemispheric albedos [*Voigt et al.*, 2013; *Stephens et al.*, 2015]. Climate models do not generally reproduce this result, though when they are tuned so that they do, they also appear to improve along other metrics [*Haywood et al.*, 2016], underlining that the symmetry is a potentially-important feature of the climate system which, if understood, could reveal model inadequacies. *Voigt et al.* [2014] deduce that a shift of the intertropical convergence zone is the main mechanism by which the hemispheric total cloud cover is regulated. This does not, however, provide a full explanation of *why* the climate system would use this mechanism to self-regulate the global albedos. Several researchers from outside of the entropy production field who I have spoken with have pointed to the tantalising possibility that entropy production rate regulation might play a causal role.

Without a more specific proposed mechanism for entropy regulation and the connection to hemispheric albedo, we are not ready to test the hypothesis of entropy production rate having an explanatory role directly, but instead focus on the background work of characterising the hemispheric symmetry of entropy production rates and related variables.

Two challenges arise in leveraging the SYN dataset for this. The first is that it does not include a measure of the meridional energy flow, in particular across the equator. This means that the true hemispheric rate of entropy storage, and also the production due to subsequent irreversible transformations of the cross-equatorial energy, cannot be estimated. I make the approximation of assuming no cross-equatorial flow, which is equivalent to the less controversial assumption that there is no further entropy production occurring with energy after it has flowed across the equator. The hemispheric top-of-atmosphere energy imbalance is taken to represent the hemispheric energy storage rate, which is again scaled with the hemispheric average ocean temperature to find

the hemispheric entropy storage rate. The hemispheric average net entropy flux is used to complete the estimate of hemispheric entropy production rates $\Sigma = J_{out} + J_{stor} - J_{in}$.

The second is that the SYN dataset, where we have access to entropy flux measurements, actually does not demonstrate the hemispheric symmetry in albedo which is present in the EBAF dataset. This is explored in Figure 5.10, in which the upper left panel shows the hemispherically averaged net rate of solar absorption in the two datasets. The EBAF datasets (dashed lines) show similarity between the northern and southern hemispheres, while the SYN southern hemisphere (solid blue) is lower by approximately $1\,\mathrm{W/m^2}$. The EBAF dataset is the more likely to be realistic and is more consistent with other lines of satellite evidence [*Voigt et al.*, 2013].
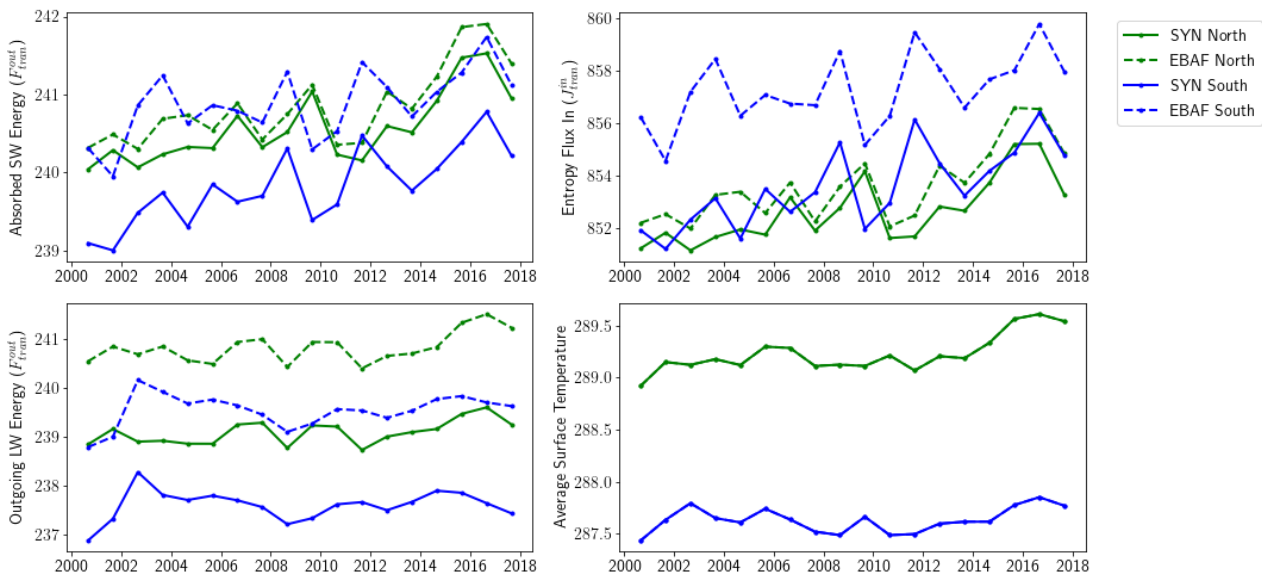

Figure 5.10: Comparison between the hemispheric symmetry in SYN (solid lines) and EBAF (dashed lines) datasets, with the annual average northern hemisphere values in green and southern hemisphere in blue. (upper left) The net absorbed shortwave radiation, calculated as incoming top-of-atmosphere solar minus scattered. This is the energy associated with incoming entropy fluxes. (lower left) The net outgoing longwave radiation. (upper right) The transfer entropy flux associated with the absorbed solar radiation. (lower right) The global mean surface temperature.

To explore the impact of this difference on entropy production rate values, the hemispheric rescaling to EBAF values of the SYN entropy dataset discussed in Equation 5.10 is applied. Because of the difference in average surface temperatures between the hemispheres (lower right panel), symmetric solar fluxes imply asymmetric entropy fluxes (EBAF dashed lines, upper right panel). However, the temperature difference (surprisingly) compensates for the hemispheric asymmetry in energy absorption to give very similar incoming entropy fluxes in the SYN dataset (solid lines, upper right panel). In the EBAF dataset, there is more emitted longwave radiation in both hemispheres than in the SYN dataset, but the difference is similar between hemispheres (lower left panel) in both datasets. The warmer northern hemisphere emits more longwave radiation.

The hemispherically-averaged net entropy fluxes and the entropy storage rates estimated from the hemispheric energy imbalance and ocean surface temperature can be combined to give estimates of the hemispheric entropy
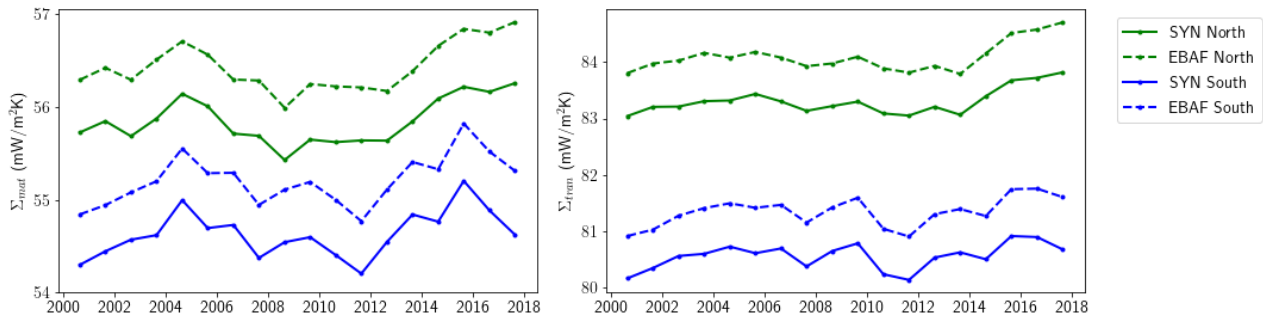
Figure 5.11: The material (left) and transfer (right) entropy production rates estimated for the northern (green) and southern (blue) hemispheres in the SYN (solid) and rescaled-to-EBAF (dashed) datasets. Both show significant hemispheric asymmetries.

production rates, shown in Figure 5.11. In the SYN dataset, the mean northern hemisphere apparent transfer entropy production rate is 83.3 mW/m^{2}K, compared to 80.6 mW/m^{2}K in the southern hemisphere. In keeping with the global estimates, the EBAF datasets are approximately 1 mW/m^{2}K higher, at 84.1 mW/m^{2}K and 81.3 mW/m^{2}K in the northern and southern hemispheres. The material entropy production rates shows significantly less difference between northern and southern hemispheres - only 1.2 mW/m^{2}K compared to 2.8 mW/m^{2}K for the transfer entropy production rate (both SYN and EBAF datasets), with a northern hemisphere mean value of 55.9 mW/m^{2}K and southern hemisphere, 54.6 mW/m^{2}K in the SYN dataset, and 56.4 mW/m^{2}K and 55.2 mW/m^{2}K in the EBAF dataset. Splitting the transfer entropy production into the components from material processes and internal radiation, means that the northern hemisphere material entropy production rate is only 2.2% higher than its southern hemisphere value, while the northern hemisphere entropy production rate due to internal radiation is 5.9% higher than its southern hemisphere value (27.5 mW/m^{2}K and 26.0 mW/m^{2}K respectively). This is echoed in the rescaled-to-EBAF dataset. It is striking and unexplained that the entropy production due to internal radiation shows such a larger hemispheric difference than that due to material processes.

5.5.4   Seasonal variability

The annual hemispheric values represent averages over their seasonal cycles. Over the course of the year, shifted by six months in the different hemisphere, there is a cycle between net positive and net negative top-of-atmosphere energy imbalance, implying intra-annual storage of entropy. This makes it an interesting challenge to calculate time-resolved entropy production rates to attempt to account for the hemispheric annually-averaged patterns revealed above.

Figure 5.12 begins to characterise the seasonal cycles of entropy-related variables in each hemisphere. The absorbed shortwave (upper left) shows a strong seasonal trend due to the change in solar radiation with the seasons, tempered by seasonal albedo variations such that the northern hemisphere shows a less pronounced
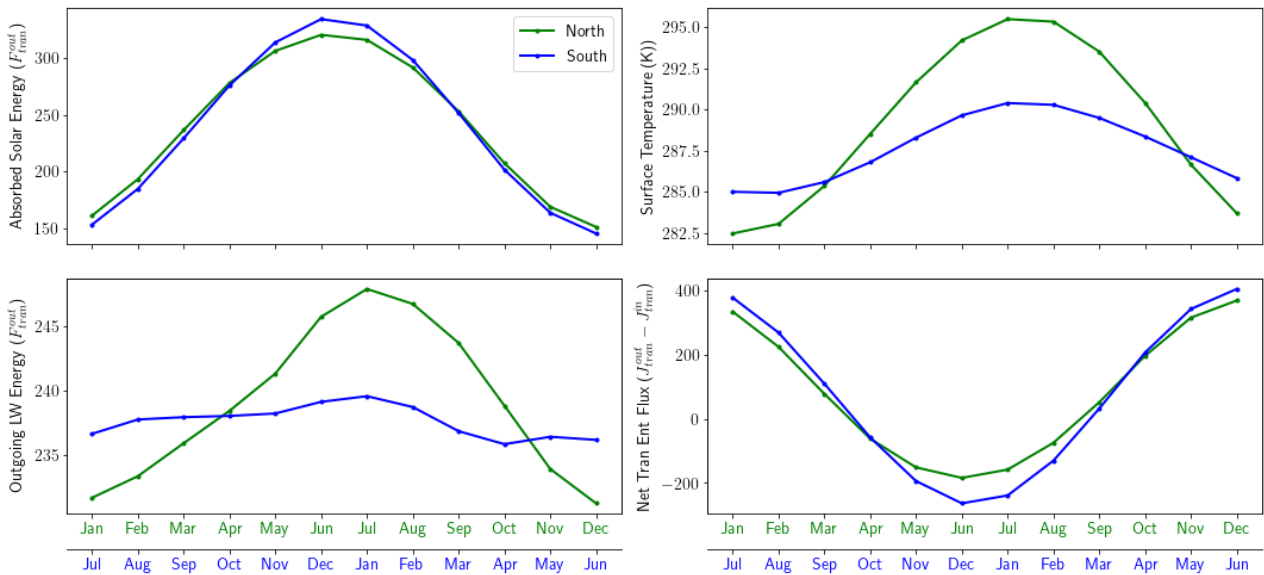
Figure 5.12: The average monthly values for the (upper left) absorbed shortwave energy, (lower left) emitted longwave energy, (upper right) mean surface temperature and (lower right) net transfer entropy flux. The green lines indicate the northern hemisphere and blue lines the southern; the SYN dataset is used.

trend than the southern. The outgoing longwave energy (lower left) matches the mean surface temperature (upper right) in having a more pronounced seasonal cycle in the northern hemisphere, which can be explained by the larger land fraction. The larger relative variations in the absorbed solar energy dominate in the net transfer entropy flux (lower right) to give a strong seasonal cycle.

As a first approximation, the monthly entropy production rate can be deduced by estimating a rate of entropy storage from the difference in monthly hemispheric energy fluxes (the stored energy) and the monthly mean ocean surface temperature (the temperature of energy storage). This gives rise to the strong seasonal cycles shown in Figure 5.13.
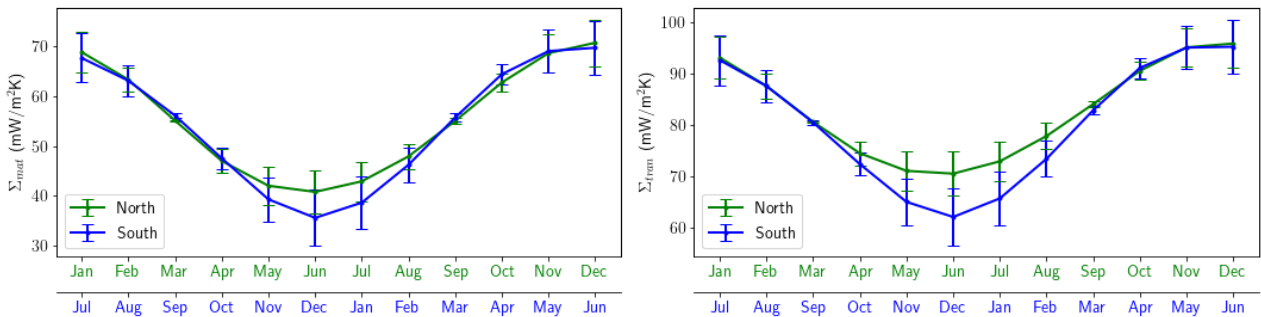
Figure 5.13: Assuming that the monthly energy imbalance is stored in the ocean at the average ocean surface temperature, the monthly entropy storage rate can be estimated and added to the net entropy flux to estimate the monthly production rate, for the material (left) and transfer (right) perspectives. The error bars indicate the impact of a 5K uncertainty above or below in the storage temperature.

The magnitude of the cycle in the material entropy production rate is 30.0 mW/m^{2}K for the northern hemisphere and 34.1 mW/m^{2}K for the southern hemisphere, and the magnitude for the transfer entropy production rate is

25.3 mW/m²K in the northern hemisphere and 33.1 mW/m²K for the southern hemisphere. These are strikingly large cycles which seem to suggest less entropy production in those months where there is more incoming solar radiation and the climate system is hotter. This raises some questions.

Might these results be spurious? As shown in Figure 5.14, the entropy storage variation is very large intra-annually (> 400 mW/m²K), and our method of estimating it using the hemispherically-averaged ocean temperature is only approximate. It is possible that this could be introducing spurious cycles in the apparent production rate; to test this, another method for approximating the entropy production rate can be used, via the climate efficiency. Firstly the top-of-atmosphere entropy and energy fluxes can be combined to estimate input and output temperatures without reference to storage. These are shown in the upper right two panels of Figure 5.14, compared to the trend in global mean surface temperature in the upper left panel. Several things are notable. Firstly, the seasonal cycle in entropic temperatures is much smaller than in the global mean surface temperature, covering $1 - 4$ K rather than $5 - 10$ K in the GMST case. Secondly, the shape of the seasonal cycle in the input temperature is not similar to that of the GSMT, and shows a significant lag between the hemispheres. This requires further explanation.
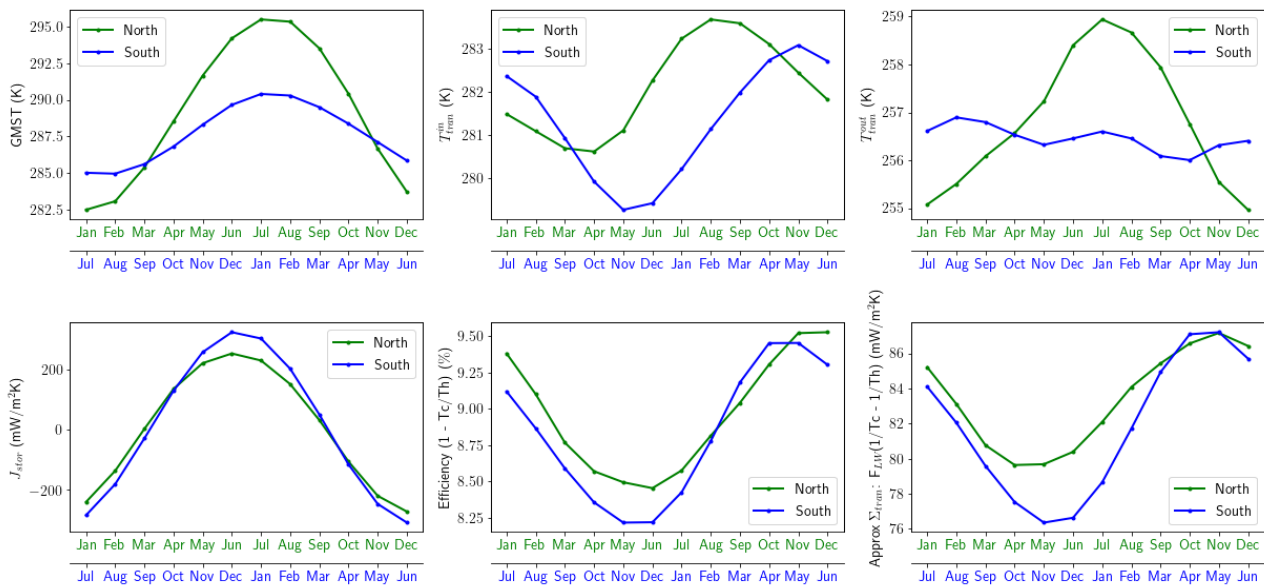

Figure 5.14: To explore and corroborate the seasonal trend in entropy production rate of Figure 5.13, the seasonal cycle of several variables related to the transfer entropy production rate is explored. (upper left) The global mean surface temperature. (upper middle) The entropic input temperature, T_{tran}^{in}. (upper right) The entropic output temperature, T_{tran}^{out}. (lower left) The estimated rate of entropy storage in the ocean. (lower middle) The efficiency of the transfer system, $(1 - T_c/T_h)$, where $T_h = T_{tran}^{in}$ and $T_c = T_{tran}^{out}$). (lower right) The approximate entropy production rate, calculated as $F_{tran}(1/T_c - 1/T_h)$.

The input and output temperatures can be taken forward to provide an independent estimate of the approximate rate of entropy production in the system, by leveraging the relationship between efficiency and entropy production discussed in *Bannon* [2015]. The efficiency, shown in the lower middle panel of Figure 5.14, is $\eta = (1 - \frac{T_c}{T_h})$ and is related to production via $\Sigma \approx \eta\frac{F}{T_c} = F(1/T_c - 1/T_h)$, which is shown in the lower right panel. This approximate production shows a notable similarity to the cycle demonstrated in Figure 5.13,

although it is shifted a few months earlier. This lends credence to the conclusion that entropy production rates may be higher in the winter months than the summer months.

Finally, I happened on a similarity between two unexpected variables as illustrated in Figure 5.15: the rate of entropy production due to internal radiation (i.e. the difference between transfer and material entropy production rates) and the hemispheric average ocean temperature. Both show a lag of the southern hemisphere relative to the northern and a similar contrast in the magnitude of the cycles between hemispheres. The internal radiation is due to temperature differences within the atmosphere so a correlation with the ocean surface temperature is not entirely unexpected, but this result requires further investigation.
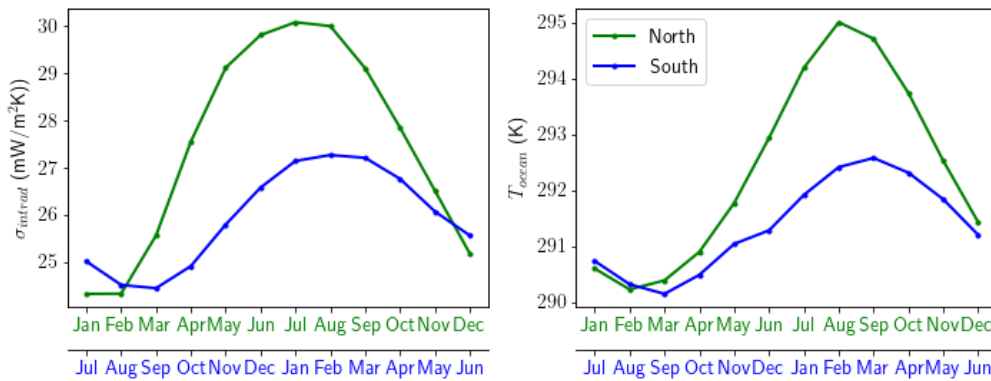

Figure 5.15: The seasonal cycles of (left) the entropy production due to internal radiation ($\sigma_{intrad} = \Sigma_{tran} - \Sigma_{mat}$) and (right) the mean ocean temperature. The reason for this similarity is as yet unexplained.

5.5.5 Albedo variability

In the paper which introduces the SYN entropy dataset, *Kato and Rose* [2020] point out a striking negative correlation between the net export of entropy and the annual mean absorbtion of solar radiation. This net export is the difference between entropy delivered to the system by absorption of shortwave radiation and exported by emission of longwave radiation, a $J_{out} - J_{in}$ in our notation (their Figure 8, third panel). In their paper, the result is described as indicating a negative correlation between shortwave absorption and the "entropy production by irreversible processes". However, rearranging Equation 5.8, we can see that in a system which is not steady and so has a non-zero rate of entropy storage, the difference in fluxes focused on in `KR2020` is actually a measure of the difference between the entropy production rate and storage rate.

The entropy storage rate is a function of the annual mean top-of-atmosphere energy imbalance and the storage temperature, which are shown in Figure 5.16 as a function of the annual top-of-atmosphere SW anomaly. There is a correlation between the entropy storage rate and the SW anomaly, dominated by the variation in the energy storage rate. The mean rate of entropy storage is $6.3\,\text{mW/m}^2\text{K}$ in the SYN dataset, with annual means ranging between 4.0 to 8.6 mW/m^{2}K in the time period considered (2000 - 2018). This correlation makes sense: in years with high absorption of solar radiation there is a smaller increase in longwave emission to space because

of a damping effect of heat uptake by the ocean (as explored in KR2020 Figure 8, first and second panel), leading to an increase in energy and entropy storage.
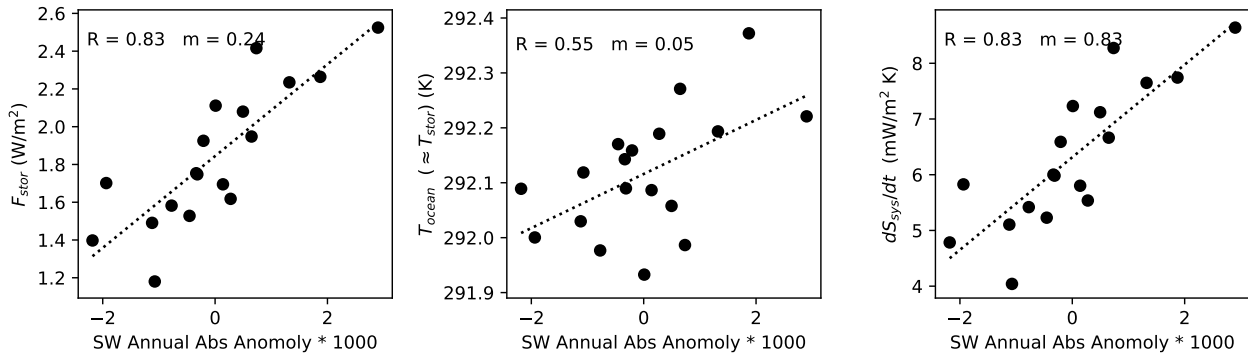

Figure 5.16: (a) The rate of storage of energy within the system (the net top-of-atmosphere radiative imbalance) correlates strongly with the top-of-atmosphere solar absorption anomaly. (b) There is also a positive correlation with the average ocean surface temperature (used here as a proxy for the entropy storage temperature). (c) The resulting trend in the estimated rate of storage of entropy within the system ($= dS_{sys}/dt$) has a similar form to the rate of storage of energy, panel (a).

The upper panel of Figure 5.17 reproduces KR2020 Figure 8(c) but uses absolute units rather than anomalies for the difference in longwave outgoing and shortwave absorbed entropy flux (y-axis). This allows us to compare it with the storage rate $\frac{dS_{sys}}{dt}$ in 5.16, which shows that the negative trend found in KR2020 can be predominately explained by the behaviour of storage within the system. In the lower panel of Figure 5.17, the corrected entropy production rate, $\Sigma = J_{out} - J_{in} + \frac{dS_{sys}}{dt}$, is plotted against the SW annual absorption anomaly. This reveals a trend of entropy production with solar absorption anomaly that is a factor of four smaller in magnitude and of *opposite sign*, increasing with a slope of 0.13 (95% confidence interval: 0.09 to 0.18) rather than decreasing with a slope of -0.70 (95% confidence interval: -1.06 to -0.47) as in the upper panel of Figure 5.17 and KR2020 Figure 8c for the difference in entropy fluxes.

These updated results should not be considered unintuitive. The increase in energy flowing through the system in high absorption years gives more opportunity for entropy production. Higher energy flow drives an increase in the temperature differences within the climate system, which also contributes to the increase in the entropy production rate, $\Sigma_{prod} = F(1/T_C - 1/T_H)$, where T_H is the representative input temperature and T_C the output temperature for the irreversible processes. In the time period under consideration, entropy flow is (for an annual average) into, not out of, the ocean storage reservoirs, and so T_H is simply the absorption temperature of solar radiation $T_a = F_{SW}/J_{in}$. The energy-weighted output temperature is an average of the cooling-to-space and storage temperatures: $T_C = (F_{LW} + F_{stor})/(J_{out} + J_{stor})$. Both temperatures increase with solar absorptivity (Figure 5.18(a) and (b)), but the effect is small compared to the change in F_{LW}, especially when the inverse difference is taken. A common way to express the temperature influence on entropy production is through the efficiency $\eta := 1 - T_C/T_H = T_C(1/T_C - 1/T_H)$ [*Bannon*, 2015], such that $\Sigma = \eta F/T_C$. There is a small positive correlation between efficiency and the SW absorption anomaly, as shown in Figure 5.18(c) which is
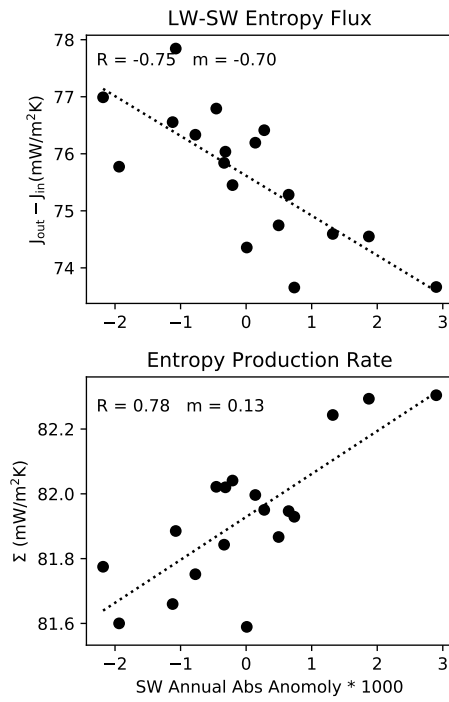
Figure 5.17: (upper) A reproduction of `KR2020` Figure 8(c) with the y-axis – the difference between longwave outgoing entropy and shortwave absorbed – in absolute units rather than anomalies. The downward trend is the result highlighted in that published study as representing a trend in the entropy production rate, however it is revealing to note that $J_{out} - J_{in} = \Sigma - J_{stor}$ and the trend is of a similar order of magnitude to the rate of storage in the system, Figure 5.16(c). (lower) The actual entropy production rate, calculated by adding the storage to panel (a), $\Sigma = J_{out} - J_{in} + dS_{sys}/dt$, shows a positive trend. This figure refers to the transfer entropy production rate.

consistent with an increase in the entropy production rate, but the dominant cause of the trend in Σ is the trend in F.

The storage of entropy in the climate system also impacts the estimate of the non-radiative material entropy production rate and its correlation with albedo. This trend is of similar form to that for the transfer entropy production rate shown in Figure 5.17, with the un-corrected difference in entropy fluxes exhibiting a negative correlation with shortwave absorptivity, ranging from $46.7 - 51.1 \, \text{mW/m}^2\text{K}$ and with an average value of $49 \, \text{mW/m}^2\text{K}$, as in `KR2020`. With the entropy storage correction, the new estimate for the non-radiative entropy production rate is $55.3 \, \text{mW/m}^2\text{K}$, the inter-annual range is $54.9 - 55.7 \, \text{mW/m}^2\text{K}$, and a positive correlation is found between the material entropy production rate and shortwave absorption.

The updated results suggest the transfer entropy production rate increases with solar absorption a as $\frac{d\Sigma_{tran}}{da} = 120 \, \text{mW/m}^2\text{K}$ per unit absorptivity (95% confidence interval: 58 to $161 \, \text{mW/m}^2\text{K}$). For the material entropy production rate, $\frac{d\Sigma_{tran}}{da} = 104 \, \text{mW/m}^2\text{K}$ per unit absorptivity (95% confidence interval: 30 to $167 \, \text{mW/m}^2\text{K}$).

The positive correlation of entropy production with shortwave absorption can even be confirmed in simple climate models. The EBM of Section 3.2.2 estimates a steady state climate configuration - there is no transient response, no seasonality, no inter-annual variability and no storage of entropy within the system. However, if the surface albedo α is artificially reduced, the increase in the absorption of solar radiation leads to an increase in the surface and atmospheric temperatures and also in the rate of energy flow through the system. Although the absolute values of entropy production rates in the EBM differ significantly from the observed climate ($\Sigma_{tran} = 67.0 \, \text{mW/m}^2\text{K}$ and $\Sigma_{mat} = 30.4 \, \text{mW/m}^2\text{K}$), the model produces a strikingly similar fractional increase in the transfer and material entropy production rates with solar absorptivity compared to the SYN case (Figure 5.19,
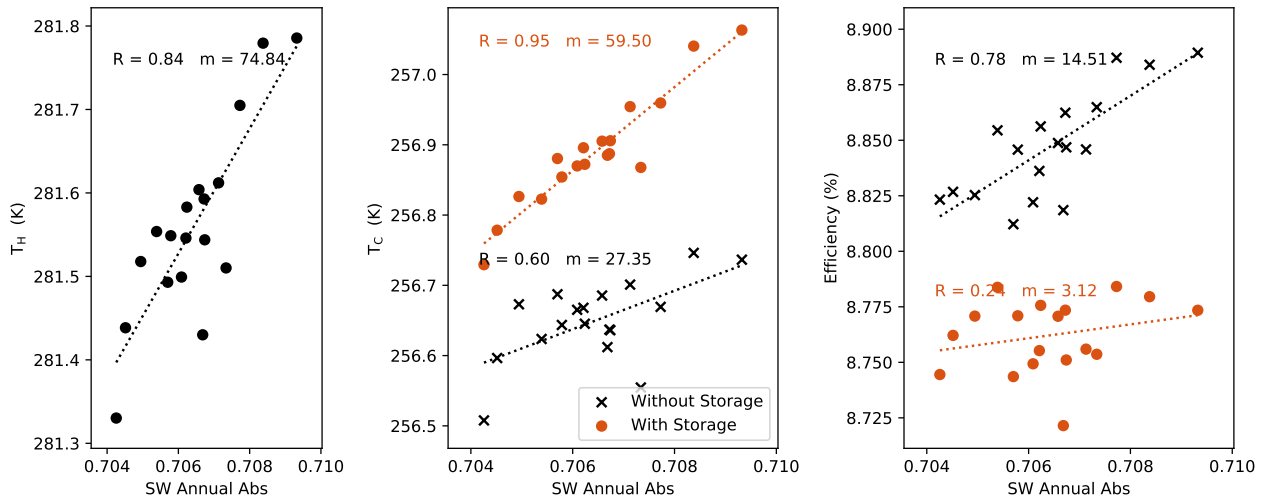
Figure 5.18: (left) The energy-averaged shortwave absorption temperature T_H, or T_a in `KR2020`, increases in high solar absorption years. (middle) There is a less pronounced trend in the system's output temperature, which is an energy-weighted average of the temperature of radiative emission to space and of storage. The values if storage is not accounted for are shown with crosses. (right) The Carnot efficiency of the climate, $1 - T_C/T_H$, therefore increases with solar absorptivity. This figure refers to the transfer entropy production view of the climate system.
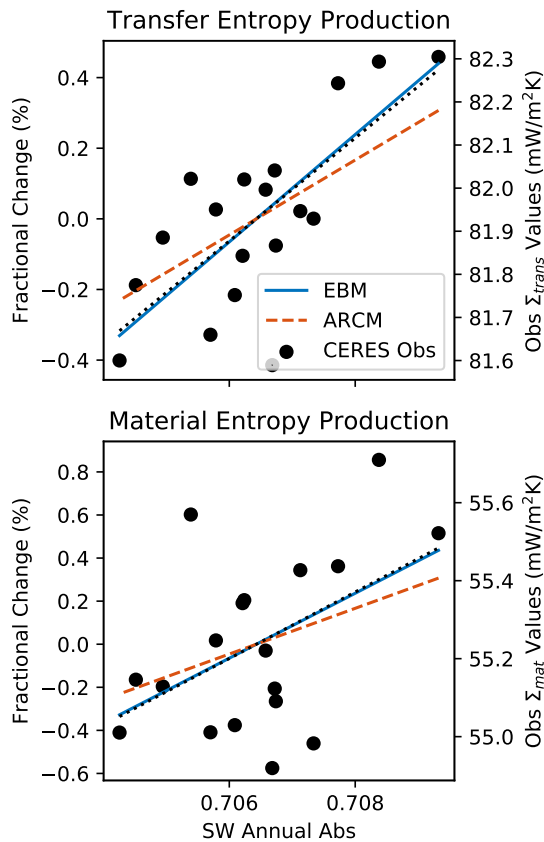
blue lines).

Figure 5.19: The fractional change (%) of the entropy production rate with the annual shortwave absorptivity anomaly. The observational SYN data (points, black dotted best fit line) of Figure 5.17 is rescaled by its mean value. The results for entropy production rate changes in response to albedo changes in an energy balance model (blue line) and an analytic radiative-convective model (red line) are compared to their control values (using standard published parameters from *Bannon* [2015]; *Tolento and Robinson* [2019]). The slope of the best fit line in the transfer entropy production rate case, upper panel, is 146 units of fractional change (%) per unit absorptivity, with a 95% confidence interval of $(70-198)$, which is consistent with the slopes of the EBM (152) and the ARCM (106). For the material entropy production rate, the slope of the best fit line is 154 with a 95% confidence interval of $(-24 - 266)$, compared to the EBM-derived slope of (151) and the ARCM slope (106).

This is a very different method of leveraging the EBM to estimate an entropy production rate from the approach taken in `KR2020`. In particular, it is claimed there that "the 1D [two-layer EBM] does not predict the change of T_a with shortwave absorption", which we would dispute, as in the EBM there is an increase of the

average absorption temperature T_a with absorptivity anomaly, $\frac{dT_a}{da} = 107\,\text{K}$, which compares well with the observed slope of $78\,\text{K}$ in Figure 5.18 (left panel), although the absolute temperatures compare less favourably ($T_{surf}(EBM) = 279.3\,\text{K}$ for the observed average albedo of 0.29 compared to the observed global mean surface temperature in the SYN1deg model of $288\,\text{K}$).

The positive correlation between solar absorption and entropy productions is also corroborated in the simple analytic radiative-convective model (ARCM) of *Robinson and Catling* [2012]; *Tolento and Robinson* [2019], used in Chapter 4 (Figure 5.19, red lines). The ARCM gives absolute values for entropy production which are again lower than the observed values ($\Sigma_{tran} = 75.9\,\text{mW/m}^2\text{K}$ and $\Sigma_{mat} = 27.2\,\text{mW/m}^2\text{K}$), but when the global top-of-atmosphere albedo is varied, however, the fractional changes in the entropy production rates are broadly consistent with observations (Figure 5.19, red lines).

That the models do not reproduce the absolute value of entropy production is not surprising; they contain a very limited range of processes, in particular they have no horizontal extent so any entropy production due to transport in the horizontal is omitted. They are, however, designed to capture the general energy and temperature trends of a climate, especially the increase of energy flux through the system and local temperatures with solar absorption, which are the variables that determine the entropy production rate. Taken together, the consistency of the positive correlation between top-of-atmosphere albedo and entropy production rates in both models *and* observations is strong evidence for that conclusion, and underlines the importance of taking storage into account.

5.5.6 Climate change trends

Over the 18-year period this data covers, there has also been a climate change trend of increasing surface temperatures. This has been driven by changes in radiative forcing due to increased greenhouse effect, but also by changes in the shortwave absorption, which has been increasing over the period as shown in Figure 5.20 [*Loeb et al.*, 2018].
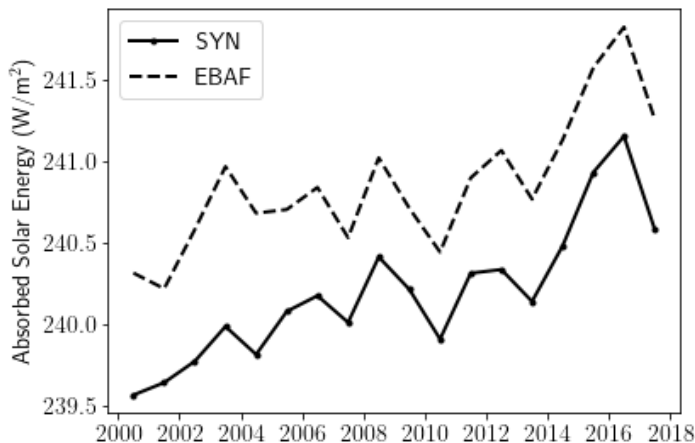

Figure 5.20: The annual mean absorbed solar energy flux in the SYN and EBAF datasets, demonstrating a clear positive trend due to a decrease in global albedo over that time period. This would be contributes to an increasing surface temperature.

Because of the positive correlation between entropy production and solar absorption discovered in the previous section, the increase in solar absorption over this period suggests an increase in the entropy production rates. This is indeed the case, as shown in Figure 5.21. There is a particularly good match between GMST and entropy production rates; even the inter-annual variations in the GMST are closely tracked by the production rate.
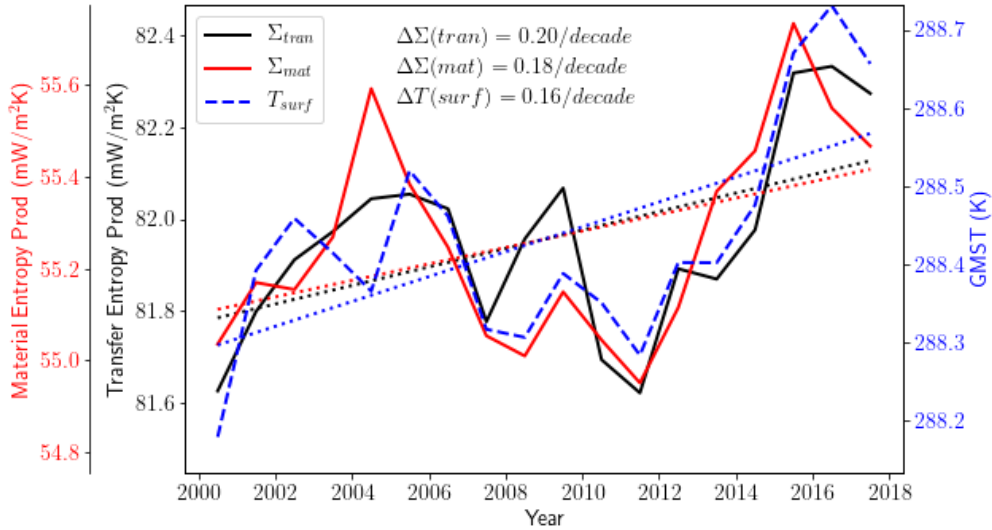
Figure 5.21: The annual global mean transfer (black) and material (red) entropy production rates in the SYN dataset, superimposed on the global mean surface temperature trend (blue). Best fit lines are shown dashed.

The similarity between the GMST and entropy production trends is striking and is further demonstrated by examining the correlation between GMST and entropy production rates, in Figure 5.22. That the correlation is stronger with the transfer entropy production rate than the material rate is suggestive of the value of that perspective, though with so few data-points this difference in R-value is not necessarily statistically significant. It may also be instructive to examine the outliers, especially on the material entropy production rate plot: what features of climate state cause certain years have very different entropy production rates but similar global mean surface temperature?

Figure 5.22: The correlation between the annual global mean material (left) and transfer (right) entropy production rates and the global mean surface temperature in the SYN dataset.

In Section 4.4, a simple analytic radiative-convective model was used to deduce the impact of a change in

the greenhouse effect on the entropy production rates, and predicted an increase of both material and transfer entropy production rates with increased optical depth. An attempt to isolate the greenhouse effect from the shortwave absorption trend has been mad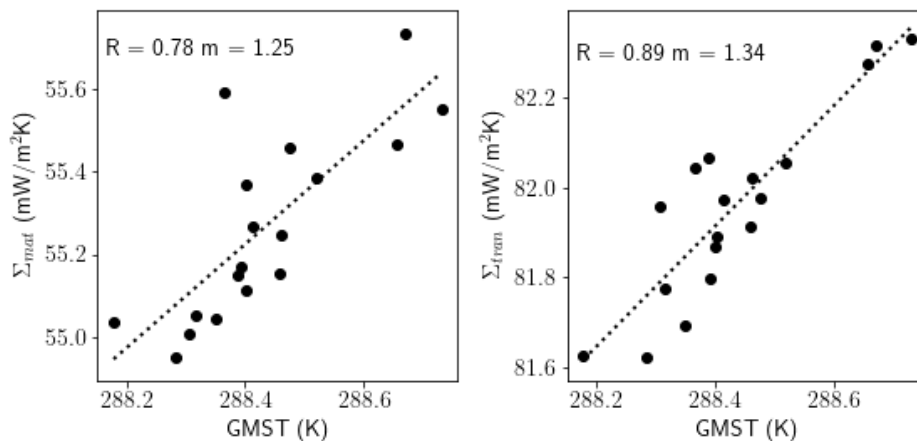e in Figure 5.23, by using the functional relationship between the shortwave absorption anomaly and entropy production rate anomaly deduced in Figure 5.17 to subtract the component of the entropy production rate trend which is correlated with this increase in shortwave absorption.
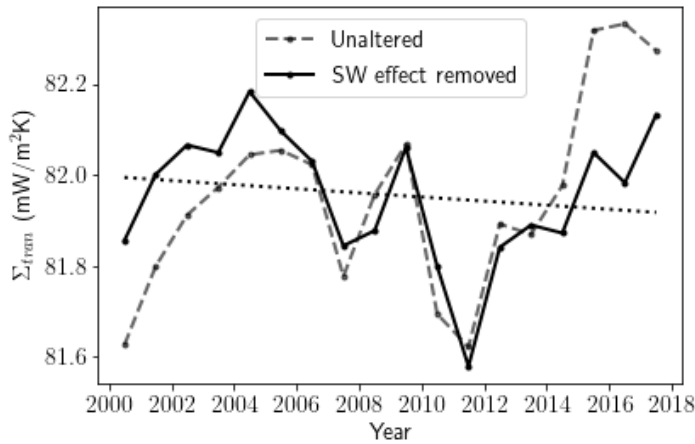

Figure 5.23: The global annual average transfer entropy production rate (dashed) with the component dependent on the shortwave absorption calculated from the trend in Figure 5.17 subtracted (solid, with dotted best fit line). The remaining variation is due to other features, including changes in the greenhouse effect.

If this trend were dominated by a relationship between the average atmospheric thermal optical depth and entropy production rates, we would expect a smoother result, as the greenhouse effect has been increasing quite steadily. Instead, the variability evident is suggestive of other internally-fluctuating features of the climate system. This is another result that warrants further investigation.

5.6 Discussion

5.6.1 Error estimation

The magnitude of potential errors in these global entropy production rate data products are fundamentally difficult to estimate because so many pieces of data are brought together to estimate entropy production. If the temperature or composition of the atmosphere in the assimilation model is incorrect, the radiative transfer will suggest heating and cooling from incorrect parts of the system, which will affect entropy production rates. More crucially, the inaccuracies in the global energy budget, as evidenced by the high apparent rate of entropy storage in the SYN dataset compared to the EBAF dataset, is very much manifested in the glfobal entropy production rates, changing the values by up to 2% as demonstrated in Table 5.3 . Furthermore, in the estimates of entropy storage, incorrect characterisation of the expected storage temperature introduces further potential errors, as discussed in Section 5.4.

In *Kato and Rose* [2020], where the SYN dataset is introduced, they estimate an uncertainty in the net radiative entropy flux of 10%. If this were an uncorrelated error, with different years experiencing different deviations

from the true estimate, a $5 \, \text{mW/m}^2\text{K}$ range on the material entropy production rate and $8 \, \text{mW/m}^2\text{K}$ on the transfer entropy production rate would easily render inconclusive the trend noted in entropy production against solar absorption (Figure 5.17) and cast doubt on the hemispheric asymmetry of global entropy production rate results, which show a difference of half of these values. However, it is more likely that such errors would be systematic and somewhat uniform across the dataset, in which case the absolute values of the trends and values measured in this chapter should be taken with only a 10% confidence, but the trends and patterns seem likely to be more robust.

5.6.2   In relation to other studies

Many of the results in this section are without precedent in the literature because we have not previously had access to such a complete, observationally-based entropy production dataset. However, there is insight to gain from the overlaps with what has previously been found.

The mean annual material entropy production rate suggested by the corrected SYN dataset of $55.3 \, \text{mW/m}^2\text{K}$ is consistent with the estimate of $51.8 \, \text{mW/m}^2\text{K}$ for the HadCM3 model in *Pascale et al.* [2011a] and higher than the direct estimates of around $40 \, \text{mW/m}^2\text{K}$ in *Lembo et al.* [2019]. The standard deviation of the annual mean entropy production rate over the 18 year observational period is only $0.2 \, \text{mW/m}^2\text{K}$ for the transfer entropy production rate and the material entropy production rate, which is much lower than the value of $1 \, \text{mW/m}^2\text{K}$ found in *Pascale et al.* [2011a].

The hemispheric asymmetry of the entropy production rate, with more produced in the Northern hemisphere, is consistent with the higher precipitation in the Northern hemisphere (see *Stephens et al.* [2016]), recalling that the hydrological cycle plays the dominant role in the non-radiative entropy production. Using the relationship between transfer entropy production rate and temperature uncovered in Chapter 4, the inter-hemispheric GMST difference is also consistent with the higher entropy production rate noted in the warmer Northern hemisphere.

Seasonal cycles in the planetary entropy perspective were studied in *Stephens and O'Brien* [1993], which, as established in Chapter 4, is not easily mappable to the transfer or material entropy perspectives. Note also that *Paillard and Herbert* [2013] investigates applying MEPP in a two-box model with seasonally-varying forcing, rather than diagnosing the observed consequences of the seasonal cycle on the entropy production rates. Neither of these are comparable to the results found here.

5.7   Conclusions

Measuring entropy production rates in realistic Earth climate states is not a solved problem, but there are hints that there will be interesting results to explore as it develops. The promisingly versatile approach of using offline

radiative transfer calculations for atmospheric columns in the `entmap` project faced significant challenges in its vast computational requirements and the difficulty in sufficiently constraining the radiation-relevant properties of an atmosphere from GCM output parameters. When *Kato and Rose* [2020] calculated material and transfer entropy fluxes from radiative transfer calculations within the existing CERES SYN1deg observational product, they ran into the challenge of combining entropy fluxes with entropy storage rates to deduce entropy production rates properly. In this chapter I have explained storage correction in detail and updated the SYN entropy production dataset accordingly, giving a novel global, observational entropy production rate dataset.

From this, many features of the global entropy production rate are elucidated. Taken together, they underline an important point: entropy production is not an incomprehensible, mysterious variable - there are patterns and stories to be told with it that are not so dissimilar from those which we are familiar exploring in other climate state metrics, but dissimilar enough not to be trivial. The material and transfer entropy production rates have been tracking the global mean surface temperature over the past two decades, showing an increase of 0.32% and 0.24% per decade, compared to 0.06% for GMST. The entropy production rates are higher in years with high shortwave absorption (a discovery which corrects the result published in *Kato and Rose* [2020]) but no trend due to the change in the greenhouse effect can be separated from the noise. Entropy production rates are higher in the northern hemisphere than the southern, by 2.1% for the material rate and 3.2% for the transfer rate. Furthermore, there is a strong seasonal cycle which is difficult to measure, because the magnitude of intra-annual entropy storage challenges our approximations, but nonetheless appears to show a lower entropy production in the summer months. This last result in particular separates entropy production from GMST in its behaviour.

5.7.1 Further research questions

The results discussed in this chapter are some of those which were attainable with the information available in the SYN dataset. There are many more questions remaining to be addressed which provide interesting lines of enquiry:

- How and why do the entropy production rates vary between climate models?

- Do the irreversible processes modelled directly within a climate model capture as much entropy production as is suggested by the indirect tally?

- How do diurnal cycles manifest in entropy production analysis, and do diurnally-averaged datasets introduce systematic errors?

- How does land albedo change affect global entropy production rates?

- What impact does ENSO have on the entropy production rates?

I hope that the improved SYN dataset, and others which might be created following similar approaches, might help answer these questions.

Chapter 6

Conclusions and Future Work

What are the key scientific implications of the results offered in this thesis? Entropy production and the climate remains a complicated, intricate topic. With this work, I have returned to fundamentals: what is the global entropy production rate, how does it capture and respond to features of the Earth's climate, how can it be measured in reality, and what patterns does that reveal. These investigations have furnished the following conclusions and ideas for future work.

6.1   The transfer entropy production rate is a promising new perspective

The most fundamental and potentially-impactful contribution in this thesis has been the re-framing of the choices available in specifying the global entropy production rate and, in particular, the advancement of the transfer entropy production rate. Building on the excellent work in *Bannon* [2015], I have laid out three primary options for defining a global entropy production rate, which differ in the extent to which they consider radiation to be part of the climate system. The material entropy production rate, which focuses on only non-radiative processes, and the planetary entropy production rate, which includes all processes, radiative and non-radiative, were standard concepts in the literature. However, the intermediate transfer entropy production rate, which separates radiation according to the role it plays within the system, had not been thoroughly appreciated or investigated.

Having introduced the transfer entropy production rate in Chapter 3, and contrasted it with the material and planetary entropy production rates in Bannon's simple energy balance model, the developments of the following two chapters revealed hints that the transfer entropy production rate might be a more natural, meaningful climate system-summarising variable than the two established entropy production rates. In an analytic radiative-convective model in Chapter 4, the transfer entropy production rate was found to respond neatly to climate changes due to variations in the albedo, greenhouse effect and latent heat in convection. Of the three

entropy production rates, the transfer entropy production rate was the only one to increase with surface temperature in all three climate change cases. Furthermore, the material entropy production rate gained intelligibility as a component of the transfer rate, remaining in fixed ratio with the transfer rate when the heat transfer processes within the climate were not directly altered (the albedo-mediated climate change), but increasing when an increased greenhouse effect suppressed heat transfer by internal radiation relative to non-radiative processes, and decreasing when latent heat transfer was suppressed. The planetary entropy production rate fared poorly in this investigation, only being able to resolve changes in the climate due to the albedo variations.

In the observational dataset introduced in Chapter 5 – a storage-corrected version of the CERES SYN1deg dataset of *Kato and Rose* [2020] – the transfer entropy production rate was again physically significant. Its behaviour in the observational record was broadly similar to the material entropy production rate but, certain features were more pronounced for the transfer entropy production rate – namely the hemispheric difference in entropy production rate, the correlation between annual shortwave absorption anomaly and entropy production rates, and the correlation between annual average global mean surface temperature and entropy production rates. These observations show that the transfer entropy production rate is able to pick up on something meaningful in the climate system, more so than other entropy production rate variables.

The transfer entropy production rate also has theoretical elegance and potential significance. By focusing on heat transfer within the climate system both by internal radiation and material processes, it does not differentiate between mechanisms which are anyway indistinguishable from the rest of the system's perspective. It focuses on the temperature at which energy is first supplied to and last leaves the climate system, which are comprehensible and intuitively meaningful variables. And it even fits well with the original *Paltridge* [1975] observation of maximisation of meridional entropy production: in the horizontal, entropy production due to internal radiation is minimal and the value Paltridge found to be maximised could equally be interpreted as either the horizontal component of the material or the transfer entropy production rates. In fact, it is even possible that the difficulty of demonstrating maximisation of entropy production in the vertical might be explained by a focus on the material component only and the outlook could be different if the transfer entropy production rate were considered.

Although this tantalising idea remains to be tested, what is clear is that the transfer entropy production rate is physically meaningful, that it is definitively different from the more common material and planetary entropy production rates and that it has the potential to shed new light on the study of Earth's entropy production.

6.2   Entropy production rates are sensitive global climate variables

The results in this thesis have also helped to situate the global entropy production rates as climate-summarising variables more generally. Even with detailed numerical simulations of the climate system available in GCMs,

global summary metrics can add value in terms of comprehension, communication and analysis, as discussed in Chapter 2. Energy conservation supplies physically-grounded global variables in the total energy budget, but there is not such an obvious candidate for incorporating temperature and the activity of the climate system; the global mean surface temperature (GMST) is accepted in the field but is a geometric rather than physically-motivated aggregate variable.

In Chapter 4, I demonstrated how the global entropy production rates respond to simple climate changes which increase the surface temperature, showing that the entropy production rate can differentiate between the manner of the climate change. This was particularly striking in the case of a simple solar radiation management scenario: although surface temperature can be restored by adjusting the albedo to compensate for a greenhouse gas change, the entropy production rates cannot, indicating that an intervention in the shortwave energy flow to compensate for longwave changes is in a fundamental way unsuited to restoring the pre-industrial climate in terms of irreversible activity.

In Chapter 5, the entropy production rates and related variables were explored in a two-decade observational dataset. In the period from March 2000 to February 2018, the mean global average transfer entropy production rate was estimated as $82.0 \, \mathrm{mW/m^2K}$ and the material entropy production rate $55.3 \, \mathrm{mW/m^2K}$. The transfer entropy-averaged input and output temperatures were calculated, at 281.6K and 256.7K, and it was shown that the entropic global average temperatures emphasise those regions which have more energy flow, with relatively less focus on the poles than the GMST. The difference in input and output temperatures is maintained by the external energy sources and sinks and represents the temperature difference necessary to ensure energy flows from input to output locations: they are meaningful global temperature metrics to consider alongside GMST.

New patterns in the global entropy production rate were also found. Some mirrored the trend in GMST - most notably, an increase in the global entropy production rate in line with the 0.16 K/decade increase of GMST of $0.18 \, \mathrm{mW/m^2K/decade}$ for the material entropy production rate and $0.16 \, \mathrm{mW/m^2K/decade}$ for the transfer. A higher material and transfer entropy production rate was also noted in the warmer Northern hemisphere. In contrast to this, in both hemispheres the transfer and material entropy production rates both seemed to show a minimum in summer months, although this results requires further investigation due to the significant role the only-approximately-calculated entropy storage rate plays on seasonal time frames.

Perhaps the most striking evidence of a new-found understanding of the entropy production rates as global climate metrics was illustrated by two instances of the ability to predict and then test the direction (and to a limited extent, the magnitude) of entropy production rate responses to climate changes. The first of these came in Section 4.3 with the conceptual model of the climate system as a hotter and colder reservoir with material and radiative heat transfer 'resistors' acting in parallel to transfer energy from influx to outflux. This picture was able to forecast and make sense of the behaviour observed in the simple analytic radiative-convective model (ARCM) of *Robinson and Catling* [2012] and *Tolento and Robinson* [2019] when the climate changes were

implemented. The second confirmation used the observed climate to confirm entropy responses predicted by the ARCM and EBM. An *increase* of the transfer and material entropy production rates with increasing solar absorption (decreasing albedo) was a robust result of Chapter 4, but was contrary to the result published in *Kato and Rose* [2020] which found a *decrease* in entropy production rate in anomalously high solar absorptivity years in their observational dataset. This led me to re-examine their result, which revealed an error in the omission of the interannual storage of entropy [*Gibbins and Haigh*, 2021]. Correcting for this reversed the apparent trend resulted in an increase of the entropy production rates with solar absorption anomaly in the observed climate that is of a similar order of magnitude to that suggested by the analytic radiative-convective model and the energy balance model.

Entropy production rates are unlikely to replace the familiar variables of global temperature and top-of-atmosphere energy imbalance in our climate discussions, but they do have potential to add to it. Generally, it is helpful to be able to summarise aspects of our climate via global scalar metrics, but it is essential to not over-simplify, and an over-reliance on the single metric of global temperature is a danger (recall the solar radiation management issue). Entropy production rates are meaningful, comprehensible climate metrics which offer a useful additional perspective.

6.3   Observational datasets have been improved to support further discoveries

In this thesis, I have also worked on constructing the tools necessary to observe and measure the entropy production rate in realistic systems. This is far from trivial because entropy production rate is not a state variable to be measured but sums the impact of all the various irreversible processes in the climate system. Here, I have explored using the properties (temperature and spectral intensity) and quantity of the energy flow at the boundaries of the system to calculate the entropy fluxes and from these (and the rate of entropy change of the system, i.e. the entropy storage) deducing the entropy production rate. Initially, this was by building a versatile offline tool for analysing a snapshot of the climate state via radiative transfer calculations and entropy fluxes deduced from these. This proved too computationally intensive and so has been put on hold, but some of the insights from this were able to be applied directly to the similar work which was undertaken in *Kato and Rose* [2020] for the observationally-based CERES SYN1deg dataset. In particular, the Libradtran-based entropy calculating tool I constructed was able to verify numerically the methodology used to create the CERES dataset, lending credence to its reliability.

Although the *Kato and Rose* [2020] analysis introduced a very detailed, public dataset, it was of limited use without estimates of the rate of entropy storage. This is because in a realistic system which is not steady in time, there is intra- and inter-annual storage of energy and entropy. If the difference in cross-boundary entropy fluxes is taken as the entropy production rate without including an entropy storage term, erroneous conclusions

can be formed (as in the issue of the trend of entropy production rate with a solar absorption anomaly), and the patterns in the true entropy production rate can be drowned out by the variation in the storage rate (for example, the close match between material and transfer entropy production rates and GMST of Figure 5.21 does not appear). Estimating the rate of entropy storage from the global mean ocean surface temperature allows entropy production rates to be calculated from the *Kato and Rose* [2020] CERES SYN1deg dataset.

Entropy production is not widely understood or studied by the broader climate science community, in large part because it is difficult to grasp and requires specialised tools to analyse. This storage-augmented dataset is an opportunity to make entropy production more accessible as a variable to study, as it fits within the established CERES project and can be freely downloaded with familiar formatting and metadata. The verifications, improvements and demonstrations of the kinds of results which are possible from the dataset offered in this thesis will be useful to improve the documentation and explanation for future users. There are many further questions which could be probed with this dataset: for example, how does the ENSO impact entropy production rates? Or, what are the features which might explain the years in which the correlation between entropy production rates and GMST diverge? Having an observational dataset is essential to ground and inspire entropy production research, both to be able to test theories but also to prompt us to notice and reckon with the features of the true climate which impact the entropy production rate.

6.4   More questions and ideas for the MEPP hypothesis

6.4.1   Broad considerations

Although this work did not set out to directly investigate the maximum entropy production principle hypothesis, the exploration did raise some ideas and questions about it which might inform further study.

The first thing of note is that our investigations of the response of the entropy production rate to climate changes underline that none of the entropy production rates is at its global maximum (or minimum) value in the climate system. The planetary entropy production rate would be increased by a lower albedo, i.e. if more of the radiation incident on the planet were absorbed and re-emitted rather than scattered. It would also be increased if the outgoing longwave radiation were more uniform, without emission temperature variations. The transfer entropy production rate would similarly be higher if there were more energy flowing through the system, via a lower albedo, or if the surface temperature were warmer because of a drier atmosphere or higher greenhouse gas concentration. A more moist atmosphere, more solar absorption and a stronger greenhouse effect would all increase the material entropy production rate. Furthermore, these higher and lower entropy production states occur in some years in the CERES SYN1deg dataset but are not maintained; the entropy production rates fluctuate without a monotonic tendency towards a maximum or minimum.

This implies that if it were the case that the climate were seeking an optimum in its entropy production rate, it must be with respect to certain constraints. There poses a challenge though (also raised by *Caldeira* [2007]): we know from our deterministic models of the climate that the full constraints of the law of physics and the climate's composition determine the climate's exact state and thus a particular entropy production rate, which is in some sense both the maximum and minimum that it can be. If the climate is self-organised for an extremum, it must be with respect to some constraints but not all.

One way to approach this is to step back and consider what types of things could conceivably be controlled by a principle like MEPP and what are unalterable. Things like the speed of light and the enthalpy of vaporisation are clearly constraints to be imposed, but variables related to the efficiency of convection and cloud characteristics are parameters with respect to which it has been speculated MEPP might act [*Wang et al.*, 2008; *Pascale et al.*, 2012]. The solar constant is another example of a constraint, but the albedo would seem to be a mode of self-regulation available to the climate system. Some are even less clear: the quantity of carbon on Earth is a constraint, but is the concentration in the atmosphere? The scattering from a particular water droplet is a physical fundamental, but are the number of cloud-nucleating particles in the atmosphere and the resulting brightness of a cloud self-regulation variables?

Another question is what do we expect the states which would be ruled out by MEPP to look like? Are they physically realisable but not the ones we happen to see on Earth or might they be states which we would not recognise as physically possible, such as a convectively unstable atmosphere which refuses to convect? If MEPP applies to a wide range of systems, it might be plausible that the states it rules out are ones which are unphysical to our intuition.

Yet another question is: which entropy production rate is to be maximised? The discussion in Chapter 3 underlines that the material, transfer and planetary entropy production rates are all valid entropy production rates, but are from three nested systems of different extents. Chapter 4 demonstrates that the entropy production rates behave differently from each other, capturing different features of the climate system, so they are unlikely to be maximised by the same climate state. An MEPP theory would have to explain why the climate's configuration should be governed by the entropy production rate(s) it proposes - why that perspective of the climate system's extent is the predictive one and not the others.

It is interesting to consider thought experiments of adjacent systems in which we might expect an MEPP-like theory to apply, were it to exist in the climate system. For example, a system identical to the climate but in which heat is still delivered to and taken from the same places by a mysterious external heating mechanism rather than radiation (with the system still translucent to internal radiation) would be expected to have exactly the same configuration but a very different planetary entropy production rate. Similarly, a climate-like system which is not translucent – and so no internal radiation exists to distinguish the material from the transfer entropy production rate – could still be governed by an extremal principle. If clouds and water vapour were

not radiatively active, either in the shortwave or the longwave, would that disrupt an extremal principle? Is the existence of an MEPP-like law in a Rayleigh-Bernard set-up or rotating annulus a necessary or sufficient condition to deduce that one does or does not exist in the climate?

These questions do not offer solutions to the MEPP debate, but perhaps enrich it, leveraging the more fundamental developments offered by this thesis.

6.4.2 A resistor analogue

The conceptual resistor model for the climate as an entropy-producing system which was introduced and tested in Chapter 4 also suggests an intriguing way of perceiving the system as seeking an extremal value in terms of its entropy production. It is an idea that is partially suggested by *Reis* [2014] but which has not yet been picked up in the MEPP literature.

Consider that one of the climate system's key features is that it has many possible mechanisms and routes by which to transfer energy from the hot places where it is deposited to the cold places where it leaves. In doing this, material processes and internal radiation act in parallel, both behaving in the most basic sense like resistors, transferring as much energy as the temperature difference implies. The natures of the heat transfer processes ('resistors') are then somewhat fixed by physical laws, but *what is free to adjust is the amount of energy transported by each*, in the same sense that the current through parallel branches of a circuit adjusts to the most efficient, balanced, configuration. When a new 'resistor' becomes available (or, equivalently, if it had been unphysically under-utilised before), the system automatically brings it online. This either increases the total amount of energy which flows through the system (in the case of fixed temperature difference) or decreases the temperature difference necessary to transport a fixed quantity of energy. In *Reis* [2014], this is taken as an example of the Constructal Law, that a system will organise itself most efficiently with respect to the flow through it. More simply, it is a consequence of a monotonic relationship between driving temperature difference and energy flow through a process, which makes an efficient sharing of the 'current' inevitable.

What is intriguing, however, is how this principle results in *either* a maximisation *or* a minimisation of the entropy production rate, depending on the boundary conditions forcing the system out of equilibrium. If the temperature difference is fixed, an additional 'resistor' increases the amount of energy which can flow through the system, *increasing* the rate of entropy production. If, on the other hand, the amount of energy flowing through a system is fixed, an additional resistor decreases the necessary driving temperature difference, *decreasing* the entropy production rate. This was pointed out by *Reis* [2014], but there it is suggested that the climate is a fixed temperature system. I would argue that the climate is not a fixed-temperature-difference system, and if anything, the climate is more approximately a system where the incoming solar energy flux is fixed[1]

---

[1]The self-regulation by the feedback of the humidity on albedo is the obvious hiccup in this picture.

and the temperature difference responds, suggesting that the system is one that we could expect might in some sense *minimise* its entropy production.

Interestingly, this update away from MEPP and towards a theory of maximisation or minimisation of entropy production depending on boundary conditions also applies to laboratory experiments. Some studies of convective heat transport between hot and cold plates in fluid-based table-top experiments have reported a maximisation of entropy production [*Ozawa et al.*, 2003], however more recent and thorough analysis have pointed out that if the current is fixed and temperature is allowed to adapt, a minimisation is instead noted [*Bartlett and Virgo*, 2016]. Another similar result can be found in *Weaver et al.* [2014], where a lattice-Boltzmann simulation of a Rayleigh-Bérnard convective system is used to study meta-stable states. It is found that depending on the nature of the forcing at the boundary conditions, the maximally stable state is either a maximisation or a minimisation of entropy production, but is reliably a maximisation of the rate of heat transfer. This is far from a direct indication of applicability in the climate system, but it suggests future investigation of this line of reasoning may be illuminating.

Could a maximisation of the efficiency of heat transport be consistent with the MEPP observations of Paltridge and others about the maximisations of meridional entropy production rates? The transfer entropy production rate is the natural one to study in relation to heat transport, because there is no reason to separate the non-radiative from radiative 'resistors' (as in the material entropy production rate), and because it points to there being two temperature reservoirs within the system (precluding the entropy production due to the thermalisation of solar photons and thus the planetary rate). Is it feasible that the horizontal component of that transfer entropy production rate could be maximised as a consequence of a minimisation of the total? One possible line of inquiry is that there is relative similarity between the vertical heat transfer 'resistors' across the globe – and recalling that the vertical is the primary source of entropy production – so it might be interesting to investigate whether a maximum entropy production configuration in the horizontal is an efficient trade off-consistent with a global minimisation of total entropy production[2].

These theoretical speculations are far from watertight, but it is hoped that they may offer openings for development of the predictive potential of entropy production rates. It remains plausible that entropy production rate optimisation is *not* a meaningful feature of our climate; it is temptingly neat and corroborations show up in some experiments, but there may be other explanations which underlie this, which themselves could be interesting scientific results that this pursuit of entropy might yet help to uncover.

---

[2]I have made a start on this investigation by considering a grid of resistors representing latitude and height. A prescribed current is applied to the lowest level representing absorbed solar radiation at the surface. At the highest level, a fixed current element is in parallel with the resistor from each node to ground for a $\sigma T^4 \approx A + BT$ representation of the thermal emission to space. For any internal resistances, the system can be solved by a single matrix inversion and entropy production rates calculated by certain matrix multiplications. A question which might be addressed with this set-up is whether the maximisation of the horizontal component of entropy production is consistent with the minimisation of the total. Another is whether constraining the vertical resistances but allowing the horizontal to vary reproduces a more recognisable climate state than if both horizontal and vertical resistances are optimised. This is an interesting model for further investigation.

6.5   Open questions and next steps

The results and ideas in this thesis raise some more specific next-step questions that might be fruitful to pursue:

- Milankovitch cycles initiate glacial-interglacial cycles not only by the quantity of annual insolation but by the timing and location of it. The temperature fluctuates throughout the course of the year and across the globe so the timing influences the amount of entropy flux a certain energy flux causes. Could the change of entropy flow into the climate system with the Milankovitch cycles explain the significance of the orbital variations?

- Is the entropy production rate of self-aggregated convective systems different from before aggregation and does that explain why aggregation happens?

- Cloud feedbacks are very significant in the climate and as a potential self-regulating system. How can an extremal hypothesis make sense of this feedback on the quantity of energy absorbed in the system?

- Does entropy production optimisation explain hemispheric symmetry in global albedo [*Voigt et al.*, 2013]?

- Convection can be adiabatic and isentropic, and yet energy moving by radiation from the lower, warmer arm of a convecting cell to the upper generates entropy. This has not been discussed neatly in the literature, but hints at a partial paradox, the clarification of which might help our understanding.

- In the climate change field, global mean surface temperature is *the* global metric, quantifying the state of the climate. What are the limitations of the geometric averaging, compared to other entropic temperature metrics, and are the assumptions inherent in GMST partially responsible for the difficulty in constraining and defining the climate sensitivity?

- For some more pure non-equilibrium thermodynamicists, the concept of an entropy production rate is questionable, because defining entropy in an out-of-equilibrium system is challenging. Does assuming local thermodynamic equilibria solve this problem or does it present or explain challenges with the study of the climate's entropy production?

- Tropopause height is a fingerprint of climate state [*Santer et al.*, 2003] which could plausibly be particularly related to entropy production via the cold emission temperature and the temperature difference between which convection acts. Tropopause pressure-height has also been noted as remarkably consistent (around 0.1 bar) among planetary climates [*Robinson and Catling*, 2014]. This might be an interesting avenue of investigation.

And some more concrete next steps:

- The ARCM used in Chapter 4 is designed to replicate extraterrestrial climates, which means our work could be combined with the published parameters for those planets [*Tolento and Robinson*, 2019] to measure the entropy production rates implied.

- In the CERES SYN1deg dataset: What is the correspondence between the ENSO index and entropy production rates? How does the diurnal cycle influence entropy production rates? What can be gleaned from investigating a 3D version of the dataset, with vertical resolution?

6.6   Closing remarks

Doing science as speculative as the study of Earth's entropy production rate is both exciting and challenging because it is such an untrodden space full of confusion and unresolved hypotheses. Questioning, going back to the basics of how we make sense of our climate, picking unorthodox routes and reframing familiar things in a different light is a way of making progress which is complementary to the more routine modes of science. This matters especially because our climate is desperately important to human existence and we, as a society, have very difficult and crucial choices to make about our impact on it. We can make those choices well only if we can make the immense, unintuitive complexity of the climate something more understandable. The results uncovered in this thesis suggest that this might be advanced by further study and clarification of the climate's entropy production.

Bibliography

Adkins, C. J., The zeroth law, in *Equilibrium Thermodynamics*, pp. 17–29, Cambridge University Press, 1983.

Anderson, G. P., J. H. Chetwynd, S. A. Clough, E. P. Shettle, and F. X. Kneizys, AFGL atmospheric constituent profiles (0-120km), p. 43, 1986.

Bala, G., P. B. Duffy, and K. E. Taylor, Impact of geoengineering schemes on the global hydrological cycle, *Proc. Natl. Acad. Sci. U.S.A*, *105*(22), 7664–7669, 2008.

Bala, G., K. Caldeira, and R. Nemani, Fast versus slow response in climate change: implications for the global hydrological cycle, *Clim Dyn*, *35*(2-3), 423–434, 2010.

Bannon, P. R., Entropy production and climate efficiency, *J. Atmos. Sci.*, *72*(8), 3268–3280, 2015.

Bannon, P. R., and S. Lee, Toward quantifying the climate heat engine: solar absorption and terrestrial emission temperatures and material entropy production, *J. Atmos. Sci.*, *74*(6), 1721–1734, 2017.

Bannon, P. R., and R. G. Najjar, Heat-Engine and Entropy-Production Analyses of the World Ocean, *J. Geophys. Res.: Oceans*, *123*(11), 8532–8547, 2018.

Bartlett, S., and N. Virgo, Maximum Entropy Production Is Not a Steady State Attractor for 2D Fluid Convection, *Entropy*, *18*(12), 431, 2016.

Caldeira, K., The maximum entropy principle: A critical discussion, *Climatic Change*, *85*(3), 267–269, 2007.

Clausius, R., Ueber eine veränderte Form des zweiten Hauptsatzes der mechanischen Wärmetheorie, *Ann. Phys.*, *169*(12), 481–506, 1854.

Clough, S. A., M. W. Shephard, E. J. Mlawer, J. S. Delamere, M. J. Iacono, K. Cady-Pereira, S. Boukabara, and P. D. Brown, Atmospheric radiative transfer modeling: a summary of the AER codes, *Journal of Quantitative Spectroscopy and Radiative Transfer*, *91*(2), 233–244, 2005.

Dewar, R. C., Information theory explanation of the fluctuation theorem, maximum entropy production and self-organized criticality in non-equilibrium stationary states, *J. Phys. A: Math. Gen.*, *36*(3), 631–641, 2003.

Dewar, R. C., Maximum entropy production and the fluctuation theorem, *J. Phys. A: Math. Gen.*, *38*(21), L371–L381, 2005.

Dewar, R. C., Maximum Entropy Production as an Inference Algorithm that Translates Physical Assumptions into Macroscopic Predictions: Don't Shoot the Messenger, *Entropy*, *11*(4), 931–944, 2009.

Dewar, R. C., A general maximum entropy framework for thermodynamic variational principles, *AIP Conference Proceedings*, *1636*(1), 137, 2014.

Dewar, R. C., and A. Maritan, The second law, maximum entropy production and Liouville's theorem, *arXiv*, 2011.

Dyke, J., and A. Kleidon, The Maximum Entropy Production Principle: Its Theoretical Foundations and Applications to the Earth System, *Entropy*, *12*(3), 613–630, 2010.

Emanuel, K. A., Hurricanes: Tempests in a greenhouse, *Physics Today*, *59*(8), 74–75, 2006.

Emde, C., et al., The libRadtran software package for radiative transfer calculations (version 2.0.1), *Geosci. Model Dev.*, *9*(5), 1647–1672, 2016.

England, J. L., Statistical physics of self-replication, *J. Chem. Phys.*, 2013.

Essex, C., Radiation and the irreversible thermodynamics of climate, *J. Atmos. Sci.*, *41*(12), 1985–1991, 1984.

Essex, C., Global thermodynamics, the clausius inequality, and entropy radiation, *Geophys. Astrophys. Fluid Dyn.*, *38*(1), 1–13, 1987.

Feistel, R., Entropy flux and entropy production of stationary black-body radiation, *J. Non-Equilib. Thermodyn.*, *36*(2), 131–139, 2011.

Fraedrich, K., and F. Lunkeit, Diagnosing the entropy budget of a climate model, *Tellus A: Dyn. Meteor. Oceanogr.*, *60*(5), 921–931, 2008.

Gibbins, G., and J. D. Haigh, Entropy production rates of the climate, *J. Atmos. Sci.*, pp. 1–46, 2020.

Gibbins, G., and J. D. Haigh, Comments on "Global and Regional Entropy Production by Radiation Estimated from Satellite Observations", *J. Climate*, *34*(9), 3721–3728, 2021.

Gjermundsen, A., J. H. LaCasce, and L. S. Graff, The Atmospheric Response to Surface Heating under Maximum Entropy Production, *J. Atmos. Sci.*, *71*(6), 2204–2220, 2014.

Goody, R., Sources and sinks of climate entropy, *Quart. J. Roy. Meteor. Soc.*, *126*(566), 1953–1970, 2000.

Goody, R., Maximum Entropy Production in Climate Theory, *J. Atmos. Sci.*, *64*(7), 2735–2739, 2007.

Goody, R., and W. Abdou, Reversible and irreversible sources of radiation entropy, *Quart. J. Roy. Meteor. Soc.*, *122*(530), 483–494, 1996.

Grassl, H., The climate at maximum entropy production by Meridional atmospheric and oceanic heat fluxes, *Quart. J. Roy. Meteor. Soc.*, *107*(451), 153–166, 1981.

Green, J. S. A., Division of radiative streams into internal transfer and cooling to space, *Quart. J. Roy. Meteor. Soc.*, *93*(397), 371–372, 1967.

Gregory, J., The CF metadata standard, 2003.

Grinstein, G., and R. Linsker, Comments on a derivation and application of the 'maximum entropy production' principle, *J. Phys. A: Math. Theor.*, *40*(31), 9717, 2007.

Haywood, J. M., et al., The impact of equilibrating hemispheric albedos on tropical performance in the HadGEM2-ES coupled climate model, *Geophys. Res. Lett.*, *43*(1), 395–403, 2016.

Herbert, C., D. Paillard, M. Kageyama, and B. Dubrulle, Present and Last Glacial Maximum climates as states of maximum entropy production, *Quart. J. Roy. Meteor. Soc.*, *137*(657), 1059–1069, 2011.

Jaynes, E. T., Information Theory and Statistical Mechanics, *Phys. Rev.*, *106*(4), 620–630, 1957a.

Jaynes, E. T., Information theory and statistical mechanics. II, *Phys. Rev.*, 1957b.

Johnson, D. R., "General Coldness of Climate Models" and the Second Law: Implications for Modeling the Earth System, *J. Climate*, *10*(11), 2826–2846, 1997.

Kato, S., and F. G. Rose, Global and regional entropy production by radiation estimated from satellite observations, *J. Climate*, *33*(8), 2985–3000, 2020.

Kleidon, A., Nonequilibrium thermodynamics and maximum entropy production in the Earth system, *Naturwissenschaften*, *96*(6), 1–25, 2009.

Kleidon, A., A basic introduction to the thermodynamics of the Earth system far from equilibrium and maximum entropy production, *Philosophical Transactions of the Royal Society B: Biological Sciences*, *365*(1545), 1303–1315, 2010.

Kleidon, A., and R. D. Lorenz, Entropy production by Earth system processes, in *Non-equilibrium Thermodynamics and the Production of Entropy*, pp. 1–20, Springer, Berlin, Heidelberg, Berlin/Heidelberg, 2005.

Laakso, A., P. K. Snyder, S. Liess, A.-I. Partanen, and D. B. Millet, Differing precipitation response between solar radiation management and carbon dioxide removal due to fast and slow components, *Earth Syst. Dynam.*, *11*(2), 415–434, 2020.

Labarre, V., D. Paillard, and B. Dubrulle, A radiative-convective model based on constrained maximum entropy production, *Earth Syst. Dynam.*, *10*(3), 365–378, 2019.

Laliberté, F., J. D. Zika, L. Mudryk, P. J. Kushner, J. Kjellsson, and K. Doos, Constrained work output of the moist atmospheric heat engine in a warming climate, *Science*, *347*(6221), 540–543, 2015.

Lembo, V., F. Lunkeit, and V. Lucarini, TheDiaTo (v1.0) – a new diagnostic tool for water, energy and entropy budgets in climate models, *Geosci. Model Dev.*, *12*(8), 3805–3834, 2019.

Lesins, G. B., On the relationship between radiative entropy and temperature distributions, *J. Atmos. Sci.*, *47*(6), 795–803, 1990.

Li, J., and P. Chylek, Entropy in climate models. Part II: horizontal structure of atmospheric entropy production, *J. Atmos. Sci.*, *51*(12), 1702–1708, 1994.

Li, J., P. Chylek, and G. B. Lesins, Entropy in climate models. Part I: vertical structure of atmospheric entropy production, *J. Atmos. Sci.*, *51*(12), 1691–1701, 1994.

Liu, Y., C. Liu, D. W. Entropy, and 2011, Understanding atmospheric behaviour in terms of entropy: a review of applications of the second law of thermodynamics to meteorology, *Entropy*, 2011.

Loeb, N. G., et al., Clouds and the Earth's Radiant Energy System (CERES) Energy Balanced and Filled (EBAF) Top-of-Atmosphere (TOA) Edition-4.0 Data Product, *J. Climate*, *31*(2), 895–918, 2018.

Lorenz, E. N., Generation of available potential energy and the intensity of the general circulation, 1960.

Lorenz, R. D., The two-box model of climate: limitations and applications to planetary habitability and maximum entropy production studies, *Philosophical Transactions of the Royal Society B: Biological Sciences*, *365*, 1349–1354, 2010.

Lucarini, V., Thermodynamic efficiency and entropy production in the climate system, *Phys. Rev. E*, *80*(2), 021,118, 2009.

Lucarini, V., K. Fraedrich, and F. Lunkeit, Thermodynamic analysis of snowball Earth hysteresis experiment: Efficiency, entropy production and irreversibility, *Quart. J. Roy. Meteor. Soc.*, *136*(646), 2–11, 2010a.

Lucarini, V., K. Fraedrich, and F. Lunkeit, Thermodynamics of climate change: generalized sensitivities, *Atmos. Chem. Phys.*, *10*(20), 9729–9737, 2010b.

Lucarini, V., K. Fraedrich, and F. Ragone, New results on the thermodynamic properties of the climate system, *J. Atmos. Sci.*, *68*(10), 2438–2458, 2011.

Lucarini, V., R. Blender, and C. Herbert, Mathematical and physical ideas for climate science, *Rev. Geophys.*, 2014.

Martyushev, L. M., and V. D. Seleznev, Maximum entropy production principle in physics, chemistry and biology, *Physics Reports*, *426*(1), 1–45, 2006.

Mayer, B., and A. Kylling, Technical note: The libRadtran software package for radiative transfer calculations - description and examples of use, *Atmos. Chem. Phys.*, *5*(7), 1855–1877, 2005.

Nicolis, G., and C. Nicolis, On the entropy balance of the earth-atmosphere system, *Quart. J. Roy. Meteor. Soc.*, *106*(450), 691–706, 1980.

Noda, A., and T. Tokioka, Climates at Minima of the Entropy Exchange Rate, *Journal of the Meteorological Society of Japan. Ser. II*, *61*(6), 894–908, 1983.

O'Brien, D. M., and G. L. Stephens, Entropy and climate. II: Simple models, *Quart. J. Roy. Meteor. Soc.*, 1995.

Ore, A., Entropy of radiation, *Phys. Rev.*, *98*(4), 887–888, 1955.

Ozawa, H., and A. Ohmura, Thermodynamics of a global-mean state of the atmosphere – a state of maximum entropy Increase, *J. Climate*, *10*(3), 441–445, 1997.

Ozawa, H., A. Ohmura, R. D. Lorenz, and T. Pujol, The second law of thermodynamics and the global climate system: A review of the maximum entropy production principle, *Rev. Geophys.*, *41*(4), 1075, 2003.

Paillard, D., and C. Herbert, Maximum Entropy Production and Time Varying Problems: The Seasonal Cycle in a Conceptual Climate Model, *Entropy*, *15*(7), 2846–2860, 2013.

Paltridge, G. W., Global dynamics and climate - a system of minimum entropy exchange, *Quart. J. Roy. Meteor. Soc.*, *101*(429), 475–484, 1975.

Paltridge, G. W., The steady-state format of global climate, *Quart. J. Roy. Meteor. Soc.*, *104*(442), 927–945, 1978.

Paltridge, G. W., Stumbling into the MEP Racket: An Historical Perspective, in *Non-equilibrium Thermodynamics and the Production of Entropy*, edited by A. Kleidon and R. D. Lorenz, pp. 33–40, Springer-Verlag, Berlin/Heidelberg, 2005.

Pascale, S., J. Gregory, M. H. P. Ambaum, and R. Tailleux, Climate entropy budget of the HadCM3 atmosphere–ocean general circulation model and of FAMOUS, its low-resolution version, *Clim Dyn*, *36*(5-6), 1189–1206, 2011a.

Pascale, S., J. Gregory, M. H. P. Ambaum, and R. Tailleux, A parametric sensitivity study of entropy production and kinetic energy dissipation using the FAMOUS AOGCM, *Clim Dyn*, *38*(5-6), 1211–1227, 2011b.

Pascale, S., J. Gregory, M. H. P. Ambaum, R. Tailleux, and V. Lucarini, Vertical and horizontal processes in the global atmosphere and the maximum entropy production conjecture, *Earth Syst. Dynam.*, *3*(1), 19–32, 2012.

Pauluis, O. M., and I. M. Held, Entropy budget of an atmosphere in radiative–convective equilibrium. Part I: maximum work and frictional dissipation, *J. Atmos. Sci.*, *59*(2), 125–139, 2002a.

Pauluis, O. M., and I. M. Held, Entropy budget of an atmosphere in radiative–convective equilibrium. Part II: latent heat transport and moist processes, *J. Atmos. Sci.*, *59*(2), 140–149, 2002b.

Peixoto, J. P., A. H. Oort, M. De Almeida, and A. Tomé, Entropy budget of the atmosphere, *J. Geophys. Res. Atmos.*, *96*(D6), 10,981–10,988, 1991.

Pelkowski, J., Towards an accurate estimate of the entropy production due to radiative processes: results with a gray atmosphere model, *Meteor. Atmos. Phys.*, *53*(1), 1–17, 1994.

Pelkowski, J., Of entropy production by radiative processes in a conceptual climate model, *Meteorol. Z.*, *21*(5), 439–457, 2012.

Planck, M., *The Theory of Heat Radiation*, P. Blackiston's Sons & Co, Philadelphia, 1914.

Pujol, T., and J. Fort, States of maximum entropy production in a onedimensional vertical model with convective adjustment, *Tellus A: Dyn. Meteor. Oceanogr.*, *54*(4), 363–369, 2002.

Pujol, T., and J. E. Llebot, Extremal principle of entropy production in the climate system, *Quart. J. Roy. Meteor. Soc.*, *125*(553), 79–90, 1999.

Raymond, D. J., Sources and sinks of entropy in the atmosphere, *J. Adv. Model. Earth Syst*, *5*(4), 755–763, 2013.

Reis, A. H., Use and validity of principles of extremum of entropy production in the study of complex systems, *Annals of Physics*, *346*, 22–27, 2014.

Robinson, T. D., and D. C. Catling, An analytic radiative-convective model for planetary atmospheres, *ApJ*, *757*(1), 104, 2012.

Robinson, T. D., and D. C. Catling, Common 0.1bar tropopause in thick atmospheres set by pressure-dependent infrared transparency, *Nature Geosci*, *7*(1), 12–15, 2014.

Rodgers, C. D., Comments on paltridge's 'minimum entropy exchange' principle, *Quart. J. Roy. Meteor. Soc.*, *102*(432), 455–458, 1976.

Rodgers, C. D., and C. D. Walshaw, The computation of infra-red cooling rate in planetary atmospheres, *Quart. J. Roy. Meteor. Soc.*, *92*(391), 67–92, 1966.

Rosen, P., Entropy of radiation, *Phys. Rev.*, *96*, 555, 1954.

Rutan, D. A., S. Kato, D. R. Doelling, F. G. Rose, L. T. Nguyen, T. E. Caldwell, and N. G. Loeb, CERES Synoptic Product: Methodology and Validation of Surface Radiant Flux, *Journal of Atmospheric and Oceanic Technology*, *32*(6), 1121–1143, 2015.

Samset, B. H., et al., Fast and slow precipitation responses to individual climate forcers: A PDRMIP multimodel study, *Geophys. Res. Lett.*, *43*(6), 2782–2791, 2016.

Santer, B. D., et al., Contributions of Anthropogenic and Natural Forcing to Recent Tropopause Height Changes, *Science*, *301*(5632), 479–483, 2003.

Schreier, F., S. G. García, P. Hochstaffl, and S. Städt, Py4CAtS—PYthon for Computational ATmospheric Spectroscopy, *Atmosphere*, *10*(5), 262, 2019.

Shettle, E. P., Models of aerosols, clouds, and precipitation for atmospheric propagation studies, in *In AGARD Conf Proc No. 454*, 1989.

Singh, M. S., and P. A. O'Gorman, Scaling of the entropy budget with surface temperature in radiative-convective equilibrium, *J. Adv. Model. Earth Syst*, *8*(3), 1132–1150, 2016.

Stephens, G. L., and D. M. O'Brien, Entropy and climate. I: ERBE observations of the entropy production of the earth, *Quart. J. Roy. Meteor. Soc.*, *119*(509), 121–152, 1993.

Stephens, G. L., D. O'Brien, P. J. Webster, P. Pilewski, S. Kato, and J. l. Li, The albedo of Earth, *Rev. Geophys.*, *53*(1), 141–163, 2015.

Stephens, G. L., M. Z. Hakuba, M. Hawcroft, J. M. Haywood, A. Behrangi, J. E. Kay, and P. J. Webster, The Curious Nature of the Hemispheric Symmetry of the Earth's Water and Energy Balances, *Curr Clim Change Rep*, *2*(4), 135–147, 2016.

Tolento, J. P., and T. D. Robinson, A simple model for radiative and convective fluxes in planetary atmospheres, *ICARUS*, *329*, 34–45, 2019.

Trenberth, K. E., J. T. Fasullo, and M. A. Balmaseda, Earth's Energy Imbalance, *J. Climate*, *27*(9), 3129–3144, 2014.

Virgo, N., and T. Ikegami, Possible dynamical explanations for Paltridge's principle of maximum entropy production, *AIP Conference Proceedings*, *1636*(1), 172–179, 2015.

Voigt, A., B. Stevens, J. Bader, and T. Mauritsen, The Observed Hemispheric Symmetry in Reflected Shortwave Irradiance, *J. Climate*, *26*(2), 468–477, 2013.

Voigt, A., B. Stevens, J. Bader, and T. Mauritsen, Compensation of hemispheric albedo asymmetries by shifts of the ITCZ and tropical clouds, *J. Climate*, 2014.

Volk, T., and O. M. Pauluis, It is not the entropy you produce, rather, how you produce it, *Philos. Trans. R. Soc., B*, *365*(1545), 1317–1322, 2010.

Wallace, J. M., and P. V. Hobbs, *Atmospheric Science: An Introductory Survey*, An Introductory Survey, Elsevier, 2006.

Wang, B., T. Nakajima, and G. Shi, Cloud and water vapor feedbacks in a vertical energy-balance model with maximum entropy production, *J. Climate*, 2008.

Weaver, I., J. Dyke, and K. Oliver, Can the Principle of Maximum Entropy Production be Used to Predict the Steady States of a Rayleigh-Bérnard Convective System?, in *Beyond the Second Law*, edited by R. C. Dewar, C. H. Lineweaver, and K. Regenauer-Lieb, pp. 277–290, Springer Berlin Heidelberg, Berlin, Heidelberg, 2014.

Whitfield, J., Order out of chaos, *Nature*, *436*(7053), 905–907, 2005.

Wild, M., et al., The energy balance over land and oceans: an assessment based on direct observations and CMIP5 climate models, *Clim Dyn*, *44*(11), 3393–3429, 2015.

Woollings, T., and J. Thuburn, Entropy sources in a dynamical core atmosphere model, *Quart. J. Roy. Meteor. Soc.*, *132*(614), 43–59, 2006.

Wu, W., and Y. Liu, Radiation entropy flux and entropy production of the Earth system, *Rev. Geophys.*, *48*(2), 1075, 2010a.

Wu, W., and Y. Liu, A new one-dimensional radiative equilibrium model for investigating atmospheric radiation entropy flux, *Philosophical Transactions of the Royal Society B: Biological Sciences*, *365*(1545), 1367–1376, 2010b.

Wyant, P. H., A. Mongroo, and S. Hameed, Determination of the heat-transport coefficient in energy-balance climate models by extremization of entropy production, *J. Atmos. Sci.*, *45*(2), 189–193, 1988.

Zika, J. D., M. H. England, and W. P. Sijp, The Ocean Circulation in Thermohaline Coordinates, *J. Phys. Oceanogr.*, *42*(5), 708–724, 2012.

Zika, J. D., F. Laliberté, L. R. Mudryk, W. P. Sijp, and A. J. G. Nurser, Changes in ocean vertical heat transport with global warming, *Geophys. Res. Lett.*, *42*(12), 4940–4948, 2015.

Appendices

A.1 The invalidity of the Carnot limit when work is dissipated within the system

Climate efficiency is often mentioned in the climate and entropy literature [*Bannon*, 2015; *Lucarini*, 2009]. It is based on the sensible (if extreme) simplification of the system as involving reservoirs at two temperatures only, T_H and T_C, and the heat flow between them. The energy in and out is typically taken to be the solar incoming and outgoing longwave radiations, while the down-gradient heat transport is the steady-state net impact of the multitude of irreversible climate processes and transports.
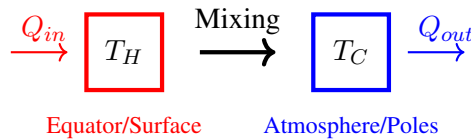
For a heat engine, the efficiency, η, is a natural way to quantify how optimally the system is operating (see Figure A.1). The maximum efficiency (work output per unit heat input) can be calculated by considering the work done if the system were acting reversibly, with no entropy produced.

By the Second Law:
$$\frac{Q_{in}}{T_H} = S_{in} \leq S_{out} = \frac{Q_{out}}{T_C}$$

So:
$$W = Q_{in} - Q_{out}$$
$$\leq Q^* \left(1 - \frac{T_C}{T_H}\right)$$
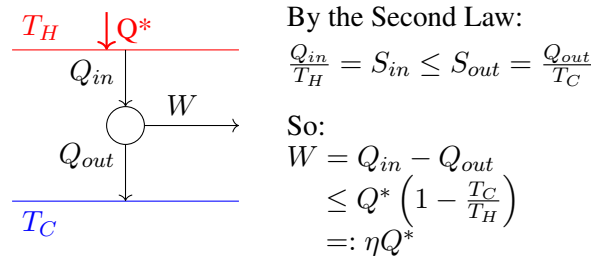$$=: \eta Q^*$$

Figure A.1: The canonical Carnot engine and efficiency calculation.

When analysing the climate system, the observed or estimated hot and cold temperatures are often combined into an efficiency using the same formula, which is often interpreted as representing the maximum amount of kinetic energy which could be generated by the atmosphere were it maximally efficient. In that scenario, however, there is work being done to maintain motion against an equal amount of dissipation which balances

to keep the system steady but, in so doing, produces entropy. The reversibility assumption key to the Carnot limit is not invocable.

One way [*Bannon*, 2015] tries to maintain a use for climate efficiency is to drop the concept of work and instead relate it to the amount of irreversible entropy produced within the system at steady state via:

$$\eta Q_{in} = T_C \Sigma \tag{A.1}$$

However, there the concept is a diversion from the fundamental physics: in steady state, heat (Q) enters the hot reservoir from an external source, is somehow mixed and transported in the middle, and leaves from the cold. The total entropy change to the universe can be calculated from the temperatures T_H and T_C at which energy is absorbed and emitted:

$$\Sigma = \frac{Q}{T_C} - \frac{Q}{T_H} = \frac{Q}{T_C}\left(1 - \frac{T_C}{T_H}\right) =: \eta_{\text{H,C}}Q/T_C \tag{A.2}$$
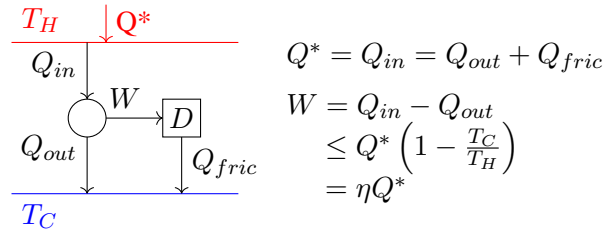
and it can be seen that the significance of the efficiency $\eta_{\text{H,C}}$ is on the basis of algebraic similarities only. It is the common ancestry of the amount of entropy produced by irreversible processes and the amount of work which can be exported in the Second Law of thermodynamics that ties them to each other mathematically, not a universality of the "efficiency" concept.

More fundamentally, it is not physically correct to apply the Carnot limit to a system like the climate in which there is no work exported out of the system, and doing so does not supply an upper bound of work generated (as mentioned briefly in *Volk and Pauluis* [2010]). In the Carnot engine of Figure A.1, work is exported to an unknown final destination, while in the planetary system, all work is dissipated somewhere within the system, returning as heat via friction. Depending on where the dissipation occurs, the heat it returns can in principle be used to initiate more work (provided sufficient energy is rejected into the cold reservoir to be at least reversible each time). Consider the two-temperature system for example, shown in Figure A.2.

The input and output temperatures, which solely determine the climate efficiency, demonstrably cannot account for the amount of work produced by the system, even assuming the heat engines themselves, ◯, are reversible, the location of the dissipation, $\boxed{D}$, can skew the account significantly. For an extreme example, consider dissipation occurring at a temperature much larger than T_H: an arbitrarily large multiplying effect can be obtained.

In his 2015 paper, Bannon argues that "all these dissipative processes produce entropy, and that entropy production, always positive, is a measure of the internal activity of the climate system". Although the quantity of dissipation must equal the quantity of work produced, which *is* a measure of internal activity of the system, the entropy production associated with that dissipation is not fixed, as it depends on the temperature of the dissipa-

Dissipation into cold reservoir

$$Q^* = Q_{in} = Q_{out} + Q_{fric}$$
$$W = Q_{in} - Q_{out}$$
$$\leq Q^*\left(1 - \frac{T_C}{T_H}\right)$$
$$= \eta Q^*$$

Dissipation into hot reservoir

$$Q^* = Q_{in} - Q_{fric} = Q_{out}$$
$$W = Q_{in} - Q_{out}$$
$$\leq Q^*\left(\frac{T_H}{T_C} - 1\right)$$
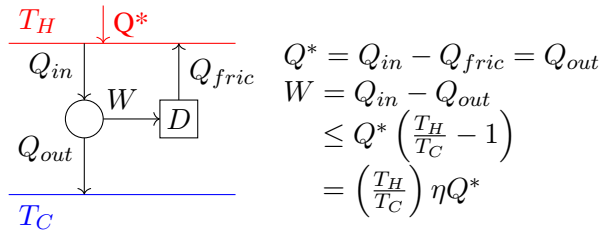$$= \left(\frac{T_H}{T_C}\right)\eta Q^*$$

Figure A.2: When work is dissipated within a system instead of being exported, the same unit of inputted energy can be multiplied into more work than a simple calculation of climate efficiency might suggest. The amount depends on the temperature of the reservoir into which the work is dissipated: cold/output temperature will have no multiplying effect while dissipation into the hot reservoir will allow for $\frac{T_H}{T_C}$ times more work to be done. Throughout, the assumption of reversibility is maintained for the heat engine (denoted by $\bigcirc$) which establishes an entropy-preserving relationship between input and output heat quantities, $\frac{Q_{in}}{T_{in}} = \frac{Q_{out}}{T_{out}}$.

tion location. For the same entropy production, that in Equation A.2, any amount of work could be done: none if the heat had simply diffused from hot to cold, up to a near-infinite amount if the dissipation of work produced by a reversible engine was fed back into an arbitrarily hot reservoir.

For these reasons, caution is warranted when using the concept of climate efficiency.

A.2 Choices in defining J_{in} and J_{out}

There is a mapping between the entropy production perspectives offered in this thesis and in the Bannon [2015] paper: the planetary entropy production rate (PEPR) to CV1, the transfer entropy production rate (TEPR) to MS3 and the material entropy production rate (MEPR) to MS1. We calculate nearly identical values for TEPR/MS3 and exactly identical for PEPR/CV1. However, the values calculated in the present manuscript for MEPR do not agree with values tabulated in Bannon [2015] for MS1. The question is why and what to make of it.

In what follows I will argue that the views presented by Bannon for MS1 and here for MEPR are *both* self-consistent and 'correct,' representing different valid perspectives on the cross-boundary flux into and out of the material climate system. However, we prefer the MEPR approach because we think it is more physically meaningful.

First note that the values for MEPR in Table 3.1 are all reflected in *Bannon* [2015], so they're not without

precedent: at issue is just their interpretation. They occur on page 3275, where Bannon's text explains that "[t]he irreversible entropy production due to convection[3] is

$$\dot{\Sigma}_{mat} = F_{CHF} \left(\frac{1}{T_{atm}} - \frac{1}{T_{sfc}} \right) \tag{5.7}$$

[...] The atmosphere gains entropy at a rate of 336 mW/m^{2}K while the surface loses entropy at a rate of 306 mW/m^{2}K for a total production of 30 mW/m^{2}K." Elsewhere in the text, the surface temperature is quoted as $T_{sfc} = 278$ K, the atmosphere temperature $T_{atm} = 253$ K (page 3274) and the convective heat flux $F_{CHF} = 85$ W/m^2 (*Bannon* [2015], Table 1). Along with the efficiency calculated from these temperatures, these are precisely the values in our Table 3.1.

Secondly, the entropy production rate suggested by Bannon's MS1 and MS2 (from his Table 3) are the same as those suggested by our MEPR[4] (within rounding errors):

For MS1:

$$\dot{\Sigma}_{mat} = F \left(\frac{1}{T_{out}} - \frac{1}{T_{in}} \right)$$
$$= 783.66 \left(\frac{1}{263.59} - \frac{1}{266.32} \right)$$
$$= 30.5 \, \text{mW/m}^2\text{K}$$

For MS2:

$$\dot{\Sigma}_{mat} = F \left(\frac{1}{T_{out}} - \frac{1}{T_{in}} \right)$$
$$= 238.51 \left(\frac{1}{265.22} - \frac{1}{274.52} \right)$$
$$= 30.4 \, \text{mW/m}^2\text{K}$$

So the values we are differing on are F, T_{in} and T_{out} (as well as J_{in}, J_{out} and η, which can be defined in terms of the first three), but not on $\Sigma_{mat} = J_{out} - J_{in}$.

So why the three versions of F, T_{in} and T_{out} in MS1, MS2 and MEPR?

It has been established (for example in Goody (2000), Equations (9) and (10)) that the the material (i.e. non-radiative) entropy production rate can be calculated from the net radiative heating rate, because any net radiative

---

[3]In our EBM, we have split our convective processes up into latent and sensible heat terms, but their summed effect is identical to Bannon's convection. They are all the non-radiative (material) processes.

[4]We've followed the definitions in Bannon in order to calculate the values below to more significant figures than are tabulated in his Table 3 so that these relationships can be verified numerically.

heating (or cooling) must be exactly balanced by non-radiative cooling (or heating) at steady state:

$$\Sigma_{mat} = \int dV \, \frac{-\dot{Q}_{rad}(\mathbf{x})}{T_{mat}(\mathbf{x})} \tag{A.3}$$

where $Q_{rad}(\mathbf{x})$ is the local radiative heating (negative for cooling) and $T_{mat}(\mathbf{x})$ is the temperature of the material where it occurs.

For the simple *Bannon* [2015] model, one can enumerate all the contributions to this integral (per unit surface area, not volume integrated):

$$\Sigma_{mat} = -\left[\frac{\beta F_{ISR}}{T_{atm}} + \frac{(1-\alpha-\beta)F_{ISR}}{T_{sfc}} - \frac{F_{sfc}}{T_{sfc}} + \frac{F_{atm}}{T_{sfc}} + \frac{\epsilon F_{sfc}}{T_{atm}} - 2\frac{F_{atm}}{T_{atm}} \right] \tag{A.4}$$

where $\beta F_{ISR} = 34.1\,\text{W/m}^2$, $(1-\alpha-\beta)F_{ISR} = 204.4\,\text{W/m}^2$, $F_{sfc} = 340.7\,\text{W/m}^2$, $\epsilon F_{sfc} = 323.7\,\text{W/m}^2$ and $F_{atm} = 221.5\,\text{W/m}^2$.

Bannon [2015] foreshadows this next point on page 3271 where he says: "the criterion for the partition of the heating into input and output components requires careful consideration for the complex climate system. The partitioning is not unique, and three different partitioning appear relevant." I agree exactly, except I would point to a different third choice for the material system alongside MS1 and MS2, and suggest instead that his MS3 belongs to a different subsetting of the climate system which should be considered separately (namely TEPR, as it includes internal radiation). The three options for how to split up the Q/T terms in Equation A.4 into two groupings corresponding to a Q_{in} and Q_{out} (or F, in since we're taking column-integrated values) are as follows:

MS1 All absorption-related terms are grouped together in F_{in} and all emission terms in F_{out} ("The case MS1 strictly distinguishes between the absorption and emission" (*Bannon* [2015], pg 3278)).

MS2 All terms related to shortwave radiation are grouped in F_{in} and all terms relating to longwave radiation in F_{out} (" [MS2] defines the input to the system as that due solely to the absorption of solar radiation. Then the output is that associated with the net emission of terrestrial radiation" (*Bannon* [2015], pg 3271)).

MEPR The net impact of the terms occurring at each location are considered, and all locations for which $F_{\text{total rad}}$ is positive are grouped in F_{in} and those where $F_{\text{total rad}}$ is negative are grouped in F_{out}. For the EBM, this is grouping the atmosphere (which has net radiative cooling) and surface (which has net radiative heating) terms separately.

It is worth acknowledging that this third option is not original: it is discussed in *Lucarini* [2009], for example.

We can use these to partition the terms from Equation A.4 and can plug in the numbers to confirm that this interpretation agrees with the values given in Table 3 of *Bannon* [2015]):

MS1:

$$\textcolor{red}{F_{in}} = \beta F_{ISR} + (1 - \alpha - \beta)F_{ISR} + F_{atm} + \epsilon F_{sfc} = \textcolor{blue}{F_{out}} = F_{sfc} + 2F_{atm} = 784\,\text{W/m}^2$$

MS2:

$$\textcolor{red}{F_{in}} = \beta F_{ISR} + (1 - \alpha - \beta)F_{ISR} = \textcolor{blue}{F_{out}} = F_{sfc} - F_{atm} - \epsilon F_{sfc} + 2F_{atm} = 239\,\text{W/m}^2$$

MEPR:

$$\textcolor{red}{F_{in}} = (1 - \alpha - \beta)F_{ISR} - F_{sfc} + F_{atm} = \textcolor{blue}{F_{out}} = -\beta F_{ISR} - \epsilon F_{sfc} + 2F_{atm} = 85\,\text{W/m}^2$$

From these the temperatures also follow:

$$\frac{1}{T_{in}} = \frac{1}{F}\sum_j \frac{F_j^{in}}{T_j}, \qquad \frac{1}{T_{out}} = \frac{1}{F}\sum_j \frac{F_j^{out}}{T_j} \tag{A.5}$$

as in Bannon's Equation 2.8. Because of the relationship with Equation A.4 and these careful definitions of the temperatures, for all cases $\Sigma_{mat} = F_{out}/T_{out} - F_{in}/T_{in}$.

We have now established that these three definitions/perspectives of the cross-boundary fluxes are internally consistent and all belong, in some sense, to the material system. The question that remains is, which is preferable? Which is most useful or meaningful? We have established above that they are all equally equipped to calculate the Σ_{mat}, but they each regard the material system as having different amounts of energy flow through it, different working temperatures and so different efficiencies. The question of preferability relies on our physical intuition of how we would like our metrics to capture the climate.

MS1 has the problem of being very difficult to scale to an atmosphere with more layers, which was an issue in this thesis because we wanted to compare the results from the EBM to the ARCM and the realistic atmospheric profile. *Bannon* [2015] in fact highlights this issue on page 3278: "Rigorous application of this approach (MS1) is impractical using accurate non-grey calculations where the photon mean-free paths in some spectral lines are less than 1m". Put another way, the issue is that radiation is so frequently absorbed and re-emitted within the atmosphere that the quantity of absorption and emission is more a function of the vertical resolution of the model and optical thickness of the atmosphere than something related to the material processes and convective activity. This makes us reluctant to use MS1, especially given the partial aim of showing continuity between the definitions as applied to EBMs and more realistic climates.

MS2 is more tractable since the total energy F is fixed by the absorbed solar energy and not a function of atmospheric absorptivity. However, if a fraction of the solar radiation is absorbed and immediately re-emitted

in the stratosphere, the stratospheric temperatures contribute to the averaged T_{in} and T_{out}, although they are arguably irrelevant to the material processes that occur in the troposphere.

By focusing on the places where there is an imbalance in net radiative heating (or cooling), we average the temperatures between which non-radiative processes actually act (since a net radiative heating imbalance in steady state implies compensating non-radiative cooling). In the EBM case, the MEPR perspective we suggest extracts F_{CHF}, the familiar energy flow through the material process, from the radiative imbalance, which is physically quite meaningful. The T_{in} and T_{out} that result are the familiar surface and atmospheric temperatures, which are the temperatures between which we would intuitively expect the atmospheric convection 'heat engine' to act. And finally, this definition is straightforward to apply to the ARCM and realistic profile cases.

This is why we have chosen to use the approach we do with MEPR to partition the radiative heating into input and output.

A similar issue for the transfer entropy production rate case:

There is a similar issue with defining TEPR. In the same way that Equation A.3 summarises the entropy production for the material system, the transfer entropy production is:

$$\Sigma_{tran} = \int dV \, \frac{-\dot{Q}_{\text{external rad}}(\mathbf{x})}{T_{mat}(\mathbf{x})} \tag{A.6}$$

where $Q_{\text{external rad}}$ is the heating due to the radiation that comes from or goes to space, as in solar heating or cooling to space.

This can be expanded again:

$$\Sigma_{tran} = -\left[\frac{\beta F_{ISR}}{T_{atm}} + \frac{(1 - \alpha - \beta)F_{ISR}}{T_{sfc}} - \frac{(1 - \epsilon)F_{sfc}}{T_{sfc}} - \frac{F_{atm}}{T_{atm}} \right]. \tag{A.7}$$

Grouping all the terms associated with shortwave radiation separately from those involved with longwave radiation (analogous to MS2 above) would return the $F = (1 - \alpha)F_0 = (1 - \epsilon F_{sfc}) + F_{atm}$ of *Kato and Rose* [2020] Equations (15) and (16) and also the temperatures of (17) and (18) and our Table 3.1. This is also the perspective we have suggested for TEPR, which we will label here TS1.

There is another choice, which we did not explore in detail but which is more analogous to the MEPR perspective above, of splitting the terms in Equation A.7 into those which occur where there is net external heating and those where there is net external cooling (which in the EBM is separating the atmosphere and surface). Then the $T_{in} = T_{surf}$ and $T_{out} = T_{atm}$ (necessarily) and the flux suggested is $F_{in} = (1 - \alpha - \beta)F_{ISR} - (1 - \epsilon)F_{sfc} = F_{out} = -\beta F_{ISR} + F_{atm} = 187.4\,\text{W/m}^2$. This is equal to $F_{CHF} + F_{intrad}$, which is quite a neat result. Let's label this perspective TS2.

TS1 has the same disadvantage as MS2: from the perspective of TS1, a stratosphere where radiation is absorbed

and immediately re-emitted will affect the T_{in} and T_{out} and change the apparent efficiency of the system, even though no material processes or internal radiation is involved; TS2 avoids this problem. But on the other hand, the output temperature for TS1 is (approximately) the brightness temperature of the outgoing radiation, which is an observable, unlike T_{out} for TS2. If the global albedo is fixed, the effective radiating temperature of the planet is fixed and the TS1 T_{out} is approximately fixed too. This has some appeal.

It is not yet certain which one of the TS1 and TS2 perspectives will be more useful in analysing and understanding the climate.